PETROGENESIS OF THE WILLIS MOUNTAIN AND EAST RIDGE KYANITE QUARTZITE, BUCKINGHAM COUNTY, VIRGINIA

by

Judith Christian Cochrane

Thesis submitted to the Faculty of the Virginia Polytechnic Institute and State University in partial fulfillment of the requirements for the degree of

Master of Science

in

Geology

APPROVED:

D. A. Hewitt, Co-chairman	J. R. Craig, Co-chairman
J. D. Rimstidt	P. H. Ribbe

October, 1986

Blacksburg, Virginia

PETROGENESIS OF THE WILLIS MOUNTAIN AND EAST RIDGE KYANITE QUARTZITE, BUCKINGHAM COUNTY, VIRGINIA

by

Judith Christian Cochrane

(ABSTRACT)

The kyanite quartzites of the Willis Mountain and East Ridge deposits in Buckingham County, Virginia hosts the world's largest kyanite mine and constitute the largest known reserves of kyanite. The stratiform kyanite quartzite is overlain and underlain by quartz-muscovite schists which are in turn enveloped by biotite-amphibole gneiss of the Cambrian Chopawamsic formation, metamorphosed volcanic and volcaniclastic rocks . The entire package of rocks has been metamorphosed to amphibolite grade peak conditions of 6.5 kb and 600° C. The kyanite quartzite is very similar in bulk composition and accessory mineralogy to high-alumina rocks of probable hydrothermal origin in North Carolina, South Carolina, and Georgia, and to active stratiform hydrothermal alteration zones in Tatun, Taiwan and Otake, Japan. The major difference among these deposits is the type of aluminosilicate phase present, a reflection of the grade of metamorphism, with kaolinite and pyrophyllite appearing in unmetamorphosed deposits, pyrophyllite and andalusite appearing in zones of greenschist grade, and kyanite appearing in zones of amphibolite grade. Data from active alteration zones and mineral equilibria suggest that the kyanite quartzite was formed from intermediate volcanic rocks by hydrothermal action of acidic fluids (pH 2 to 4) at a temperature between 100 and 200° C under mildly oxidizing conditions. Alumina and silica were residually enriched as alkali and alkaline earth cations were extracted from the rock by hydrolysis. The surrounding quartz-muscovite schist was formed in

the same manner by less acidic, cooler fluids. The adjacent biotite-amphibole gneiss also shows signs of partial hydrothermal alteration, such as residual enrichment of alumina represented by a kyanite and/or sillimanite-staurolite-gedrite assemblage.

Table of Contents

List of Figures

List of Tables

Aknowledgements

I wish to thank Mr. Gene B. Dixon, Jr., President of the Kyanite Mining Corporation of America for his generous hospitality at the Willis Mountain and East Ridge kyanite mine. Dr. Robert W. Luce of Billeton Exploration, Inc., donated an invaluable drill core and provided many useful suggestions. Prof. Werner Schreyer, Prof. Mark Barton, Mr. John Marr, and Prof. P. G. Feiss also provided many helpful suggestions. My fellow students, the staff, and the faculty of the Geology Department were of great assistance to me. I would especially like to thank Mr. Todd Solberg, Ms.Sharon Chiang, and Ms. Llyn Sharp for their technical assistance. My husband, Theodore D. Johnson, gave me many helpful suggestions, lots of field assistance, and plenty of help in the darkroom. My parents supplied unflagging encouragement. Most of all, I wish to thank my committee members for all their help and support with this project.

Introduction and Scope of Study

Aluminum is the third most abundant element in the Earth's crust, yet the only locations where it occurs in concentrations as great as 25 percent Al_2O_3 are the few rare deposits of bauxites, kaolin deposits, and kyanite deposits. Although the origin of bauxite and kaolin deposits are now moderately well understood, the genesis of kyanite deposits remains controversial. The Willis Mountain and East Ridge kyanite deposit, located in Buckingham County, Virginia, represents an extraordinarily large alumina-rich deposit. Because of its large size and the availability of fresh samples, it was chosen for study in an attempt to decipher the origin of this type of deposit.

Willis Mountain, the most prominent topographic feature in Buckingham County (Figure 1), is the largest known commercial kyanite deposit presently providing 45 percent of the world's production of kyanite (Dixon, 1980). It is located in the southern part of the county, seven kilometers (4.5 miles) southwest of the Dillwyn community and 29 kilometers (18 miles) north of Farmville at 78° 28' west longitude and 37° 29' north latitude (Figure 2). Kyanite quartzite, the dominant rock of the deposit, forms two ridges that stand high above the surrounding terraine of the Virginia Piedmont; the higher western ridge, Willis Mountain itself, is 339 meters above sea level and the lower eastern ridge, called East Ridge by Sweet (1980a), is 246 meters above sea level. Several other kyanite quartzites occur nearby at Baker, Leigh, and Woods Mountains. The Willis Mountain and East Ridge kyanite quartzite serves as the reserves of the Kyanite Corporation of America mine.

The kyanite quartzite, composed of quartz, kyanite, muscovite and/or paragonite with minor pyrite, rutile, topaz, hematite, and scarce apatite and zircon, has an unusual mineral assemblage which is abnormally high in aluminum and silica and distinctively

Figure 1: Willis Mountain viewed from the northwest along U.S. 15. The processing plant for the kyanite mine is in the center right.

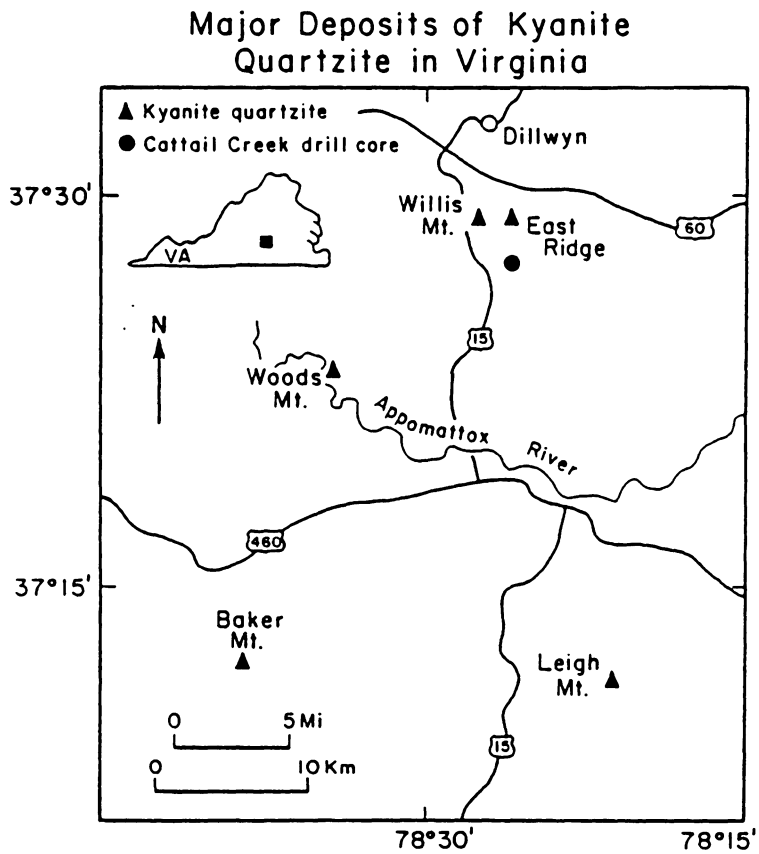

Figure 2: Map of major kyanite deposits in Virginia (after Espenshade and Potter, 1960).

low in alkalies and alkaline earths when compared to other types of alumina deposits.

Previous Work

The kyanite belt of central Virginia was studied and named by Jonas (1932), who concluded that the kyanite quartzite occurrences of the area were members of the flysch and pelitic rocks of the Wissahickon formation in northern Virginia and Maryland. Jones and Eilertsen (1954), on the basis of 32 drill holes and trenches to assess the economic value of a kyanite mine at Willis Mountain, attributed the origin of the kyanite quartzite to metamorphism of high-alumina sedimentary rocks. This mode of origin was also suggested by Espenshade and Potter (1960) in their study of these and other aluminosilicate deposits throughout the southeastern United States. They did, however, suggest that other deposits similar to the ones in central Virginia were formed by hydrothermal replacement. Bennett (1961), while recognizing the metamorphic recrystallization of the kyanite quartzite, concluded that the protolith was a quartz and kaolinite-rich residue produced by lateritic weathering or by circulating groundwaters. Brown (1969) mapped the rocks north of the Willis Mountain area, grouped the kyanite quartzites with "rocks of uncertain age", and attributed their origin to metamorphism. Conley and Marr (1980) and Marr (1980, 1981) reported relict cross-beds and other sedimentary features within the kyanite quartzite at Willis Mountain and suggested that the protolith had been an aluminous sandstone. Marr (personal communication, 1985) has subsequently stated that a sedimentary origin for the kyanite quartzite is unlikely. In the most recent work on the area, Duke (1983) emphasized that no sedimentary features could be seen in thin sections of any kyanite quartzite rocks from the Farmville district and he attributed the origin of the kyanite quartzite to hydrothermal metasomatism

followed by amphibolite grade metamorphism.

Several other authors working in Georgia, North Carolina, and South Carolina have noted similarities between their study areas and the Farmville district kyanite quartzites. Carpenter and Allard (1982) and Feiss (1985a) in their studies on the Graves Mountain, Georgia kyanite quartzite and the Carolina aluminosilicate deposits have all suggested, by comparison, that the Willis Mountain kyanite quartzite might have formed by acidic hydrothermal alteration followed by metamorphism.

Regional Geology

Stratigraphy

The oldest rocks in the Willis Mountain vicinity are the mafic to felsic metavolcanics of the Chopawamsic formation, which has its type locality in northeastern Virginia where it is 600 to 1,000 meters thick (Southwick et al., 1971). Aeromagnetic data (Higgins et al., 1973) indicate that this unit extends to the southwest into the Willis Mountain area and Glover (1974) has tentatively correlated it with the metavolcanic rocks of the Carolina Slate Belt. The Chopawamsic formation has been dated at 530 and 579 million years old (Higgins et al., 1971, Glover, 1974) and has been interpreted as representing subaqueous and subaerial volcanism of an island arc sequence (Pavlides, 1981). A 123 meter drill core into Chopawamsic rocks, drilled by Billeton Exploration, Inc., from 3 kilometers southeast of East Ridge along Cattail Creek reveals that the fresh rocks consist of biotite-amphibole gneiss with a thin unit of pyrite-rich chlorite schist and several veins of pegmatitic quartz and albite.

The kyanite quartzite lies within the biotite-amphibole gneiss but is separated from it

above and below by an approximately 50 meter thick coarse-grained quartz-muscovite schist containing quartz, muscovite and/or paragonite and hematite. The contacts between the quartz-muscovite schist and the gneiss, and between the quartz-muscovite schist and the kyanite quartzite are interleaved to gradational. The kyanite quartzite is at least 12 to 15 meters thick and is composed of a hard, light gray, foliated, granular rock which ranges from quartzite to schist depending upon the concentration of white mica. Where pyrite abounds, weathered surfaces are deep red from iron oxide stains.

The Columbia granite, actually a metamorphosed tonalite, granodiorite, and granite (Bourland, 1976), intrudes the Chopawamsic formation, and crops out 21 kilometers northeast of Willis Mountain. Gravity data (Johnson, 1981) suggest that the Columbia granite does not extend into the subsurface beneath the Willis Mountain and East Ridge area.

The 1,950 meter thick Arvonia formation unconformably overlies the Chopawamsic formation (Conley and Marr, 1980), is younger than the Columbia granite (Bourland, 1976), and is composed predominantly of slate, porphyroblastic slate, and schist (McDowell, 1964; Brown, 1969). It contains trilobites which have been correlated to a middle to late Ordovician age (Tillman, 1970). The Arvonia formation is exposed 1.3 kilometers northwest of Willis Mountain.

All of the above-mentioned units are intruded by many diabase dikes of Triassic or early Jurassic age which have a general trend of north 12° west (McCollum, 1981). They have also all been metamorphosed at the amphibolite grade.

Structure

Willis Mountain and East Ridge lie on either side of the axis of the asymmetric,

doubly plunging, northeast striking Whispering Creek anticline (Marr, 1981; Duke, 1983). Willis Mountain is formed by the steeply dipping, almost vertical, west limb and East Ridge is formed by the more gently dipping east limb. Secondary folds abound within the kyanite quartzite, the quartz-mica schist, and the biotite gneiss. Two sets of joints intersect at almost 90° giving the kyanite quartzite, especially at Willis Mountain, a blocky appearance, and Marr (1981) has identified four fold generations.

Local Ore Deposits

The Chopawamsic formation is host to an estimated 13.5 million tons of known sulfide deposits consisting of pyrite, chalcopyrite, sphalerite, and galena, most of which is located in two distinct mineralized regions: the Mineral district, 32 kilometers southwest of Fredericksburg, Virginia, and the Andersonville district which includes Willis Mountain and East Ridge within its boundaries (Pavlides et al., 1982). Furthermore, Willis Mountain is less than 3 kilometers east of Virginia's gold-pyrite belt where gold occurs in sulfide-rich veins and mineralized zones within volcanic, metamorphic, and sedimentary rocks (Sweet, 1980b). Several gold deposits in the Chopawamsic formaiton, mined from the 1830's until the Civil War, are located in the Willis Mountain vicinity. The Morrow mine and the adjacent Seay mine, 3.5 kilometers west of Willis Mountain, produced gold from pyrite-, chalcopyrite-, and pyrrhotite-containing quartz veins within a quartz-sericite schist (Luttrell, 1966). The London-Virginia mine, 9 kilometers north of Willis Mountain, produced gold from discontinuous bands of pyrite, sphalerite, galena, chalcopyrite, and tetrahedrite-tennantite within quartz-muscovite schist and associated ferruginous quartzite. Mangan et al. (1984) have suggested an exhalative process for the origin of

these deposits similar to currently active exhalatives of the Atlantis II Deep in the Red Sea.

Duke (1983) reported the concentration of gold in pyrite concentrate from the Willis Mountain kyanite quartzite as 0.2 troy ounces per ton of concentrate. An abandoned copper prospect trench (Sweet, 1980a) lies on the southern slope of Willis Mountain within a ferruginous quartzite of unknown dimensions. Blue copper alteration colors can be seen on weathered surfaces of the East Ridge kyanite quartzite though no primary, copper-containing sulfide or oxide minerals have been identified.

Petrography and Mineralogy

Figure 3 shows the location of samples taken from the kyanite quartzite and from the quartz-muscovite schist. The location of the Cattail Creek drill core into the biotite-amphibole gneiss is shown by Figure 2.

Kyanite Quartzite

Table 1 lists the modal abundances of the minerals comprising the kyanite quartzite. The dominant phase, quartz, averages 69 percent of the rock and is present as anhedral grains from 0.1 to 2.0 millimeters in size. Undulose extinction is common and annealing has produced numerous 120° dihedral grain intersections. Kyanite averages 27.6 percent of the deposit and occurs as blades, between 0.1 and 20.0 millimeters long which are often fractured, sometimes twinned, and usually have a preferred or decussate orientation. Figure 4 shows the preferred orientation of kyanite. Locally it also occurs in felty mats or radiating clusters. Microprobe analysis indicates that kyanite at Willis

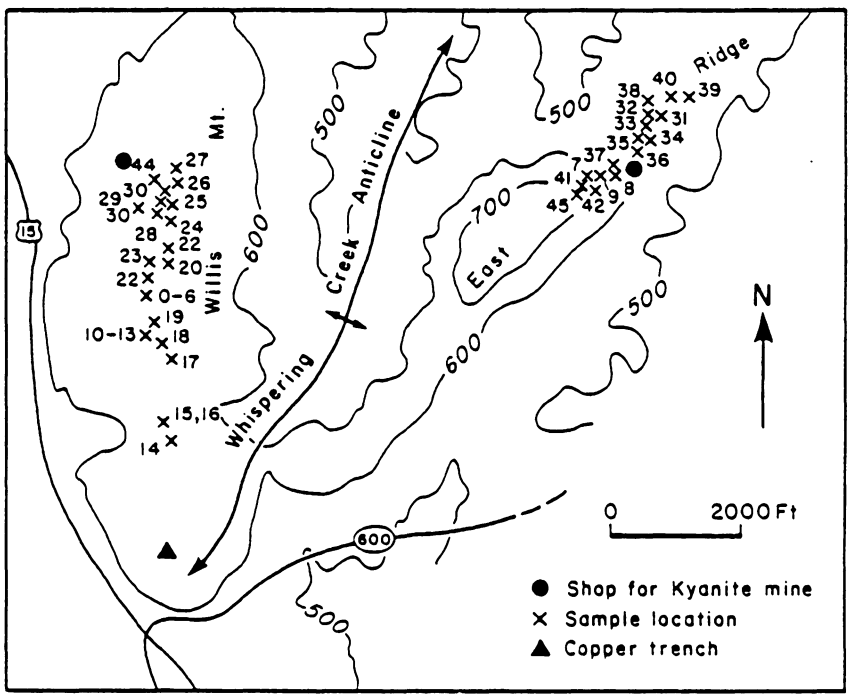

Figure 3: Sample locations at Willis Mountain and East Ridge.

Table 1: Modal abundances of minerals comprising kyanite quartzite at Willis Mountain (DW) and East Ridge (DE), Buckingham County, Virginia. 1000 counts.

Sample #:	DW5	DW10A	DW14	DW22	DW28	DE33	DE36	DE40	DE42	AVERAGE
Mineral:										
Quartz	75.5	72.5	77.1	72.6	60.9	70.7	60.0	68.7	62.6	69.0
Kyanite	23.1	24.8	22.2	25.2	30.2	28.3	38.7	28.4	27.5	27.6
Pyrite	0.2	0.1	0.0	0.0	4.4	0.0	0.0	1.0	4.9	1.2
Mica*	0.2	0.7	0.4	1.0	3.5	0.0	1.2	0.6	0.7	0.9
Topaz	0.7	1.3	0.0	0.1	0.3	0.4	0.0	0.8	3.6	0.8
Rutile	0.3	0.6	0.3	1.1	0.7	0.6	0.1	0.4	0.7	0.7
Hematite	0.0	0.0	0.1	0.0	0.0	0.0	0.0	0.1	0.0	< 0.1
Total	100.0	100.0	100.0	100.0	100.0	100.0	100.0	100.0	100.0	

*Muscovite and/or paragonite

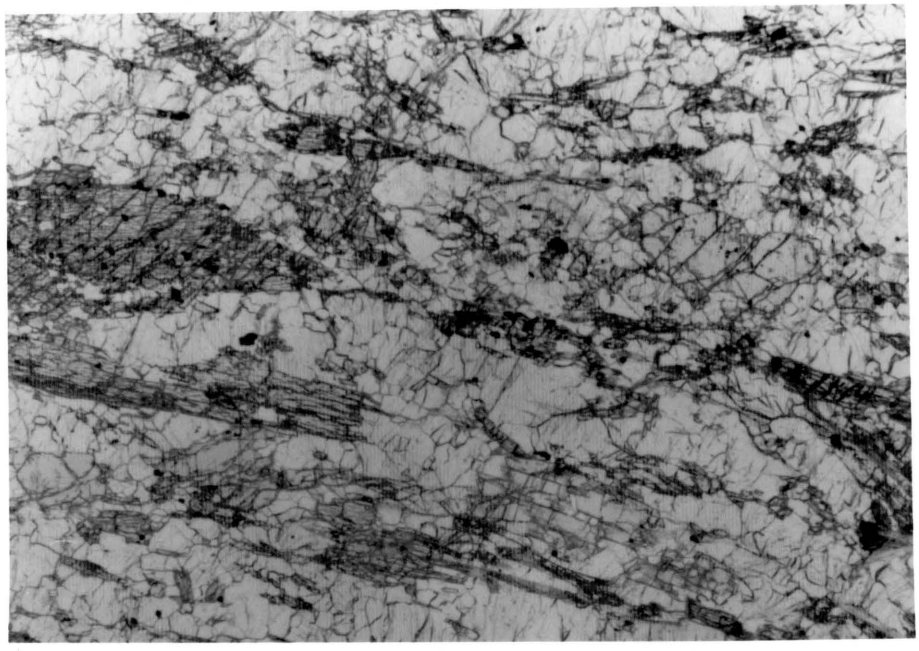

Figure 4: Photomicrograph of kyanite quartzite from Willis Mountain showing preferred orientation of kyanite. Width of field: 2.8 mm.

Mountain and East Ridge is stoichiometric Al_2SiO_5within one percent, the precision of the analysis. It frequently contains many quartz and rutile inclusions and alters upon weathering to kaolinite. Pyrite occurs as disseminated euhedral to subhedral pyritohedrons from 0.1 to 0.5 millimeters in diameter and, like kyanite, it is also slightly more abundant on East Ridge than on Willis Mountain. Also pyrite-rich quartz veins, ranging in size from microsopic to 0.5 meters thick, are scattered throughout the kyanite quartzite in apparently random orientations. Pyrite frequently reaches concentrations of 35 percent or more in these veins and sometimes occurs as large, 30 to 40 millimeter long, strained cubes.

Muscovite and paragonite occur together in concentrations up to 3.5 percent as 0.3 to 0.5 millimeter long flakes and show a preferred orientation parallel to that of the kyanite. Microprobe or X-ray analysis is necessary to distinguish muscovite from paragonite because they appear identical in thin section. Analyses (Table 2) of representative samples show that they are extremely low in iron, magnesium, calcium, barium, titanium, and fluorine and, therefore, are very close to ideal muscovite-paragonite compositions (Guidotti, 1984). Generally, paragonite in the kyanite quartzite is more fluorine-rich than is muscovite (Figure 5), though neither mica is distinctively high in fluorine (Munoz, 1984). Guidotti (1984) has noted that muscovite tends to deviate from the ideal composition more than paragonite by enrichment in iron, magnesium, and silica (phengite substitution). Although the total amount of substitution is low, this same pattern is demonstrated by white micas in the kyanite quartzite (Figure 6).

Coexisting muscovite and paragonite and paragonite were observed in two samples, DW14 (muscovite; X_K=0.70; d_{002}= 9.903 - paragonite; X_K= 0.15; d_{002}= 9.645) and DE34 (muscovite; X_K= 0.67; d_{002}= 9.900 - paragonite; X_K= 0.17; d_{002} not

Table 2: Representative microprobe analyses of muscovite (mu) and paragonite (pa) from Willis Mountain (DW) and East Ridge (DE) kyanite quartzite.

Sample #	DW2	DW14	DW14	DE36	DE40
Phase	mu	mu	pa	mu	pa
Grain#	5	6	2	1	11
SiO_2	45.91	45.65	47.89	47.22	45.66
Al_2O_3	37.36	36.08	39.80	37.38	39.33
TiO_2	.43	.57	.15	.38	.19
FeO*	.07	.13	.05	.03	.00
MgO	.61	.78	.12	.36	.02
Na_2O	2.56	2.01	5.49	2.64	6.23
K_2O	7.30	6.95	1.59	6.73	1.58
F	.24	.35	.26	.55	.16
Total	94.48	92.52	95.35	95.29	93.17
Si	3.03	3.07	3.04	3.08	2.99
Al	2.91	2.86	2.98	2.87	3.03
Ti	.02	.03	.01	.02	.01
Fe*	.00	.01	.00	.00	.00
Na	.26	.23	.68	.33	.79
K	.60	.71	.13	.56	.13
OH=2-F	1.93	1.96	1.95	1.89	1.97
F	.07	.04	.05	.11	.03

*FeO represents total iron.

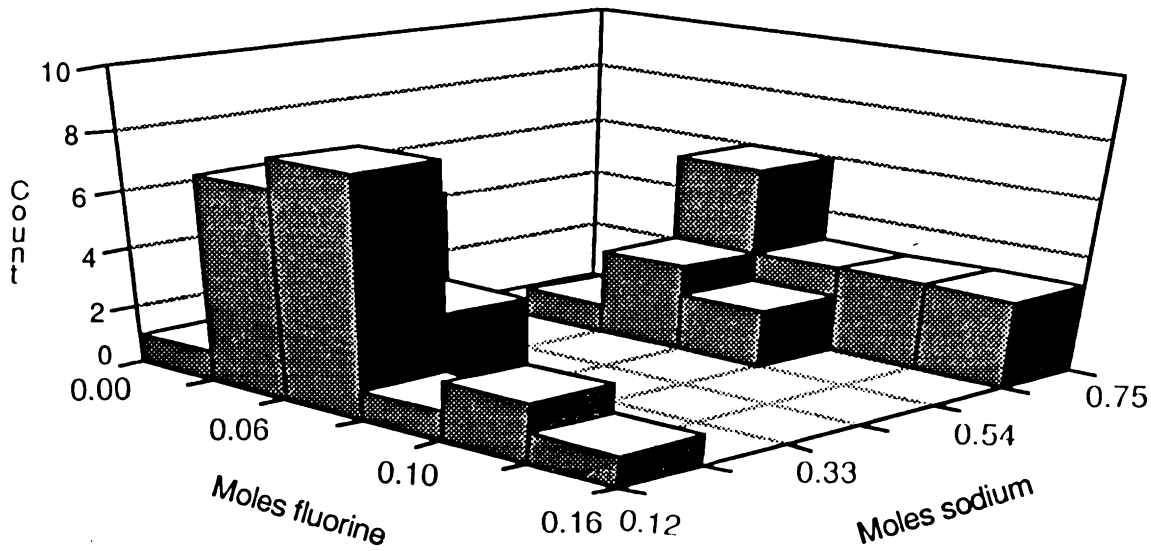

Figure 5: Graph of fluorine content of white mica in kyanite quartzite.

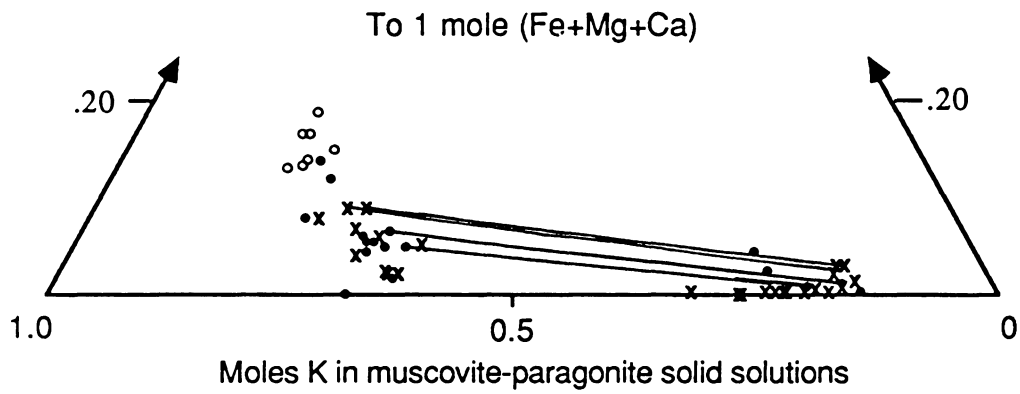

Figure 6: Composition of muscovite and paragonite in the Willis Mountain (x's), and East Ridge (filled dots) kyanite quartzite and the quartz-muscovite schist (o's). Tie lines are drawn between coexisting muscovite and paragonite pairs.

determined). These compositions fall well inside the experimentally determined solvi of Eugster et al. (1972), Thompson (1974), and Chatterjee and Froese (1975), however their unreversed experiments were performed at low pressures and the kyanite quartzite reached a peak metamorphic pressure of 6.5 kilobars. Blencoe and Luth (1973) suggest that mutual muscovite-paragonite solubility increases significantly with increasing pressure and Blencoe (1977) calculated the compositions of coexisting muscovite and paragonite at a high pressure and temperature using the experimental solvus from Eugster et al. (1972) along with the W_v parameters of 1) Eugster et al. (1972) and 2) Chatterjee and Froese (1975). The observed paragonite compositions fall between the two calculated positions for the solvus, but the muscovites contain far more sodium than predicted by any of these models. A comparison of muscovite d-spacings with the data of Guidotti (1984) shows agreement between X-ray and microprobe compositions and indicate that these high Na contents of the muscovite are not due to submicroscopic intergrowths.

The recently proposed polybaric muscovite-paragonite solvi (Chatterjee and Flux, 1986) based on reversed experimental data (Flux and Chatterjee, 1986) may be more applicable than those previously discussed to coexisting white micas in the kyanite quartzite. Figure 7 shows mica compositions from samples DW14 and DE34 superimposed on the Chatterjee and Flux (1986) solvi at 600° C, which is the calculated temperature of peak metamorphism and will be discussed in a later section. The paragonites are quite close to the predicted composition. The muscovites, however, now contain more potassium than predicted. This could be due to re-equilibration during retrograde metamorphism or to slight phengite substitution which widens the solvus (Grambling, 1984; Chatterjee and Flux, 1986). Sample DW14 muscovite contains 3.07 moles Si and DE34 muscovite contains 3.05 moles Si. Chatterjee and Flux (1986) warn

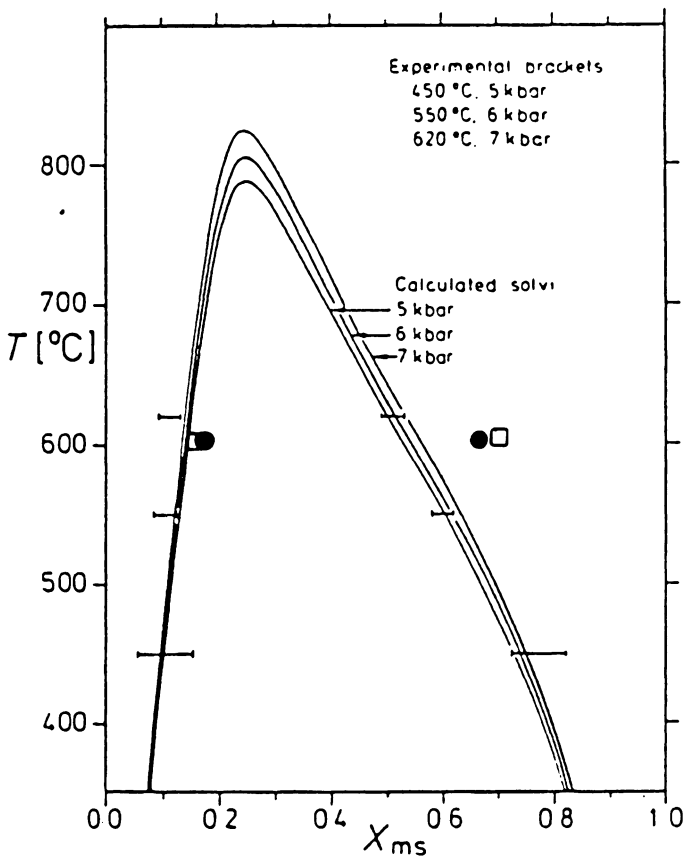

□DW14 ($Pa_{0.15K}$-$Mu_{0.70K}$)

●DE34 ($Pa_{0.17K}$-$Mu_{0.67K}$)

Figure 7: Muscovite-paragonite polybaric solvi from Chatterjee and Flux (1986) with compositions of coexisting muscovite-paragonite pairs from the Willis Mountain and East Ridge kyanite quartzite superimposed upon it.

against applying their solvi to muscovites with more than 3.05 moles Si and show examples where similar deviations from the solvus occur at even these low levels of phengite substituion.

Topaz (Table 3) comprises an average of 0.8 percent of the kyanite quartzite although its occurrence is always as dessiminated, rounded, embayed crystals between 0.1 and 0.3 millimeters in diameter (Figures 4 and 8). Topaz never occurs as an inclusion within other phases, although it often contains quartz inclusions. The calculated hydrogen content of the topaz varies between 14 and 38 percent hydroxyl-topaz but the topaz from East Ridge (averaging 21 percent hydroxyl-topaz) is usually more fluorine-rich than the topaz from Willis Mountain (averaging 32 percent hydroxyl-topaz) (Figure 9). The topaz is always richer in fluorine than coexisting white micas, an observation consistent with Barton's (1982a; 1982b) experimental work.

Rutile is ubiquitous but averages only 0.7 percent of the rock. It occurs most commonly as tiny, 0.1 millimeter long inclusions within kyanite but within the pyrite-rich quartz veins it is observed as euhedral 5 millimeter long crystals. Hematite averages 0.7 percent of the kyanite quartzite and is mostly red ocher although some specularite occurs on East Ridge. Rare zircon and apatite also occur sporadically in the kyanite quartzite.

Quartz Muscovite Schist

The quartz-muscovite schist, which immediately underlies the kyanite quartzite, is a coarse-grained, lepidoblastic, gray to reddish rock with 69 percent coarse-grained, strained quartz and 30 percent very coarse-grained to fine-grained iron-rich muscovite. Table 4 shows modal abundances and Figure 6 depicts the composition of the

Table 3: Representative microprobe analyses of topaz (top) from Willis Mountain (DW) and East Ridge (DE) kyanite quartzite.

Sample #	DW5	DW10	DW10D	DE31	DE40
Phase	top	top	top	top	top
Grain#	6	1	1	4	2
SiO_2	32.03	32.35	32.16	33.17	31.02
Al_2O_3	55.35	55.10	56.25	58.69	53.99
Fe_2O_3	.02	.04	.02	.00	.00
F	14.58	13.96	14.66	17.65	16.72
Total	101.98	101.45	103.09	109.51	101.73
Si	.99	1.00	.98	.98	.98
Al	2.01	2.00	2.02	2.03	2.02
OH=2-F	.58	.64	.58	.36	.32
F	1.42	1.36	1.42	1.64	1.68

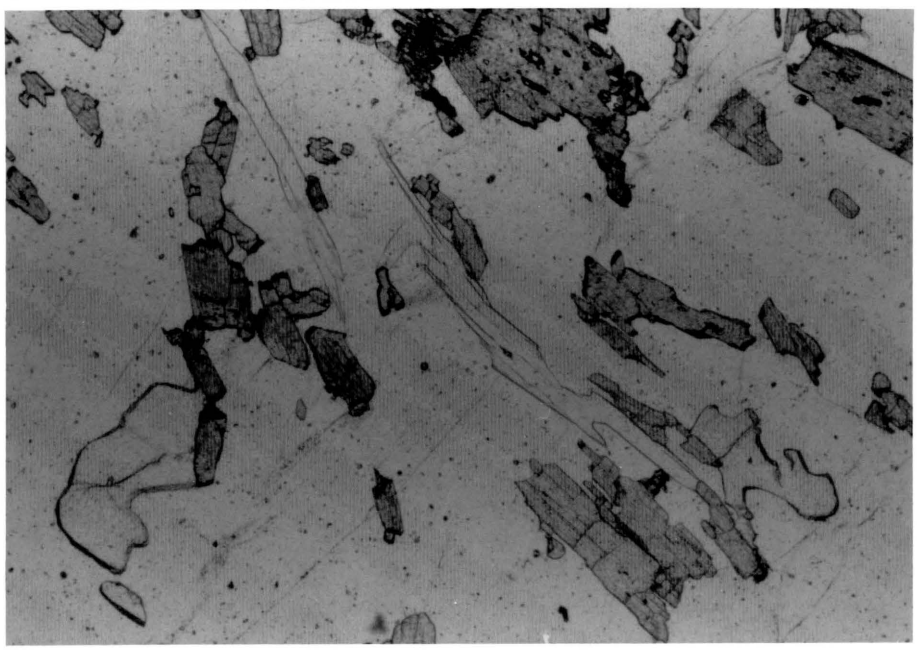

Figure 8: Photomicrograph of rounded, embayed topaz, kyanite, and quartz from kyanite quartzite at East Ridge. Width of field: 1.1 mm.

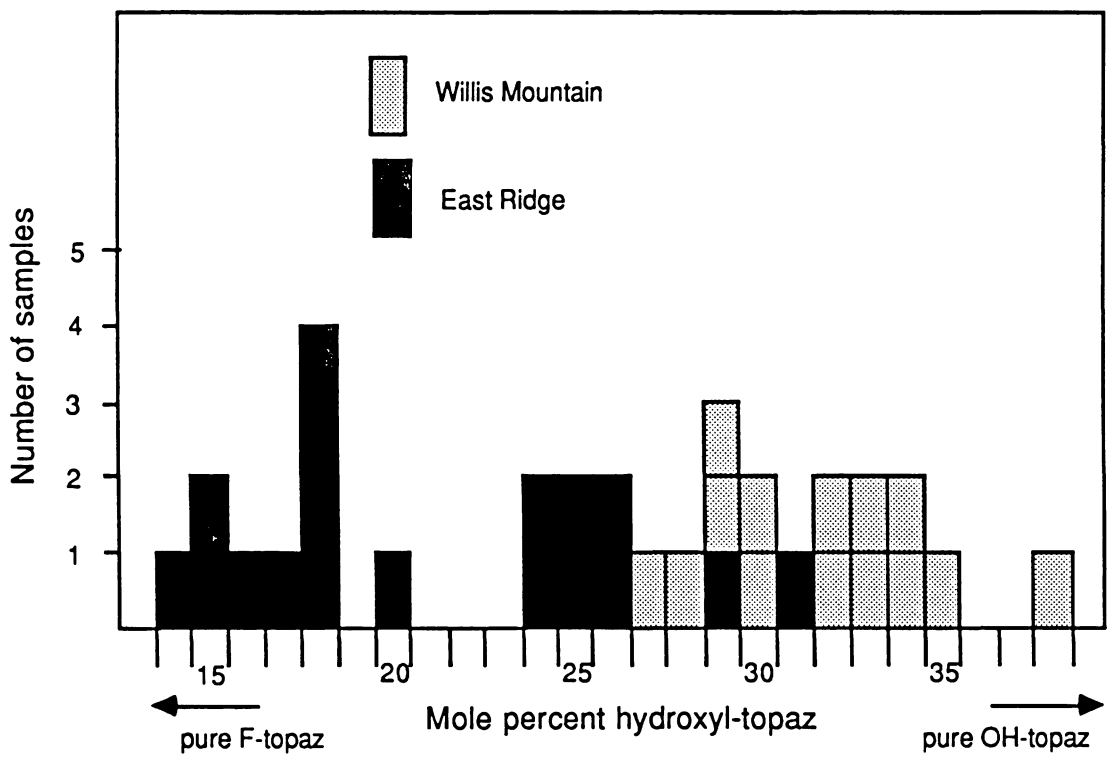

Figure 9: Graph of hydroxyl-topaz content in kyanite quartzite at Willis Mountain and East Ridge; 25 percent hydroxyl-topaz has the formula $Al_2SiO_4(OH)_{.50}F_{1.50}$.

Table 4: Modal abundances of minerals in quartz-muscovite schist at Willis Mountain (DW) and East Ridge (DE).

Mineral	DW30	DE43a	Average
Quartz	68.0	70.0	69.0
Muscovite	31.0	29.0	30.0
Hematite	1.0	1.0	1.0
Total	100.0	100.0	100.0

muscovite. Typically red iron oxides occur along the mica cleavage planes and zircon and rutile are accessory minerals.

Biotite-Amphibole Gneiss

A 123 meter long drill core of biotite-amphibole gneiss from the banks of Cattail Creek, 3 kilometers southeast of East Ridge (Figure 2) was examined as an example of the country rock surrounding the kyanite quartzite. The heterogenous gneiss (Table 5 and Figure 10) is greenish gray, nematoblastic and usually equigranular though garnet porphyroblasts appear in a few 10 centimeter thick zones. Numerous fold noses within the drill core attest to the highly deformed nature of the rocks. A one- to three-centimeter thick conformable seam of pyrite and magnesium-rich chlorite, with traces of calcite, were observed within the gneiss. Thin quartz-albite pegmatites are also present.

The gneiss generally consists of plagioclase, quartz, amphibole, biotite, and garnet. The coarse to fine-grained subhedral plagioclase comprises 45 percent of the gneiss and microprobe analysis reveals the compositions (Table 6) to range from albite to andesine with an average anorthite composition of 20 mole percent. Quartz, averaging 25 percent of the gneiss, is subhedral and between 0.01 to 1.0 millimeter in size; it has regular grain boundaries and often exhibits undulose extinction.

Nematoblastic amphiboles comprise 15 percent of the gneiss and have varying compositions (Table 7). Clear amphibole with straight extinction has a wide range of tetrahedral aluminum per formula unit and, classified according to Hawthorne (1971), ranges from anthophyllite to gedrite. Green pleochroic hornblende either coexists with anthophyllite, often rimming it (Figure 11), or occurs in samples with no other amphibole. Gedrite never appears in samples which contain anthophyllite or

Table 5: Modal abundances of minerals comprising biotite-amphibole gneiss from near Cattail Creek. 1000 counts.

Sample:	CC53	CC75	CC95	CC157	CC239	CC264	CC296	CC357	CC410
Minerals:									
Quartz	4.3	22.3	33.4	22.6	12.8	19.1	18.5	11.7	18.7
Plagioclase	24.8	42.6	46.1	47.2	44.7	13.2	53.7	24.3	41.3
Hornblende	0.0	0.0	0.0	18.3	32.1	0.0	0.0	49.6	13.8
Anthophyllite	34.2	0.0	0.0	2.1	3.6	2.8	0.0	7.1	6.3
Gedrite	0.0	11.4	0.0	0.0	0.0	0.0	8.1	0.0	0.0
Garnet	7.1	3.1	0.0	5.4	0.0	0.0	4.2	0.0	0.0
Biotite	12.0	10.1	6.7	0.0	3.8	0.0	14.0	2.9	17.1
Kyanite	0.0	0.0	3.1	0.0	0.0	0.0	0.0	0.0	0.0
Sillimanite	0.0	5.8	6.8	0.0	0.0	0.0	0.0	0.0	0.0
Staurolite	0.0	2.0	1.2	0.0	0.0	0.0	0.0	0.0	0.0
Chlorite*	14.1	0.0	0.0	0.0	0.0	46.7	0.0	0.0	0.0
Muscovite	0.0	0.0	0.0	0.0	0.0	0.9	0.0	0.0	0.0
Calcite	0.0	0.0	0.0	0.0	0.0	8.1	0.0	0.0	0.0
Opaques	3.1	1.6	1.3	1.8	1.6	9.2	1.3	4.1	2.2
Rutile	0.0	0.8	0.7	0.0	0.0	0.0	0.0	0.0	0.6
Other	0.4	0.3	0.7	2.6	1.4	0.0	0.2	0.3	0.0
Total	100.0	100.0	100.0	100.0	100.0	100.0	100.0	100.0	100.0
Plagioclase An%	27	4	5	28	29	14	18	28	20

*Only primary chlorite was counted.

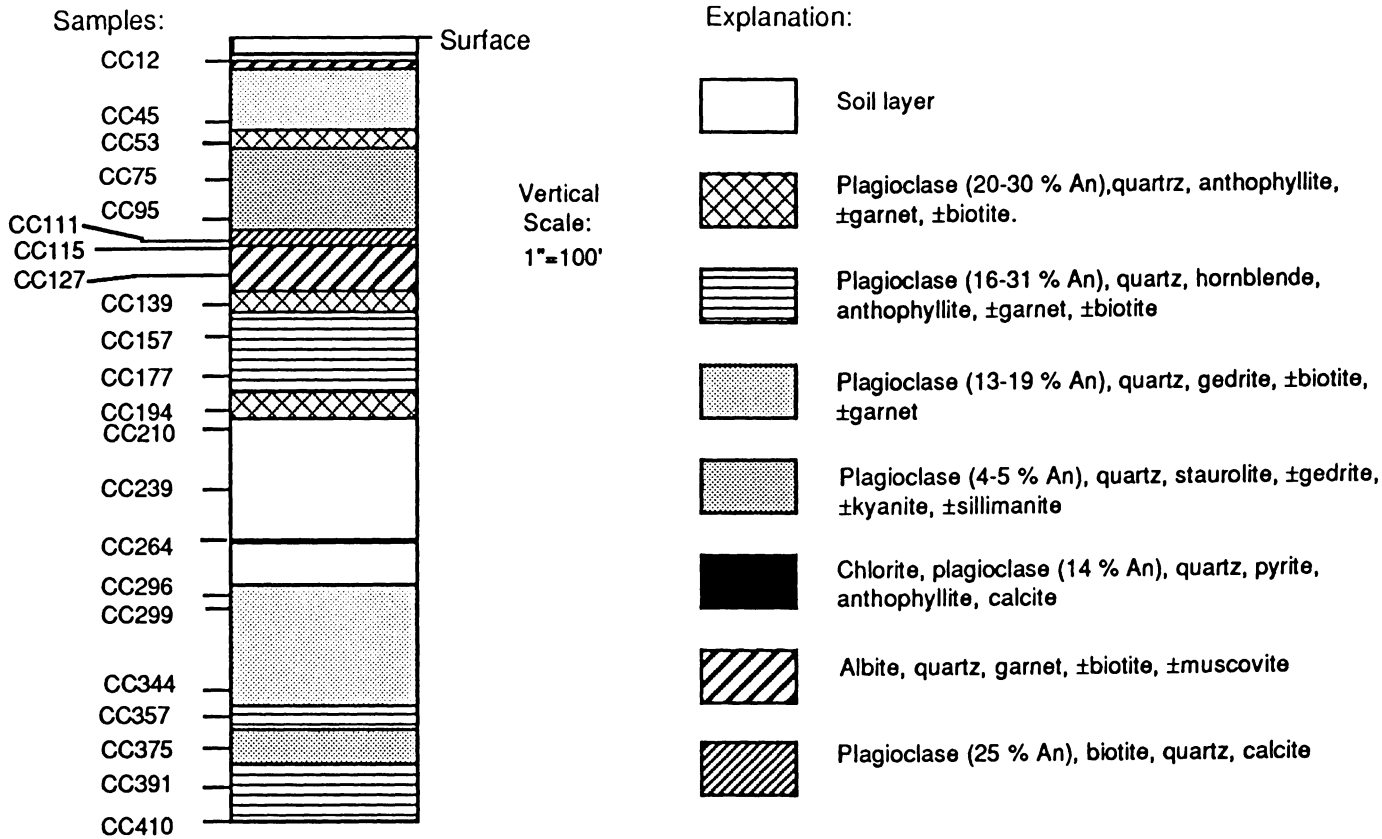

Figure 10: Log of drill core into biotite-amphibole gneiss at Cattail Creek.

Table 6: Representative microprobe analyses of feldspars (feld) from biotite-amphibole gneiss along Cattail Creek.

Sample #	CC12	CC53	CC95	CC210	CC357
Phase	feld	feld	feld	feld	feld
Grain#	1	4	4	13	9
SiO_2	64.60	58.70	64.31	62.34	60.95
Al_2O_3	22.79	23.92	19.77	23.47	24.32
TiO_2	.00	.02	.01	.01	.01
FeO*	.04	.01	.02	.04	.09
CaO	3.65	5.59	1.08	4.83	6.20
Na_2O	9.05	6.96	9.88	8.54	7.86
K_2O	.06	.04	.04	.04	.04
Total	100.19	95.24	95.11	99.27	99.47
Anorthite content	An_{17}	An_{29}	An_5	An_{23}	An_{30}

Table 7: Representative microprobe analyses of amphiboles from biotite- amphibole gneiss along Cattail Creek. Anthophyllite (anth), gedrite (ged), and hornblende (hbl) formulas are shown. Note the coexisting anthophyllite and hornblende in sample CC357.

Sample #	CC53	CC95	C296	CC357	CC357
Phase	anth	ged	ged	anth	hbl
Grain#	1	2	4	18	19
SiO_2	48.23	41.00	45.22	52.97	43.95
Al_2O_3	9.62	18.04	15.26	3.47	13.77
TiO_2	.23	.28	.20	.09	.70
FeO*	19.43	19.08	20.35	19.66	14.79
MgO	16.72	13.17	14.90	19.75	11.80
MnO	1.89	.41	.54	.58	.27
CaO	.84	.11	.36	.42	9.42
Na_2O	.95	2.03	2.08	.31	1.85
K_2O	.02	.02	.01	.01	.23
F	.10	.00	.13	.05	.07
Total	98.03	94.14	99.05	97.31	96.85
Si	7.00	6.19	6.51	7.64	6.50
Al	1.65	3.21	2.59	.59	2.40
Ti	.03	.03	.02	.01	.08
Fe*	2.36	2.41	2.45	2.37	1.83
Mg	3.62	2.96	3.20	4.25	2.60
Mn	.23	.05	.07	.07	.03
Ca	.13	.02	.06	.06	1.49
Na	.27	.59	.58	.09	.53
K	.00	.00	.00	.00	.04
OH	1.95	2.00	1.94	1.98	1.97
F	.05	.00	.06	.02	.03

*FeO represents total iron.

Figure 11: Photomicrograph of hornblende-rimmed anthophyllite surrounded by plagioclase and quartz in biotite-amphibole gneiss. Width of field: 1.1 mm.

hornblende. Exsolution textures were not observed in any of the amphiboles.

Figure 12 illustrates the varying chemical compositions of the amphiboles. Figure 12A shows a constant calcium content in the orthoamphiboles while the amount of tetrahedral aluminum ranges between 0 to 1.79 moles per formula unit. Robinson et al. (1971) postulated a gedrite-anthophyllite solvus which Spear (1980) inferred from natural assemblages to crest at 600 ± 25° C. The orthoamphiboles of this study must have equilibrated above that crest as they completely bridge the solvus. Other solvus-bridging anthophyllites and gedrites have been described by Robinson et al. (1971) in rocks with peak metamorphic conditions determined by Tracy et al. (1976) to be between 625 and 650° C and pressure approximately equal to 6 kilobars, and by James et al. (1978) in rocks with peak metamorphic conditions at 635° C and pressure between 3 and 6 kilobars. Figure 12A does show a solvus relationship between hornblende and the orthoamphiboles.

Figure 12B illustrates a direct relationship between amount of tetrahedral aluminum and sodium content in amphiboles. This is due to the so-called edenite substitution where $NaAl^{IV} \Leftrightarrow [\ ]\ Si$, whose common occurrence in gedrite has been documented by Robinson et al. (1971). Tschermak's substitution, where $Al^{VI}Al^{IV} \Leftrightarrow Mg\ Si$, also increases the amount of tetrahedral aluminum in the amphiboles.

Figure 12C shows an almost uniform Fe/(Fe+Mg) ratio for these amphiboles except for one extremely magnesium-rich amphibole occurring in the chlorite-pyrite vein. Gedrite and hornblende are generally slightly more magnesium-rich than anthophyllite but all are richer in magnesium than in iron, consistent with the description by Robinson et al. (1971) of magnesium-rich calcic amphibole-orthoamphibole pairs.

Biotite is present in most areas of the gneiss in concentrations up to five percent. It

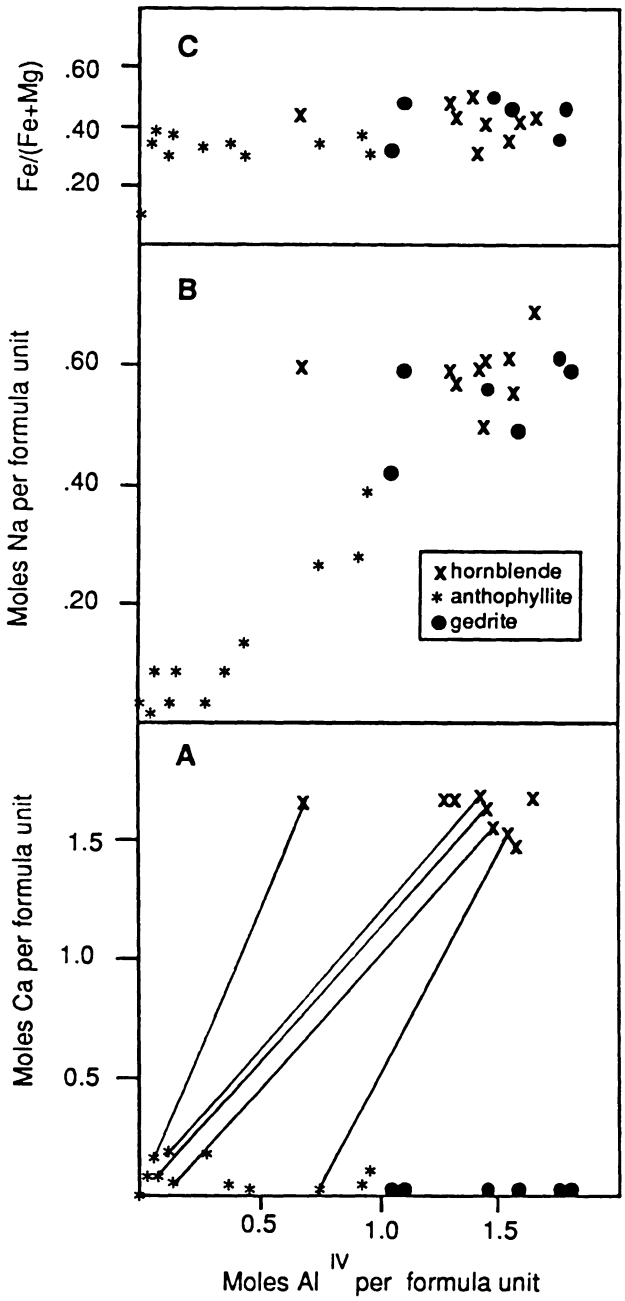

Figure 12: A: Number of moles of tetrahedral aluminum, *vs.* number of moles calcium per formula unit with lines drawn between anthophyllite and the hornblende rimming it., B: Number of moles of tetrahedral aluminum *vs.* number of moles sodium per formula unit, and C: Number of moles of tetrahedral aluminum *vs.* Fe/(Fe+Mg) in amphiboles in biotite-amphibole gneiss.

is lepidoblastic, small, light tan to light brown pleochroic flakes of magnesium-rich composition (Table 8). Like amphibole, it contains up to 0.1 moles of fluorine.

Garnets range from small anhedra to large (up to 1 centimeter in diameter) poikiloblasts with inclusions of quartz and chlorite. They exhibit little or no compositional zoning although, in one sample, a clear-rimmed garnet with a pink center showed a slight decrease in manganese from the center to the rim (0.73 to 0.67 moles of manganese per formula unit). Garnet composition (Table 9) is consistent throughout the gneiss and averages:

$$Fe_{1.90}Mg_{0.76}Mn_{0.19}Ca_{0.15}Al_{2.00}Si_{3.00}O_{12.00.}$$

Accessory minerals disseminated throughout the gneiss include apatite, zircon, rutile, ilmenite, and magnetite.

Staurolite and aluminosilicate appear in aluminum-rich zones of the biotite-amphibole gneiss and often coexist with gedrite. The staurolite occurs as rare, small, isolated crystals and lacks the frequently observed sieve texture. Microprobe analyses are given in Table 10. Kyanite and fibrolitic sillimanite appear, both separately and together, parallel to the rock foliation, in association with staurolite and gedrite. In one aluminous zone of the biotite-amphibole gneiss, fibrolitic sillimanite is altering from kyanite. The total combined amount of staurolite, sillimanite, and kyanite comprise less than one percent of the samples in which they occur.

Table 8: Representative microprobe analyses of biotite (bt) from biotite-amphibole gneiss along Cattail Creek.

Sample #	CC75	CC210	CC296	CC357	CC410
Phase	bt	bt	bt	bt	bt
Grain#	3	4	2	1	13
SiO_2	36.73	40.09	38.15	38.60	37.62
Al_2O_3	18.26	16.72	17.46	17.27	16.65
TiO_2	1.54	1.31	1.21	1.37	1.41
FeO*	13.66	10.41	13.88	12.09	15.32
MgO	14.60	18.41	15.04	16.04	13.55
MnO	.04	.03	.06	.04	.13
CaO	.10	.02	.01	.02	.04
Na_2O	.53	.41	.31	.39	.19
K_2O	7.36	8.44	8.16	8.04	8.12
F	.09	.42	.14	.25	.15
Total	92.23	96.26	94.42	94.11	93.18
Si	2.77	2.87	2.82	2.84	2.85
Al	1.62	1.41	1.52	1.50	1.49
Ti	.08	.07	.07	.08	.08
Fe*	.82	.62	.86	.74	.97
Mg	1.64	1.96	1.66	1.76	1.53
Mn	.00	.00	.00	.00	.01
Ca	.01	.00	.00	.00	.00
Na	.08	.06	.04	.06	.03
K	.71	.77	.77	.76	.78
OH=2-F	1.96	1.90	1.97	1.94	1.96
F	.04	.10	.03	.06	.04

*FeO represents total iron.

Table 9: Representative microprobe analyses of garnet (gar) from biotite-amphibole gneiss along Cattail Creek.

Sample #	CC45	CC75	CC157	CC296	CC357
Phase	gar	gar	gar	gar	gar
Grain#	1	1	9	1	4
SiO_2	38.53	38.64	39.53	38.75	39.83
Al_2O_3	20.97	21.06	20.97	20.74	20.99
TiO_2	.10	.09	.11	.02	.08
FeO*	30.54	29.80	30.60	29.77	26.57
MgO	6.23	6.31	7.32	6.06	6.51
MnO	1.17	3.15	1.27	2.55	2.06
CaO	.88	.20	3.43	1.71	3.66
Total	98.42	99.25	103.23	99.60	99.70
Si	3.06	3.05	3.01	3.05	3.09
Al	1.96	1.96	1.88	1.93	1.92
Ti	.01	.01	.01	.00	.00
Fe*	2.03	1.97	1.95	1.96	1.72
Mg	.74	.74	.83	.71	.75
Mn	.08	.21	.08	.17	.14
Ca	.07	.02	.28	.14	.28

*FeO represents total iron.

Table 10: Representative microprobe analyses of staurolite (staur), calculated on the basis of 48 oxygens, and kyanite (ky), calculated on the basis of 5 oxygens, from biotite-amphibole gneiss along Cattail Creek.

Sample #	CC75	CC75	CC95	CC95	CC95
Phase	staur	staur	staur	staur	ky
Grain#	10	11	1	5	3
SiO_2	28.57	28.43	28.21	28.37	36.95
Al_2O_3	48.14	48.80	49.26	48.53	58.76
TiO_2	.72	.71	.47	.49	.00
FeO*	13.31	13.10	12.98	13.01	.89
MgO	3.05	3.02	2.63	2.70	.06
MnO	.23	.22	.12	.14	.00
ZnO	.60	.62	.76	.75	.00
Total	94.62	94.90	94.44	93.99	96.66
Si	8.23	8.16	8.13	8.21	1.03
Al	16.34	16.50	16.72	16.56	1.94
Ti	.16	.15	.10	.11	.00
Fe*	3.21	3.14	3.13	3.15	.02
Mg	1.31	1.29	1.13	1.17	.00
Mn	.06	.05	.03	.03	.00
Zn	.13	.13	.16	.16	.00
OH=F-2	3.97	3.98	3.98	3.95	.00

*FeO represents total iron.

Conditions of Metamorphism

Peak metamorphic conditions of the Willis Mountain area rocks were calculated from the garnet-biotite geothermometer of Ferry and Spear (1978) and the garnet-rutile-aluminosilicate-ilmenite-quartz (GRAIL) geobarometer of Bohlen et al. (1983). Table 11 lists those results and Appendix I presents the calculations in detail. Garnet and biotite assemblages in samples CC75, CC296, and CC357 all yield a calculated temperature of 600° C. Calculations for CC45 result in a temperature of 665° C. GRAIL assemblages in sample CC75 yield calculated pressures of 6.3 and 6.5 kilobars using a temperature of 600° C. Two other samples, CC157 and CC344 contain garnet plus rutile, not the complete GRAIL assemblage, and they indicate minimum peak metamorphic pressures of between 5.0 and 6.2 kilobars.

Figure 13 is a pressure-temperature diagram depicting some pertinent phase equilibria. The abundant kyanite at Willis Mountain and East Ridge requires kyanite-field pressures and temperatures; sillimanite in the biotite-amphibole gneiss may be caused by a slightly higher temperature of metamorphism to the east of Willis Mountain and East Ridge or could be due to decompression during retrograde metamorphism. Abundant paragonite (0.80-0.85 Na) and the absence of albite in the kyanite quartzite indicate that pressure and temperature conditions where paragonite plus quartz react to form albite plus aluminosilicate plus vapor were not reached. The wide range of tetrahedral aluminum content in the orthoamphiboles of the biotite-amphibole gneiss indicates that the temperature of the crest of the anthophyllite-gedrite solvus, $600 \pm 25°$ C (Spear, 1980), was exceeded. Conditions where pyrite incongruently melts to form pyrrhotite and sulfur melt clearly were not reached.

Embayed, rounded topaz of varying and sometimes zoned compositions (Figure 14)

Table 11: Calculated pressure and temperature of peak metamorphism of biotite-amphibole gneiss.

A: garnet-biotite geothermometry using method of Ferry and Spear (1978), calculated for P=6000 bars:

Sample	Temperature (° C)
CC45	665
CC75	600
CC296	600
CC357	585, 600

B: GRAIL (garnet-rutile-aluminosilicate-ilmenite-quartz) geobarometry using method of Bohlen (1983), calculated for T=600° C.

Sample	Pressure (kb)
CC75	6.3 6.5
CC157*	>6.2 >5.5 >5.0
CC344*	>5.8

*These samples only contain garnet + rutile, not the complete GRAIL assemblage, and yield a minimum pressure.

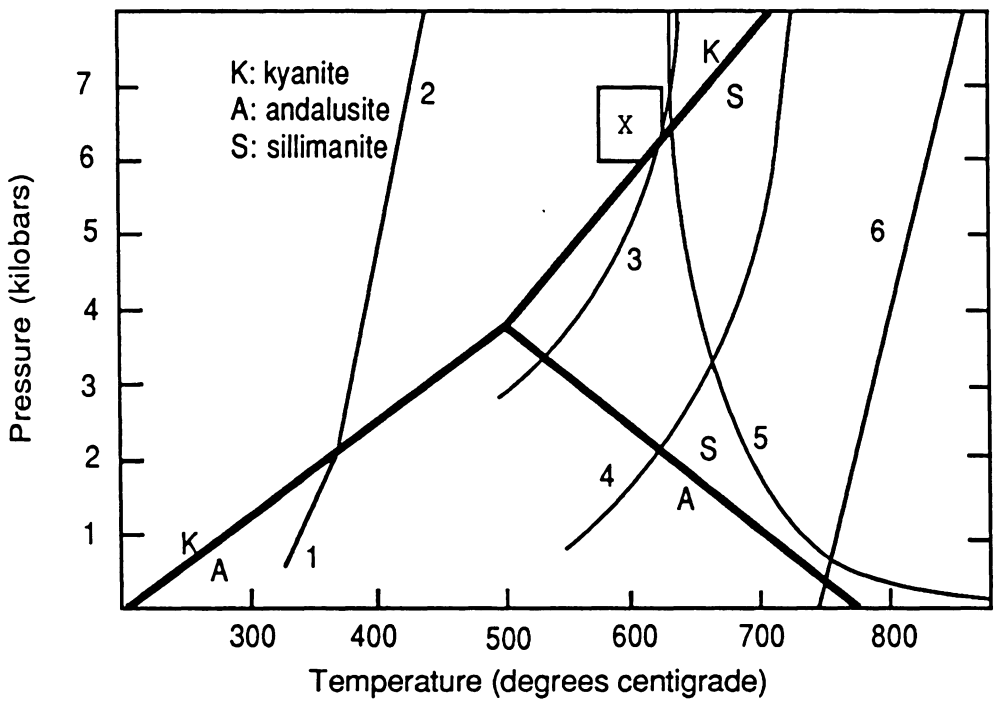

Figure 13: Pressure-temperature diagram depicting univariant curves: 1: pyrophyllite = andalusite + quartz + vapor (Haas and Holdaway, 1973), 2: pyrophyllite = kyanite + quartz + vapor (Haas and Holdaway, 1973), 3: paragonite + quartz = albite + aluminosilicate + vapor (Chatterjee, 1972), 4: muscovite + quartz = k-feldspar + aluminosilicate + vapor (Chatterjee and Johannes, 1974), 5: granite minimum melt (Yoder and Tilley, 1962), and 6: pyrite = pyrrhotite + sulfur melt (Barton, 1974). The aluminosilicate phase relations are from Holdaway (1971). The "x" marks the maximum pressure and temperature of metamorphism (6.5 kb, 600° C) of the Willis Mountain and East Ridge kyanite quartzite calculated from geothermo-barometric models and the enclosing box encompasses estimated errors.

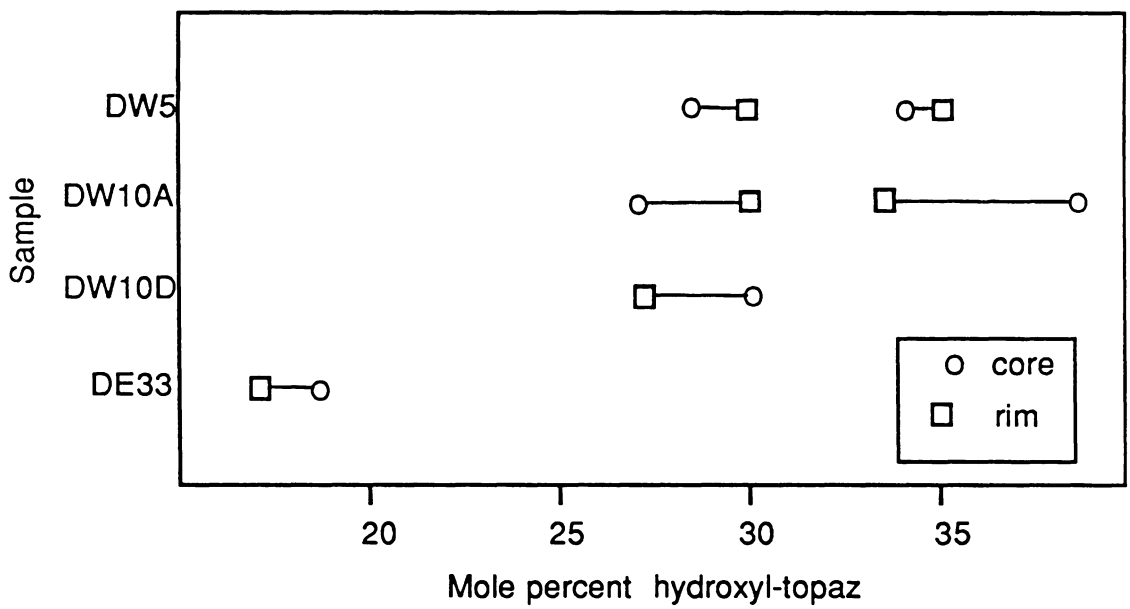

Figure 14: Compositional zoning of topaz in terms of hydroxyl-topaz component ($Al_2SiO_4[OH]_2$) in the kyanite quartzite at Willis Mountain (DW) and East Ridge (DE).

suggest resorption of topaz. Barton (1982a, b) has demonstrated experimentally the relationship between the pressure, temperature and fluorine content of topaz formed in the presence of aluminosilicate, quartz, and vapor. Figure 15 is Barton's (1982b) pressure-temperature diagram contoured for hydroxyl-topaz ($Al_2SiO_4[OH]_2$) content with the composition range of topaz from Willis Mountain and East Ridge superimposed upon it. Most of the topazes analyzed have compositions greater than 23 percent hydroxyl-topaz (Figure 9) which is consistent with the pressure and tamperature of metamorphism. However, some topaz on East Rdge has between 14 and 20 percent hydroxyl-topaz component. Several possibilities could account for this:
1) If P_{H2O} were much less than P_{total} the topaz would become more fluorine-rich; except, under these conditions, paragonite + quartz would react to form albite + aluminosilicate + vapor; two of the three samples containing fluorine-rich topaz (DE33, DE40) contain paragonite and no albite is present in these or any other samples from the kyanite quartzite, 2) isothermal decompression during retrograde metamorphism could increase the fluorine content of topaz though it should also be accompanied by the breakdown of paragonite as discussed previously, 3) the topaz could represent relict disequilibrium compositions.

The diversity of the amphiboles is a function of variations in the bulk composition of the biotite-amphibole gneiss. Gedrite occurs in zones rich in alumina and poor in calcium and coexists with staurolite, kyanite and/or sillimanite, and albite. Anthophyllite, where it occurs in the absence of hornblende, usually coexists with a plagioclase containing 20-25 percent anorthite. Where hornblende occurs, either as the only amphibole or as rims around anthophyllite, the coexisting plagioclase is generally 25-30 percent anorthite and the rock is in general more calcic than those that are anthophyllite-bearing or gedrite bearing.

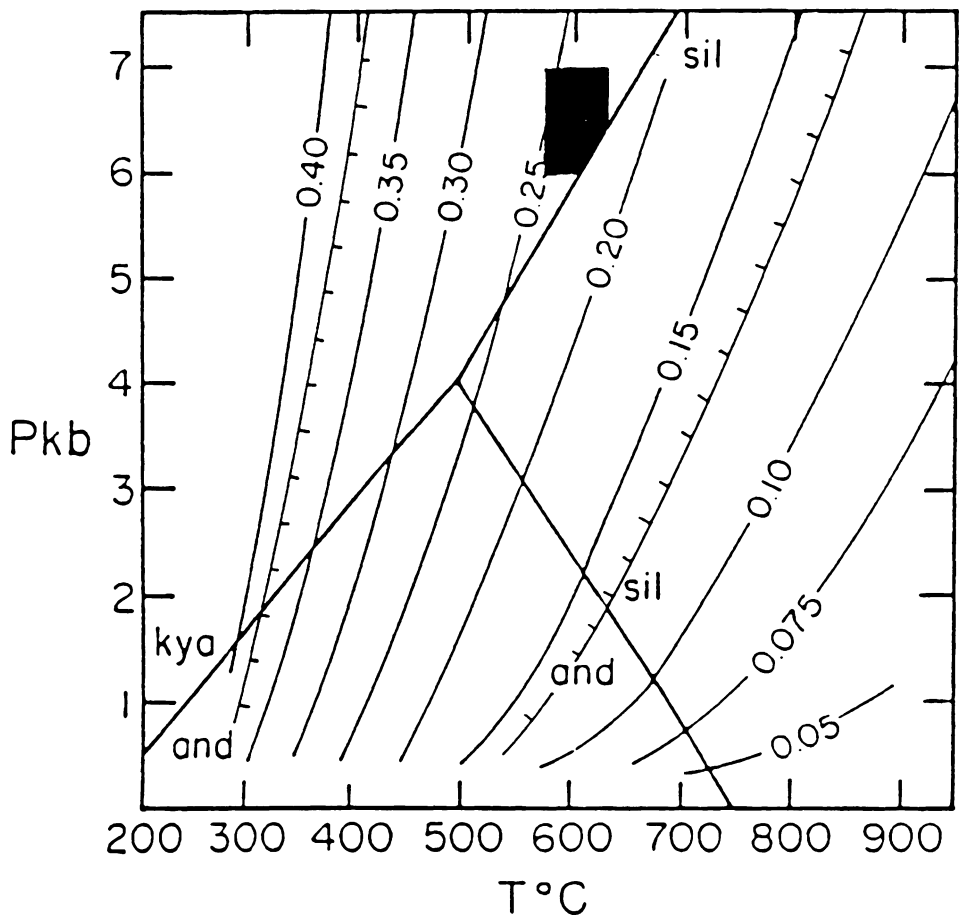

Figure 15: Calculated isopleths of hydroxyl-topaz in topaz solid solution coexisting with aluminosilicate and quartz as a function of pressure and temperature (Barton, 1982b) with topaz compositions from Willis Mountain-East Ridge kyanite quartzite occurring between the hatchured lines. The solid box represents pressure and temperature of peak metamorphism.

Comparisons With Other High-Alumina Rocks

A comparison of the Willis Mountain-East Ridge kyanite quartzite to the aluminum-rich rocks discussed in the introduction leads to the following conclusions: (1) The Willis Mountain and East Ridge kyanite quartzite is not a metamorphosed bauxite deposit because the kyanite quartzite contains far more silica and sulfide than do bauxite deposits (Overstreet, 1964; Patterson, 1967; Norton, 1973). (2) The kyanite quartzite does not represent a china clay deposit because china clays are either intimately associated with the granitic rock from which they were derived and are not stratiform or they occur within sedimentary rocks (Highley, 1984) whereas the kyanite quartzite occurs within metamorphosed volcanic rocks. (3) Striking similarities exist between the host rock, bulk composition, and major and accessory mineralogy of the Willis Mountain and East Ridge kyanite quartzite and those of the volcanic-hosted high-alumina rocks of the North Carolina, South Carolina, and Georgia Piedmont Province described by Espenshade and Potter (1960), Zen (1961), Sykes and Moody (1978), Carpenter and Allard (1980, 1982), Schmidt (1982, 1985a, b), and Feiss (1985a).

Figure 16 is a map showing occurrences of high-alumina deposits in the southeastern United States. Where they occur within areas of low grade metamorphism, these high-alumina rocks contain quartz, pyrophyllite, kaolinite, sericite, pyrite, and rutile with varying amounts of andalusite, diaspore, and topaz. As metamorphic grade increases, particularly in the Kings Mountain Belt and the southernmost portion of the Carolina Slate Belt, kyanite replaces pyrophyllite, kaolinite, or andalusite and muscovite and/or paragonite is present rather than sericite. A few of the high-alumina deposits contain trace minerals such as barite, lazulite, and zunyite. Host rocks are always

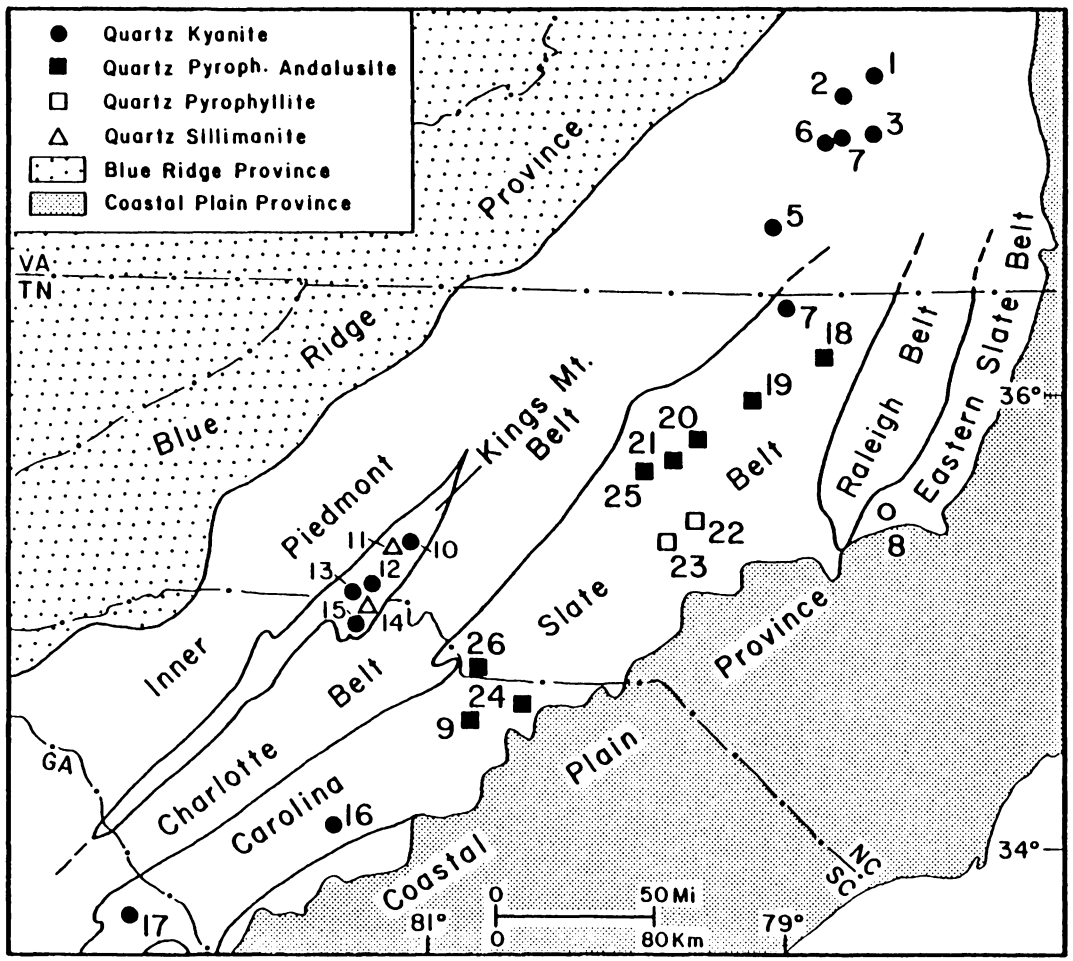

Figure 16: Map of aluminosilicate deposits in the southeastern United States (after Espenshade and Potter, 1960; Williams, 1978). Numbers correspond with deposits described in Appendix II.

metamorphosed volcanic or volcaniclastic rocks and their compositions range from felsic to intermediate.

The origin of the North Carolina, South Carolina, and Georgia aluminosilicate deposits has been the subject of keen debate but the current, widely-held view (Spence, 1975; Carpenter and Allard, 1980,1982; Schmidt, 1982, 1985a, b; Feiss, 1985a, b) is that they represent metamorphosed zones of hydrothermal alteration which occured contemporaneously with calc-alkaline volcanism, probably in a compressive tectonic regime. Conley (1962) has defined the zoning around these deposits as consisting of an inner high-alumina zone surrounded by a potassic, or alkali-rich zone, and then by a siliceous or a magnesium- and iron-enriched zone. Distinct hydrothermal alteration zones are more easily perceived in deposits of lowest metamorphic grade such as those at Glendon, Hillsborough, and Snow Camp, all in North Carolina. They have inner zones composed of quartz-pyrophyllite ± andalusite surrounded by sericitic zones which, in turn are surrounded by zones of chlorite and occasional chloritoid that gradually decrease in abundance away from the center of the deposit.

Several of these high-alumina alteration zones in the southeastern United States contain gold. The Brewer, Haile, and Nesbit gold mines are located in the Carolina Slate Belt near the North Carolina-South Carolina boundary. The Brewer mine contains vein gold in the highly altered silicified inner zone (Worthington et al., 1980; Butler, 1985). The Nesbit mine contains gold within dessiminated pyrite in the pyrophyllitic zone (McKee, 1985), and the Haile mine, the most productive gold mine in the eastern United States, contains vein gold as well as gold within pyrite (Spence et al., 1980).

Figure 17 compares the mineralogy and the bulk composition as a function of Al_2O_3-SiO_2-[Na_2O+K_2O] of the Willis Mountain and East Ridge kyanite quartzite to two representative North Carolina pyrophyllite deposits, the Glendon and the Hillsborough.

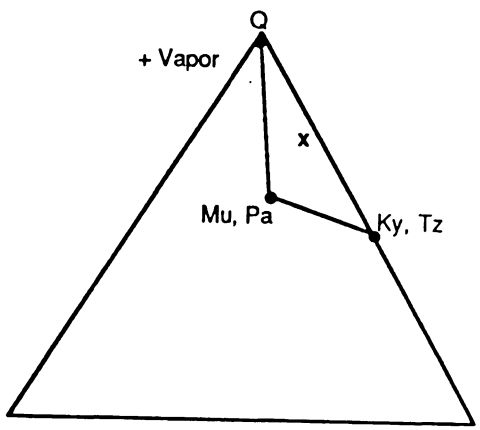

Willis Mountain
Kyanite Quartzite

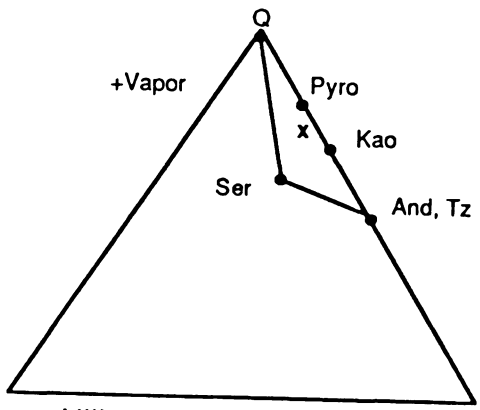

Hillsborough Pyrophyllite
Deposit

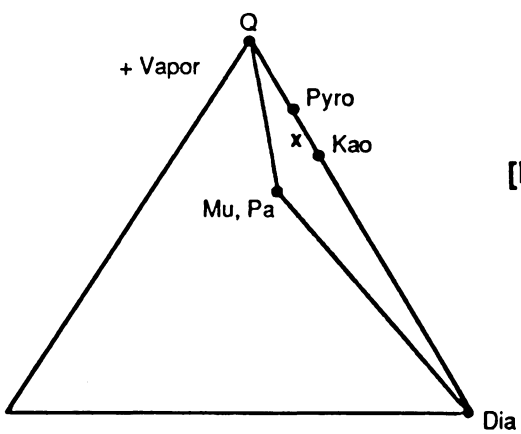

Glendon Pyrophyllite
Deposit

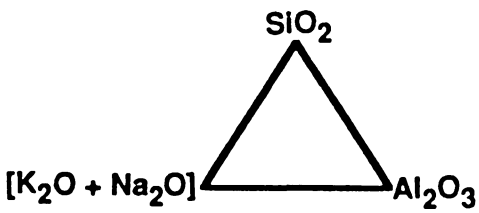

And = Andalusite
Dia = Diaspore
Kao = Kaolinite
Ky = Kyanite
Mu = Muscovite
Pa = Paragonite
Q = Quartz
Ser = Sericite
Tz = Topaz

x = Bulk composition

Figure 17: Mineralogy and bulk composition as a function of SiO_2-Al_2O_3-$[Na_2O+K_2O]$ for Willis Mountain, Virginia kyanite quartzite, Glendon, North Carolina pyrophyllite deposit (Klein, 1985), and Hillsborough, North Carolina pyrophyllite deposit (Sykes and Moody, 1978).

Since all deposits contain pyrite and rutile as the only other abundant phases, it is obvious that the deposits are quite similar and that the major difference is one of metamorphic grade.

Microprobe analyses of pyrite samples from kyanite quartzite at Willis Mountain and East Ridge, the biotite-amphibole gneiss along Cattail Creek, the kyanite quartzite at Graves Mountain, Georgia, the kyanite quartzite at Henrys Knob, South Carolina, and the pyrophyllite schist at Glendon, North Carolina indicated them to be stoichiometric FeS_2. Nickel, cobalt, manganese, selenium, and arsenic showed no significant concentrations at or above the 500 ppm level, which was the approximate limit of detection under the conditions of analysis.

The geometry of the Willis Mountain and East Ridge kyanite quartzite is similar to some high-alumina alteration zones in the Carolinas and Georgia but it differs from others. The Bowlings Mountain and Hillsborough deposits in North Carolina and the Graves Mountain deposit in Georgia all have stratiform alteration zones analogous to the Willis Mountain and East Ridge kyanite quartzite but the high-alumina deposits of Pilot Mountain and Fox Mountain in North Carolina and the Brewer mine, South Carolina have alteration zones which tend to cut across stratigraphic layers and are enclosed by highly silicified zones. Schmidt (1985a, b) interprets these patchy, irregular deposits as porphyry-type alteration systems similar to those at Butte, Montana and El Salvadore, Chile. He interprets the stratiform variety as shallow-seated alteration zones below hot springs and fumaroles.

A comparison of the mineralogy, bulk chemistry, and deposit geometry of the Willis Mountain and East Ridge kyanite quartzite to shallow-seated hydrothermal deposits in North Carolina, South Carolina, and Georgia suggests that the protolith of the Willis Mountain and East Ridge kyanite quartzite formed by similar, if not identical

hydrothermal processes.

Several active hot springs in Japan and Taiwan are altering Pliocene and Pleistocene volcanic rocks to high-alumina mineral assemblages. The Tatun volcanic region on Taiwan contains an 18 kilometer by 3 kilometer zone of 13 hot spring areas within andesitic and basaltic lavas, pyroclastic rocks, and detritus (Chen, 1970). Most of the hot springs issue acid sulfate-chloride waters with maximum temperatures reaching 240° C and pH ranging from 3.9 to 6.7. Common minerals in the shallow, most intensely altered zones include alunite, kaolinite, halloysite, α-cristobalite, and α-tridymite; deeper, less acidic zones contain kaolinite, halloysite, pyrite, sericite, chlorite, and epidote. Chlorite and calcite occur in partly or highly altered rocks at depths, indicating a higher pH in deeper zones.

The Otake geothermal area on north-central Kyushu Island, Japan is the site of a power plant which has produced electricity from hydrothermal energy since 1967. Variation in fluid pH produces different types of alteration assemblages within a 1000 meter thick pile of homogenous andesitic volcanic rocks. Hayashi and Yamasaki (1974) have divided stratiform zones of hydrothermal alteration according to their mineral assemblages (Table 12). The highly silicified zones (Type I) are usually only a few meters wide, are created by neutral, alkaline, and acidic waters, and occur at various depths but are often surrounding hydrothermal vents. Type II alteration occurs at shallow levels, less than 360 meters below the surface, in acidic waters (pH ranges from 1.5 to 4.5), and often with minerals of Type III but never with minerals of Type V. Type III assemblages appear in zones more than 1000 meters thick at levels beginning at the surface, and in slightly less acidic waters than Type II (pH ranges from 2 to 5). Type IV assemblages can be formed under a wide range of pH values, from 4 to 8, and sometimes contains interstratified chlorite and montmorillonite. Type V assemblages are

Table 12: Types of alteration assemblages at Otake geothermal area, Kyushu Island, Japan (Hayashi and Yamasaki, 1974).

Type I: silica minerals such as amorphous silica, low-cristoblalite, low-tridymite, and low-quartz.

Type II: alunite, jarosite, and similar sulfates such as halotrichite and melanterite.

Type III: aluminosilicate clay minerals such as halloysite, kaolinite, dickite, and pyrophyllite.

Type IV: aluminosilicate clay minerals such as montmorillonite, sericite, and magnesium-rich chlorite.

Type V: Zeolites such as heulandite and laumontite, wairakite, and alkali-feldspar.

Other minerals present include epidote, diaspore, anhydrite, gypsum, rutile, pyrite, and native sulfur.

caused by neutral to weakly alkaline fluids and appear in the hottest parts of the geothermal system. In the southern area of Otake where fluids are mostly acidic, Types II, III, and IV dominate but in the northern area where fluids are more alkaline, much thicker Type V alteration zones are present.

In all likelihood, the geological processes forming the protoliths of quartz-pyrophyllite rocks at places like Hillsborough and of kyanite quartzite at Willis Mountain and East Ridge were quite similar to the active hydrothermal alteration processes at Tatun and Otake. Table 13 compares the bulk rock geochemistry of kyanite quartzite from Willis Mountain to several other high-alumina deposits.

Many stratiform acidic hydrothermal alteration zones are found in the United States and throughout the world. Iwao (1949), Iwao et al. (1969), Tanaguchi et al. (1978), and Togashi et al. (1978) describe quartz, alunite, and pyrophyllite bearing rocks with accessory rutile, hematite, pyrite, and topaz scattered throughout the entire length ofJapan and they attribute their origin to hydrothermal alteration of volcanic rocks with ages ranging from late Mesozoic to Quaternary. Prakash et al. (1970) describe the lens-shaped Berwar pyrophyllite and diaspore deposit of Jhansi district, Uttar Pradesh, India as a hydrothermal alteration zone. Bartlett (1983) attributes the origin of a quartz-alunite-clay alteration zone at the Sugarloaf prospect, San Luis Hills, Conejos and Costilla Counties, Colorado to near-surface hydrothermal activity in intermediate volcanic rocks and he reports a temperature of homogenization from fluid inclusion data of approximately 250° C. Hofstra (1983) describes the NG alunite area in the southern Wah Wah range, southwestern Utah (the largest alunite deposit in the United States), as a large, funnel-shaped, zoned body formed by hydrothermal vapor-dominated activity in calc-alkaline ignimbrites and he reports homogenization temperatures between 275 and 325° C. Schreyer (1982) attributes the origin of fuchsite-andalusite-corundum rocks at

Table 13: Bulk Rock Chemistry of Some Hydrothermally Altered Rocks in Virginia, North Carolina, South Carolina, Newfoundland, and Japan.

	1	2	3	4	5	6	7
SiO_2	68.71	73.56	68.70	63.93	56.86	40.98	63.89
Al_2O_3	27.61	17.01	23.90	28.28	34.05	21.14	30.00
Fe_2O_3	0.57	0.00	0.00	0.29	0.31	1.39	0.11
FeO	0.04	5.25	0.65	0.14	n.r.	n.r.	n.r.
MgO	0.14	0.01	<0.05	0.02	0.34	n.r.	0.07
CaO	0.41	0.00	0.11	0.11	0.34	n.r.	0.00
Na_2O	0.00	0.00	0.46	tr.	0.24	1.02	0.16
K_2O	0.14	0.00	0.32	0.02	tr.	3.34	0.95
H_2O-	0.04	0.01	n.r.	n.r.	n.r.	0.05	n.r.
H_2O+	0.32	0.12	n.r.	n.r.	n.r.	7.86	n.r.
TiO_2	1.02	0.48	0.55	0.31	0.90	n.r.	0.18
CO_2	0.02	0.01	n.r.	n.r.	n.r.	n.r.	n.r.
P_2O_5	0.32	0.11	n.r.	n.r.	n.r.	n.r.	n.r.
F	0.21	n.r.	n.r.	n.r.	n.r.	n.r.	n.r.
S	n.r.	4.62	n.r.	n.r.	n.r.	19.27*	n.r.
MnO	0.00	0.00	n.r.	n.r.	n.r.	n.r.	n.r.
L.O.I.	n.r.	n.r.	4.85	6.14	6.92	n.r.	5.10
Total	99.55	101.18	99.47	99.24	99.96	95.05	100.41

n.r. = not reported
tr. = trace (<.01%)
* reported as SO_3

1. Willis Mt., Va. kyanite quartzite (Espenshade and Potter, 1960).
2. Henry Knob, S.C. kyanite quartzite (Espenshade and Potter, 1960).
3. Glendon, N.C. pyrophyllite deposit (Klein, 1985).
4. Hillsborough, N.C. pyrophyllite deposit (Sykes and Moody, 1978).
5. Udago, Yamaguchi Prefecture, Japan pyrophyllite deposit (Iwao and Udagawa, 1969).
6. Nishina, Izu Peninsula, Japan alunite deposit (Iwao, 1949).
7. Foxtrap pyrophyllite mine, Avalon Peninsula, Newfoundland (Papezik and Keats, 1978).

O'Briens, Zimbabwe to metamorphism of a near-surface hydrothermal alteration zone within ultramafic rocks and he suggests that chromium-rich ultramafic rocks may be the source for chromium in the fuchsite. He also suggests a hydrothermal mode of origin for the controversial (Schreyer and Chinner, 1966) kyanite quartzite at Big Rock, Rio Arriba County, New Mexico.

Discussion

Kyanite Quartzite As Hydrothermal Alteration Zone

It is fairly easy to "look through the metamorphism" of the rocks in the Willis Mountain and East Ridge area and draw approximate analogies between them and the hydrothermally altered rocks at Otake, Japan. Type I alteration is not seen directly at Willis Mountain or East Ridge for two possible reasons: Type I alteration at the surface (siliceous sinter) may have been eroded before burial or after exposure during this erosional cycle, and the abundant quartz veins, frequently rich in pyrite and rutile, cross-cutting the kyanite quartzite and the biotite-amphibole gneiss may represent Type I silica remobilized during metamorphism. However, Espenshade and Potter (1960) report massive layers of barren quartzite up to 3.3 meters thick which may once have been siliceous sinter present at Woods Mountain. Assemblage zones of Type II and Type III alteration, frequently admixed at Otake, probably composed the protolith for the kyanite quartzite. Kaolinite (as well as halloysite or dickite) would have produced pyrophyllite during early metamorphism by the reaction (Haas and Holdaway, 1973):

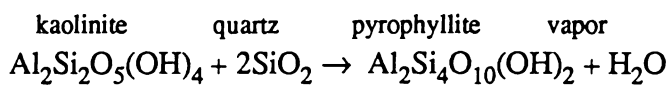

And as metamorphism progressed pyrophyllite would have produced kyanite by the reaction (Figure 12):

$$\underset{\text{pyrophyllite}}{Al_2Si_4O_{10}(OH)_2} \rightarrow \underset{\text{kyanite}}{Al_2SiO_5} + \underset{\text{quartz}}{SiO_2} + \underset{\text{vapor}}{H_2O}.$$

Alunite is formed in near-surface areas where H_2S oxidizes to SO_4^{2-} and frequently coexists with pyrite, but is not stable above approximately 400° C. (Hemley et al., 1969). Had alunite ever been present in the protolith it would have decomposed during metamorphism possibly by the following reaction:

$$\underset{\text{alunite}}{KAl_3(SO_4)_2(OH)_6} + \underset{\text{quartz}}{SiO_2} \rightarrow \underset{\text{muscovite}}{KAl_3Si_3O_{10}(OH)_2} + \underset{\text{vapor}}{H_2SO_4}.$$

Paragonite may have been similarly produced by the breakdown of natroalunite, $NaAl_3(SO_4)_2(OH)_6$. Conversely, if alunite or natroalunite were not present in the kyanite quartzite protolith, muscovite and paragonite may simply be the result of sericite increasing in grain size during metamorphism. Rutile, pyrite, and hematite, accessory minerals within the kyanite quartzite, are present in the altered rocks at Otake. Topaz, although not present at Otake, is present in other Japanese hydrothermal alteration deposits (Iwao, 1949).

Type IV alteration is represented by the quartz-muscovite schist, sericite becoming muscovite during metamorphism by an increase in grain size. The interstratified chlorite and montmorillonite at Otake may be analogous to chloritoid in partially altered rocks surrounding quartz pyrophyllite deposits of lower greenschist metamorphic grade in the Carolina Slate Belt and to staurolite in the biotite-amphibole gneiss of amphibolite metamorphic grade in the Willis Mountain and East Ridge area. The amphiboles within

the biotite-amphibole gneiss probably represent three different intensities of alteration: Zones containing anthophyllite and/or hornblende may represent a metamorphosed protolith that did not experience hydrothermal alteration and zones containing staurolite, gedrite, and aluminosilicates probably represent a metamorphosed partial Type III or IV hydrothermal alteration zone. Chlorite in Type V alteration zones at Otake is Mg-rich as is the chlorite in the biotite-amphibole gneiss

A Model for Stratiform Hydrothermal Alteration

Hydrothermal activity is common in regions of active or recently active volcanism and alteration type depends upon a wide variety of factors, the most important of these being temperature, pressure, fluid composition, original rock composition, rate of fluid flow, and permeability of the rocks (Ellis and Mahon, 1977). Most fluids have a meteoric source, as indicated by stable isotope data, though some magmatic fluids may also be present (Henley and Ellis, 1983). Figure 18 is a proposed model of the type of hydrothermal alteration system which probably created the protolith of the stratiform kyanite quartzite at Willis Mountain. A subvolcanic pluton is a the likely source of heat even though evidence for plutonic rocks in the Willis Mountain and East Ridge area is absent. The entire Chopawamsic volcanic belt has been thrust faulted (Pavlides et al.,1982) and any evidence for underlying plutons may have been lost at the time of faulting. An impermeable, silicified rock layer, probably between 1 and 1.5 kilometers deep (Facca and Tonani, 1967), generally confines the hydrothermal circulation. Occasionally, when hot, pressured fluids escape through fractures in the impermeable layer, boiling partitions the fluid into a basic, saline liquid phase and into an acidic, volatile-rich steam phase. The alkaline, saline liquid is enriched in KOH, KCl, NaOH,

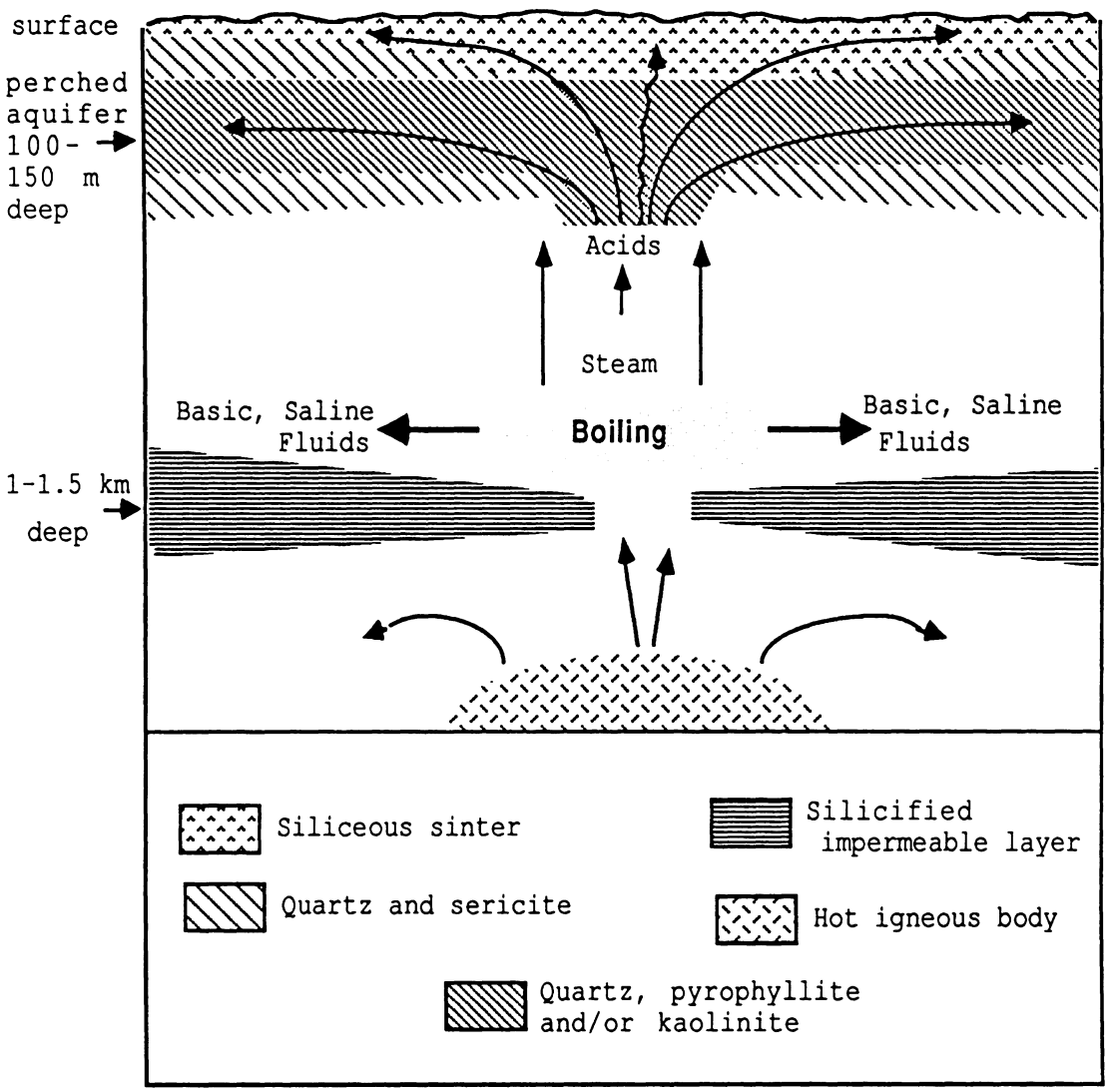

Figure 18: Model of stratiform acidic hydrothermal alteration system. Boiling partitions the fluid into an acidic vapor phase and an alkaline liquid phase. Where hydrothermal fluids reach the surface, hot springs, fumaroles, and mud pots occur. Adapted from Henley and Ellis (1983).

NaCl, and $CaCO_3$, which are more soluble in the liquid phase, and it moves laterally through the rock. The acidic vapor phase is enriched in SO_2, HCl, H_2CO_3, HF, and H_3BO_3 ,which are more volatile, and it rapidly travels upward through fractures and fissures (White et al., 1971; Ellis and Mahon, 1977; and Burt, 1981). If this process occurs in a submarine environment, seawater, which is slightly alkaline, quickly neutralizes the acidic fluid, limiting extensive alteration. But if this process occurs in a subaerial environment, the fluid remains acidic until it interacts with the wall rockcausing alteration.

Arnorsson (1978) has demonstrated that calcite precipitates when geothermal fluids flash to steam as the pH is raised by the loss of acidic volatiles. The 8.1 percent abundance of calcite in pyrite-chlorite vein within the biotite-ampohibole gneiss may indicate the zone of boiling in the Willis Mountain and East Ridge area. Laterally migrating alkaline fluids cause Type V alteration, as evidenced by the deep Type V zones at Otake where fluid pH ranges from neutral to weakly alkaline. If the rising acidic steam encounters a highly permeable stratigraphic layer above the groundwater table, that is, a perched aquifer, the steam will invade that layer creating a stratiform alteration zone. The acidic steam has a low cation/H^+ ratio and will extract cations from the surrounding rock by hydrolysis reactions (Hemley and Jones, 1964). The high alumina content of the alteration zone represents residual enrichment because silica and alumina are less soluble than other lithophile cations in acidic hydrothermal fluids (Norton, 1973; Baes and Mesmer, 1976). Figure 19 demonstrates that, with increasing acidity, alkali feldspar will alter by hydrolysis to white mica, which will then alter to kaolinite or pyrophyllite depending on the temperature. By this method, the kyanite quartzite protolith was formed in the most intensely altered part of the perched aquifer and the quartz-muscovite schist protolith was formed around it where the altering fluid obtained a higher pH as

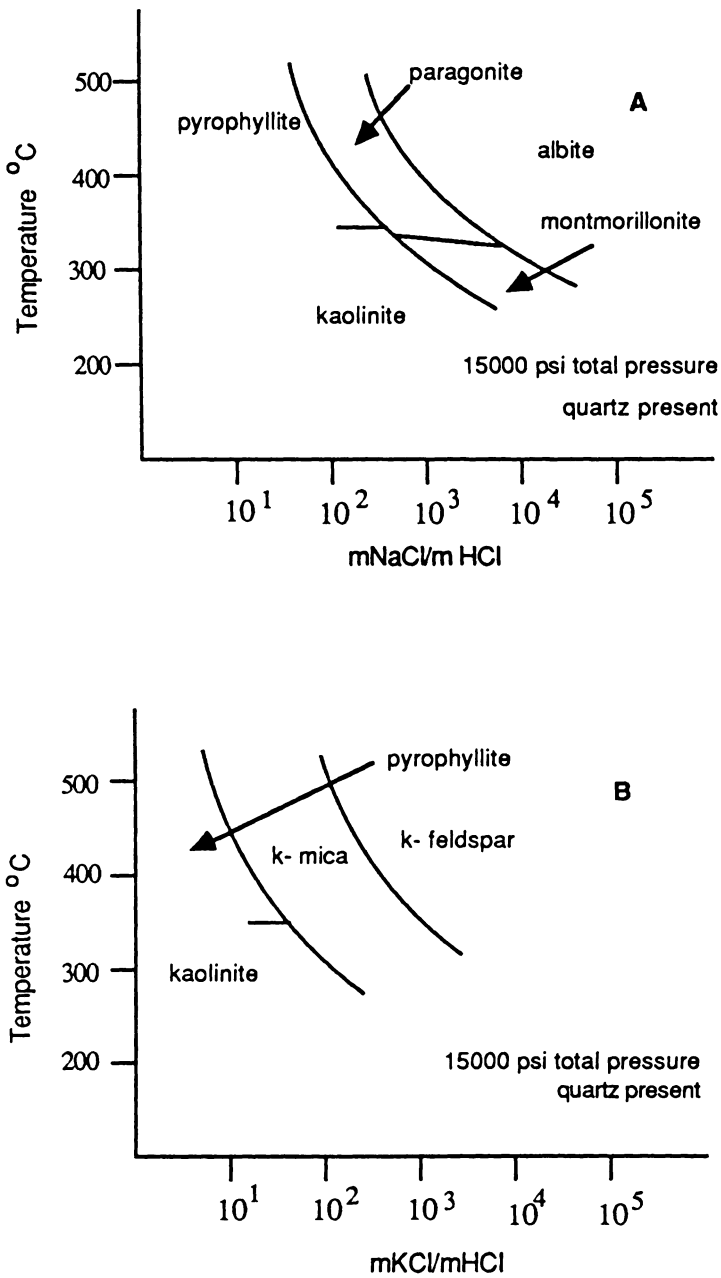

Figure 19: **A**: Reaction curves for the system Na_2O- Al_2O_3-SiO_2-H_2O and **B**: Reaction curves for the system K_2O-Al_2O_3-SiO_2-H_2O from Hemley and Jones (1964).

hydrogen ions were consumed by hydrolysis reactions. Pyrite was probably formed by the reaction (Giggenbach, 1981):

$$Fe(AlS) + 2H_2S + 1/2O_2 \rightarrow FeS_2 + H_2O + (AlS)H_2O$$

where (AlS) represents aluminosilicate component. Specular hematite was probably part of the pre-metamorphic alteration assemblage because hematite is stable in acidic, oxidizing solutions. Titanium, apparently immobile in acidic hydrothermal systems, formed rutile as Ti-bearing phases such as biotite and ilmenite disintegrated. Small amounts of topaz were formed by the interaction of HF in the altering fluid and aluminosilicates in the altered rock.

As the hot fluids reached the surface, resulting in hot springs, fumaroles, and mud pots, siliceous sinter precipitated from the rapidly cooling and oxidizing fluids.

Relationship to Ore Minerals

Though many hydrothermal alteration zones are often enriched in gold, silver, copper, lead, and zinc the Willis Mountain and East Ridge area rocks appear to be nearly barren. Gold and copper are present in the kyanite quartzite but not in economic abundances. At oxygen fugacities in pH ranges where pyrite and hematite coexist, chalcopyrite is not stable (Guilbert and Park, 1985) and slight variations in pH and oxygen fugacity among high-alumina alteration zones might explain why some (such as the Brewer deposit) contain gold and others do not. Feiss (1985a) shows that coexisting pyrite and hematite in equilibrium with fluids of pH similar to those found in active acidic hydrothermal systems are generally in zones of low gold solubility.

The close proximity of the London-Virginia ore deposit of submarine origin (Mangan et al., 1984) to a subaerial hydrothermal deposit appears incongruous.

However, Mitchell and Garson (1976) describe how incipient rifting in island arc settings initiates exhalative ore deposits, and possible shortening during folding and thrust faulting could have moved the two seemingly incompatible ore depositional environments closer together than they were originally.

Conclusions

Comparisons of the rocks in the Willis Mountain and East Ridge area, the aluminosilicate deposits in the Carolina Slate Belt and the Kings Mountain Belt, and the active hydrothermal alteration zones at Tatun, Taiwan and Otake, Japan combined with an analysis of the metamorphism in the Willis Mountain-East Ridge area suggest the following paragenesis for the Willis Mountain and East Ridge kyanite quartzite:

1. Subaerial island arc volcanism of calc-alkaline type in early Cambrian time.
2. Penecomtemporaneous hydrothermal alteration of intermediate volcanic rocks by acidic fluids at a pH between 2 and 4 and a temperature between 100 and 200° C which leached out almost all metal cations except Ti in rutile and Fe in pyrite and hematite. Only Si and Al remain in relatively unaltered abundances. Two distinct acidic alteration zones were present:
   a) A most intensely altered zone containing quartz, crystobalite, tridymite, or opalline silica, pyrophyllite and/or kaolinite, and sericite with minor amounts of pyrite, hematite, rutile, and topaz. Alunite may or may not have been present.
   b) A moderately altered zone, which formed as fluids became less acidic,

cooler, and more oxidized, containing quartz, sericite, and hematite.

3. Regional metamophism to a temperature of 600 ± 25° C and a pressure of approximately 6.5 kb caused the following prograde reactions:

Opal, trydimite, and/or cristoballite → quartz.

Pyrophyllite and/or kaolinite → kyanite + quartz + water.

Sericite → muscovite and/or paragonite.

Topaz became more fluorine-rich.

Such an intense grade of metamorphism was probably caused by very deep burial (19-20 km) of these rocks under a thrust faulted pile at a convergent margin. As metamorphism progressed the kyanite quartzite protolith probably passed through a stage where it contained a mineral assemblage similar to those found in pyrophyllite schists of greenschist grade.

Further evidence for hydrothemal alteration is found in the biotite-amphibole gneiss. Partial alteration by acidic fluids occured in the zone where gedrite, staurolite, and aluminosilicate appear, and calcite within veins of pyrite and chlorite may represent the boiling zone.

References

Albee, A., and Ray, L., 1970, Correction factors for electron-probe microanalysis of silicates, oxides, carbonates, phosphates, and sulfates: Anal. Chem., vol. 42, p. 1408-1414.

Arnorsson, S., 1978, Precipitation of calcite from flashed geothermal waters in Iceland: Contrib. Mineral. Petrol., vol. 66, p. 21-28.

Baes, C. F. and Mesmer, R. E., 1976, The Hydrolysis of Cations, New York: John Wiley and Sons, 489 p.

Bartlett, R. D., 1983, Geology and hydrothermal alteration of the Sugarloaf Prospect, San Luis Hills, Conejos and Costilla Counties, Colorado: Geol. Soc. America abstracts with programs, vol. 15, p. 326.

Barton, M. D., 1982a, The thermodynamic properties of fluor-topaz: Am. Min., vol. 67, p. 350-355.

Barton, M. D., 1982b, The thermodynamic properties of topaz solid solutions and some petrologic applications: Am. Min., vol. 67, p. 956-974.

Barton, P. B., Jr., 1970, Sulfide Petrology: Mineralogical Society of America Spec. Pap. 3, p. 187-198.

Bennett, P. J., 1961, The economic geology of some Virginia kyanite deposits: Ph.D. thesis, University of Arizona, 131 p.

Blencoe, J. G., 1977, Molal volumes of synthetic paragonite-muscovite micas: Am. Min., vol. 62, p. 1200-1215.

Blencoe, J. G. and Luth, W. C., 1973, Muscovite-paragonite solvi at 2, 4, and 8 kb pressure: Geol. Soc. America Abstracts with Programs, vol. 5, p. 553-554.

Bohlen, S. R., Wall, V. J., Boettcher, A. L., 1983, Experimental investigations and geological applications of equilibria in the system FeO-TiO_2-Al_2O_3-SiO_2-H_2O: Am. Min., vol. 68, p.1049-1058.

Bourland, W. C., 1976, Tectogenesis and metamorphism of thePiedmont from Columbia to Westview, Virginia along the James River: M.S. thesis, Virginia Polytechnic Institute and State University, 114 p.

Brown, W. R., 1969, Geology of the Dillwyn Quadrangle, Virginia: Virginia Division of Mineral Resources Rept. Inv. 10, 77 p.

Burt, D. M., 1981, Acidity-salinity diagrams--Application to greisen and porphyry deposits: Econ. Geol., vol. 76, p. 832-843.

Butler, J. R., 1985, The Brewer mine *in* Volcanic-hosted gold and high-alumina rocks of the Carolina slate belt, P. G. Feiss, ed.: Soc. Econ. Geol. Field Trip Guidebook, p.143-171.

Carpenter, R. H., and Allard, G. O., 1980, Mineralization, alteration, and volcanism in the Lincolnton-McCormick district, Georgia and South Carolina (abs.): Geol. Soc. America Abstracts with Programs, vol. 12, no. 7, p. 398-399.

Carpenter, R. H., and Allard, G. O., 1982, Aluminosilicate assemblages: an exploration tool for metavolcanic terrains of the Southeast: Exploration for Metallic Resources Conference at Univ. of Georgia, Athens, Georgia, Sept. 28-29, 1982, p.19-22.

Chatterjee, N. D., 1972, The upper stability limit of the assemblage paragonite + quartz and its natural occurrence: Contr. Mineralogy Petrology, vol. 34, p. 288-303.

Chatterjee, N. D., and Flux, S., 1986, Thermodynamic mixing properties of muscovite-paragonite crystalline solutions at high temperatures and pressures, and their geologic applications: J. Petrol., vol. 27., p. 677-693.

Chatterjee, N. D., and Froese, E., 1975, A thermodynamic study of the pseudobinary join muscovite-paragonite in the system $KAl_3Si_3O_8$-$NaAlSi_3O_8$-Al_2O_3-SiO_2-H_2O: Am. Min., vol. 60, p. 985-993.

Chatterjee, N. D., and Johannes, W., 1974, Thermal stability and standard thermodynamic properties of synthetic $2M_1$-muscovite, $KAl_2[Al\ Si_3O_{10}(OH)_2]$: Contr. Mineralogy Petrology, vol. 48, p. 89-114.

Chen, C. H., 1970, Geology and geothermal power potential for the Tatun volcanic region: Geothermics (Special Issue 2), vol. 2, pt. 2, p. 1134-1143.

Conley, J. F., 1962, Geology of the Albermarle quadrangle, North Carolina: North Carolina Department of Conservation and Development, Division of Mineral Resources Bulletin 76, 40 p.

Conley, J. F., and Marr, J. D., Jr., 1980, Evidence for the correlation of the kyanite quartzites of Willis and Woods Mountains with the Arvonia formation, *in* Contributions to Virginia Geology: Virginia Division of Mineral Resources Publication 27, p. 1-11.

Dixon, G. B., Jr., 1980, Kyanite mining in Virginia: Virginia Minerals, vol. 26, no. 1., p.12.

Duke, N. A., 1983, A metallogenic study of the central Virginian gold-pyrite belt: Ph.D. thesis, University of Manitoba.

Ellis, A. J., and Mahon, W. A. J., 1977, Chemistry and Geothermal Systems, New York: Academic Press, 392 p.

Espenshade, G. H., and Potter, D. B., 1960, Kyanite, sillimanite, and andalusite deposits in the southeastern United States: U.S. Geol. Survey Prof. Paper 336, 121 p.

Eugster, H. P., Albee, A. L., Bence, A. E., Thompson, J. B., and Waldbaum, D. R., 1972, The two-phase region and excess mixing properties of paragonite-muscovite crystalline solutions: J. Petrol., vol. 13, p. 147-179.

Facca, G., and Tonani, F., 1967, The self-sealing geothermal field: Bull. Volcanol., vol.30, p. 271-273.

Feiss, P. G., ed., 1985a, Volcanic-hosted gold and high-alumina rocks of the Carolina slate belt: Soc. Econ. Geol. Field Trip Guidebook, 217 p.

Feiss, P. G., 1985b, Henry Knob kyanite deposit*in* Volcanic-hosted gold and high-alumina rocks of the Carolina slate belt, P. G. Feiss, ed.: Soc. Econ. Geol. Field Trip Guidebook, p. 174-182.

Ferry, J. M., and Spear, F. S., 1978, Experimental calibration of the partitioning of Fe and Mg between biotite and garnet: Contrib. Min. Petrology, vol. 66, p. 113-117.

Flux, S., and Chatterjee, N. D., 1986, Experimental reversal of the Na-K exchange reaction between muscovite-paragonite crystalline solutions and a 2 molal aqueous (Na, K) Cl fluid: J. Petrol., vol. 27, p. 665-676.

Ganguly, J., Saxena, S. K., 1984, Mixing properties of aluminosilicate garnets: constraints from natural and experimental data, and applications to geothermo-barometry: Am. Min., vol. 69, p. 88-97.

Giggenbach, W. F., 1981, Geothermal mineral equilibria: Geochim. Cosmochim. Acta, vol. 45, p. 393-410.

Glover, L. G., III, 1974, Speculation on the relation between eastern and western Piedmont vulcanism (abs.): Geol. Soc. America Abstracts with Program, vol. 6, no. 7, p. 757.

Grambling, J. A., 1984, Coexisting paragonite and quartz in sillimanitic rocks from New Mexico: Am. Min., vol. 69, p. 79-87.

Guidotti, C. V., 1984, Micas in metamorphic rocks *in* Micas: Mineralogical Society of America Reviews in Mineralogy, vol. 13, S. W. Bailey, ed., p.357-467.

Guilbert, J. M., and Park, C. F., 1985, The Geology of Ore Deposits, New York: W. H. Freeman, 985p.

Haas, H., and Holdaway, M. J., 1973, Equilibrium in the system Al_2O_3-SiO_3-H_2O involving the stability limits of pyrophyllite, and thermodynamic data of pyrophyllite: Am. Jour. Sci., vol. 273, p. 449-464.

Hawthorne, F. C., 1971, Crystal chemistry of the amphiboles *in* Amphiboles and other hydrous pyriboles--mineralogy: Mineralogical Society of America Reviews in Mineralogy, vol. 9A, D. R. Veblen, ed., p.1-102.

Hayashi, M., and Yamasaki, T., 1974, Hydrothermal alteration of pyroxene

andesites in the Otake geothermal area, Japan: Int. Symposium on Water-Rock Interactions Proc. (Cadek and Paces, eds.), Prague, p. 158-163.

Hemley, J. J., Hostetler, P. B., and Gude, A. J., 1969, Some stability relations of alunite: Econ. Geol., vol. 64, p. 599-612.

Hemley, J. J., and Jones, W. R., 1964, Chemical aspects of hydrothermal alteration with emphasis on hydrogen metasomatism: Econ. Geol., vol. 59, p. 538-569.

Henley, R. W., and Ellis, A. J., 1983, Geothermal systems ancient and modern: a geochemical review: Earth Science Reviews, vol. 19, p. 1-50.

Higgins, M. W., Fischer, G. W., Johnson, S. S., and Zeitz, I., 1973, Preliminary interpretation of an aeromagnetic map of the crystalline rocks of Virginia (abs): Geol. Soc. America Abstracts with Programs, vol. 5, no. 2, p. 178.

Higgins, M. W., Sinha, A. K., Tilton, G. R., and Kirk, W. S., 1971,Correlation of metavolcanic rocks in the Maryland, Delaware and Virginia Piedmont (abs.): Geol. Soc. America Abstracts with Programs, vol. 3, no. 5, p. 320-321.

Highley, D. E., 1984, China clay *in* Mineral Dossier No. 26: British Geol. Survey, London, Her Majesty's Stationery Office, 65 p.

Hofstra, A. H., 1983, Geology and alteration of the NG alunite area, southern Wah Wah range, southwestern Utah: Geol. Soc. America Abstracts with Programs, vol. 15, p. 326.

Holdaway, M. J., 1971, Stability of andalusite and the aluminum silicate phase diagram: Am. Jour. Sci., vol. 271, p. 97-131.

Iwao, S., 1949, The alunite deposits in Japan: Geological Survey of Japan report

no. 130, 98 p. (abstract in English)

Iwao, S. and Udagawa, S., 1969, Pyrophyllite and "Roseki" clays *in* The Clays of Japan, S. Iwao, ed.: Japan Geological Survey, p. 71-87.

James, R. S., Grieve, R. A. F., and Pauk, L., 1978, The petrology of cordierite-anthophyllite gneisses and associated mafic and pelitic gneisses at Manitouwadge, Ontario: Am. Jour. Sci., vol. 278, p. 41-63.

Johnson, S. S., 1981, Regional geophysics *in* Investigations in Willis Mountain and Andersonville quadrangles, Virginia: Virginia Division of Mineral Resources Publication 29, p. 9-16.

Jonas, A. I., 1932, Geology of the kyanite belt of Virginia *in* Kyanite in Virginia: Virginia Geol. Survey Bull. 38, p. 1-37.

Jones, J. O., and Eilertsen, N. A., 1954, Investigation of the Willis Mountain kyanite deposit, Buckingham County, Virginia: Bureau of Mines Report of Investigations 5075, U.S. Dept. of Interior, 41 p.

Klein, T. L., 1985, Glendon pyrophyllite deposits *in* Volcanic-hosted gold and high-alumina rocks of the Carolina slate belt, P. G. Feiss, ed.: Soc. Econ. Geol. Field Trip Guidebook, p. 48-72.

Klein, T. L., and Schmidt, R. G., 1985, Geology of the Pilot Mountain-Fox Mountain alteration system *in* Volcanic-hosted gold and high-alumina rocks of the Carolina slate belt, P. G. Feiss, ed.: Soc. Econ. Geol. Field Trip Guidebook, p.74-107.

Luttrell, G. W., 1966, Base- and precious-metal and related ore deposits of Virginia: Virginia Division of Mineral Resources Report 7, 167 p.

Mangan, M., Craig, J. R., Rimstidt, J. D., 1984, Submarine exhalative gold mineralization at the London-Virginia Mine, Buckingham County, Virginia: Min. Dep., vol. 19, no. 3, p. 227-236.

Marr, J. D., Jr., 1980, The geology of the Willis Mountain quadrangle, Virginia: Virginia Division of Mineral Resources Publication 25, text and 1:24,000 scale map.

Marr, J. D., Jr., 1981, Stratigraphy and structure (Triassic system by M. B. McCollum) *in* Geologic investigations in the Willis Mountain and Andersonville quadrangles, Virginia: Virginia Division of Mineral Resources Publication 29, p. 3-8.

McCollum, M. B., 1981, Triassic system *in* Geologic investigations in the Willis Mountain and Andersonville quadrangles, Virginia: Virginia Division of Mineral Resources Publication 29, p. 6.

McDowell, R. C., 1964, Geology of the Arvonia Slate Quarries, Buckingham County, Virginia: M.S. thesis, Virginia Polytechnic Institute and State University, 109 p.

McKee, L. H., 1985, The Nesbit gold mine *in* Volcanic-hosted gold and high-alumina rocks of the Carolina slate belt, P. G. Feiss, ed.: Soc. Econ. Geol. Field Trip Guidebook, p. 124-142.

Mitchell, A. H. G., and Garson, M. S., 1967, Mineralization at plate boundaries: Minerals Sci. Engineering, vol. 8, p. 129-169.

Munoz, J. L., 1984, F-OH and Cl-Oh exchange in micas with applications to hydrothermal ore deposits *in* Micas: Mineralogical Society of America Reviews

in Mineralogy, vol. 13, S. W. Bailey, ed., p. 469-493.

Norton, S. A., 1985, Laterite and bauxite formation: Econ. Geol., vol. 68, p. 353-361.

Overstreet, E. P., 1964, Geology of the southeastern bauxite deposits: U.S. Geol. Survey Bull. 1199-A, 19 p.

Patterson, S. H., 1967, Bauxite reserves and potential aluminum resources of world: U.S. Geol. Survey Bull. 1228, 176 p.

Papezik, V. S., and Keats, H. G., 1976, Diaspore in a pyrophyllite deposit on the Avalon Peninsula, Newfoundland: Can. Mineral., vol. 14, p. 442-449.

Pavlides, L., 1981, The central Virginia volcanic-plutonic belt: An island arc of Cambrian (?) age: U. S. Geol. Survey Prof. Paper 1231-A, p. A1-A34.

Pavlides, L., Gair, J. E., and Cranford, S. L., 1982, Massive sulfide deposits of the southern Appalachians: Econ. Geol., vol. 77, no. 2, p.233-272.

Prakash, R., Singh, J. N., and Saxena, P. N., 1970, Geology of the pyrophyllite and diaspore deposits of Jhansi District, U. P.: Directorate of Geology and Mining, Uttar Pradesh, India, monograph no. 1, part 1-A, 54 p.

Robie, R. A., Hemingway, B. S., and Fisher, J. R., 1979, Thermodynamic properties of minerals and related substances at 298.15 K and 1 bar (10^5 pascals) pressure and at higher temperatures: U. S. Geol. Survey Bull. 1452, 456p.

Robinson, P., Ross, M., and Jaffe, H. W.,1971, Composition of the anthophyllite-gedrite series, comparisons of gedrite and hornblende, and the

anthophyllite solvus: Am. Min., vol. 56, p. 1005-1041.

Schmidt, R. G., 1982, High-alumina hydrothermal systems in volcanic rocks of the Carolina Slate Belt: Geol. Soc. America Abstracts with Programs, vol. 14, p. 80.

Schmidt, R. G., 1985a, High-alumina hydrothermal systems in volcanic rocks and their significance to mineral prospecting in the Carolina slate belt: U.S. Geol. Survey Bull. 1562, 59 p.

Schmidt, R. G., 1985b, Snow Camp pyrophyllite mine *in* Volcanic-hosted gold and high-alumina rocks of the Carolina slate belt, P. G. Feiss, ed.: Soc. Econ. Geol. Field Trip Guidebook, p. 37-47.

Schreyer, W., 1982, Fuchsite-aluminum silicate rocks in Archaean greenstone belts: Are they metamorphosed alunite deposits?: Sonderdruk aus der Geologischen Rundschau, band 71, p. 347-360.

Schreyer, W., and Chinner, G. A., 1966, Staurolite-quartzite bands in kyanite quartzite at Big Rock, Rio Arriba County, New Mexico: Contrib. Min. Petrology, vol. 12, p. 223-244.

Solberg, T. N., 1982, Fluorine electron microprobe analysis: variations of x-ray peak shape *in* Microbeam Analysis, K. F. J. Heinrich, ed., San Francisco: San Francisco Press, Inc., p. 148-150.

Solberg, T. N., and Speer, J. A., 1982, QALL, a 16-element analytical scheme for efficient petrologic work on an automated ARL-SEMQ: application to mica reference samples *in* Microbeam Analysis, K. F. J. Heinrich, ed., San Francisco: San Francisco Press, Inc. p. 422.

Southwick, D. L., Reed, J. C., Jr., and Mixon, R. B., 1971, The Chopawamsic formation--a new stratigraphic unit in the piedmont of northeastern Virginia: U.S. Geol. Survey Bull. 1324-D, 11 p.

Spear, F. S., 1980, The gedrite-anthophyllite solvus and the composition limits of orthoamphibole from the Post Pond Volcanics, Vermont: Am. Min., vol. 65, p. 1103-1118.

Spence, W. H., 1975, A model for the origin of the pyrophyllite deposits in the Carolina slate belt (abs.): Geol. Soc.America Abstracts with Programs, vol. 7, p. 536.

Spence, W. H., Worthington, J. E., Jones, E. M., and Kiff, I. T., 1980, Origin of the gold mineralization at the Haile mine, Lancaster County, South Carolina: Mining Engineering, vol. 32, p. 70-73.

Sweet, P. C., 1980a, Economic geology *in* The geology of the Willis Mountain quadrangle, Virginia: Virginia Division of Mineral Resources Publication 25, text and 1:24,000 scale map.

Sweet, P. C., 1980b, Gold in Virginia: Virginia Division of Mineral Resources Publication 19, 77 p.

Sykes, M. L. and Moody, J. B., 1978, Pyrophyllite and metamorphismin the Carolina slate belt: Am. Min., vol. 63, p. 96-108.

Taniguchi, M., Makita, T., and Kawai, Y., 1978, Geological study on hydrothermal rock alteration in Hijiori geothermal area, Yamagata Prefecture, Japan: Japan Geological Survey report no. 259, p. 377-414. (abstract in English)

Thompson, A. B., 1974, Calculation of muscovite-paragonite- alkali feldspar phase relations: Contrib. Min. Pet., vol. 44, p. 173-194.

Tillman, C. G., 1970, Metamorphosed trilobites from Arvonia,Virginia: Geol. Soc. America Bull., vol. 81, p. 1189-1200.

Togashi, Y., Kubota, Y., Yamada, E., and Nishimura, S., 1978, Geothermal rock alteration at Ubayu Hot Springs and vicinity, Yamagata Prefecture, Japan: Japan Geological Survey report no. 259, p.415-436. (abstract in English)

Tracy, R. J., Robinson, P., Thompson, A. B., 1976, Garnet composition and zoning in the determination of temperature and pressure of metamorphism, central Massachusetts: Am. Min., vol. 61, p. 762-775.

White, D. E., Muffler, L. J. P., and Truesdell, A. H., 1971, Vapor-dominated hydrothermal systems compared with hot water systems: Econ. Geol., vol. 66, p. 75-97.

Williams, H., 1978, Tectonic lithofacies map of the Appalachian orogen, Memorial University of Newfoundland.

Worthington, J. E., Kiff, I. T., Jones, E. M., and Chapman, P. E., 1980, Applications of the hot springs or fumarolic model in prospecting for lode gold deposits: Mining Engineering, vol. 32, p. 73-79.

Yoder, H. S., and Tilley, C. E., 1962, Origin of basalt magmas: an experimental study of natural and synthetic rock systems: J. Petrol., vol. 3, p. 342-532.

Zen, E., 1961, Mineralogy and petrology in the system Al_2O_3-SiO_2-H_2O in some North Carolina pyrophyllite deposits: Geochim. Cosmochim. Acta., vol. 26, p.1055-1067.

Appendix I

Sample Calculations for Determining Pressure and Temperature of Peak Metamorphism

Garnet-biotite geothermometry

According to Ferry and Spear (1978), partitioning of Mg and Fe between garnet and biotite at equilibrium has the following relationship:

$$0 = 12{,}454 - 4.662T(K) + 0.057P(b) + 3RT\ln K$$

where R = 1.987

and $K = (Mg/Fe)_{garnet}/(Mg/Fe)_{biotite}$ in weight percent.

Sample CC75 contains biotite and garnet in apparent equilibrium with the following composition:

Garnet: 6.31 wt. % Mg

29.80 wt.% Fe.

Biotite: 14.60 wt. % Mg

13.05 wt. % Fe.

so: ln K = -1.665 and $T(K) = \{12{,}454 + 0.057P(b)\}/14.586$.

Pressure (kb)	Temperature (K)	Temperature (°C)
5.0	873	600
5.5	875	602
6.0	877	604
6.5	879	608

GRAIL geobarometry

Given the GRAIL assemblage (almandine garnet-rutile-aluminosilicate- ilmenite-quartz), geobarometry may be calculated from the reaction (Bohlen et al., 1983):

(ilm) (AlS) (qtz) (alm) (rut)

3 ilmenite + aluminosilicate + quartz = almandine + rutile

and from the relation:

$$\Delta G = 0 = -RT\ln K + P\Delta V$$

pressure can be calculated by:

$$\Delta P = -RT\ln K/2.303\Delta V$$

where R = 1.982 and

$$K = (a_{ilm}^3)(a_{qtz}^2)(a_{AlS})/(a_{alm})(a_{rut}).$$

The following are necessary to perform this calculation:

1. GRAIL assemblage at equilibrium.
2. Composition of phases.
3. Solution models for activity of end-member components in impure phases.
4. A reasonable estimate of temperature.

From Ganguly and Saxena (1984) we have a summary of mixing data for garnets and a solution model:

Margules Parameters:

$W^{Fe-Mg} = 200$ $W^{Mg-Fe} = 2{,}500\pm500$

$W^{Ca-Mg} = 4047\pm77$ $W^{Mg-Ca} = 1000\pm77$

$W^{Ca-Fe} = -630\pm400$ $W^{Fe-Ca} = 4620\pm660$

$W^{Fe-Mn} = W^{Mn-Fe} = W^{Ca-Mn} = W^{Mn-Ca} = 0$

$W^{Mg-Mn} = W^{Mn-Mg} = 3000\pm500.$

Binary interaction terms:

$C_{CaFeMg} = -5300$ $C_{CaMgMn} = -1523$

$C_{CaFeMn} = 2625$ $C_{MgFeMn} = -1150$

Solution model for Fe in almandine:

$$\Delta RT\ln\gamma = X_{Fe}^2[W^{Fe\text{-}Mn} + 2X_{Fe}(W^{Mn\text{-}Fe} - W^{Fe\text{-}Mn})] + X_{Fe}X_{Mg}[1/2(W^{Mn\text{-}Fe} + W^{Fe\text{-}Mn} + W^{Mg\text{-}Fe} + W^{Fe\text{-}Mg} - W^{Mn\text{-}Mg} - W^{Mg\text{-}Mn}) + X_{Fe}(W^{Mn\text{-}Fe} - W^{Fe\text{-}Mn} + W^{Mg\text{-}Fe} - W^{Fe\text{-}Mg}) + (X_{Mg} - X_{Mn})(W^{Mg\text{-}Mn} - W^{Mn\text{-}Mg}) - (1 - 2X_{fe})(C_{MgFeMn})] + X_{Fe}X_{Ca}[1/2(W^{Mn\text{-}Fe} + W^{Fe\text{-}Mn} + W^{Ca\text{-}Fe} + W^{Fe\text{-}Ca} - W^{Mn\text{-}Ca} - W^{Ca\text{-}Mn}) + X_{Fe}(W^{Mn\text{-}Fe} - W^{Fe\text{-}Mn} + W^{Ca\text{-}Fe} - W^{Fe\text{-}Ca}) + (X_{Ca} - X_{Mn})(W^{Ca\text{-}Mn} - W^{Mn\text{-}Ca}) - (1 - 2X_{Fe})C_{CaFeMn}] + 2X_{Mg}X_{Ca}X_{Mn}(W^{Mn\text{-}Mg} - W^{Mg\text{-}Mn} + C_{CaMgMn}).$$

Assume the activity of pure phases = 1 so:

$$K = a_{ilm}^3/a_{alm}.$$

Sample CC75 has the GRAIL assemblage in apparent equilibrium and microprobe analyses yield the following garnet compositions:

$$X_{Fe} = .67$$
$$X_{Mg} = .22$$
$$X_{Ca} = .01$$
$$X_{Mn} = .07$$

and substituting into the above solution model:

$$RT\ln\gamma_{Fe} = 144.60.$$

Assuming T = 600° C = 873K:

$$\gamma_{Fe} = 1.09$$
$$a_{alm} = [(1.09)(.67)]^3 = .39$$
$$(a_{ilm})^3 = (X_{ilm})^3 = .86$$
$$\log K = .34$$

At this point, we can read the pressure from the graph in Fig. 3 of Bohlen et al. (1983) and, assuming T = 600° C, P = 6.5 kb.

Appendix II

Comparison Table of Southeastern United States Aluminum Silicate Deposits of Probable Hydrothermal Origin

Mineral abbreviations: And=andalusite, Ap=apatite, Chl=chlorite, Ctd=chloritoid, Dia=diaspore, Dick=dickite, Hem=hematite, Kao=kaolinite, Ky=kyanite, Laz=lazulite, Mt=magnetite, Mu=muscovite, Pa=paragonite, Py=pyrite, Pyro=pyrophyllite, Q=quartz, Rut=rutile, Ser=sericite, Sill=sillimanite, St=staurolite, Tz=topaz, Zr=zircon.

Deposit	Alteration minerals	Host rocks	References	Remarks
1. Willis Mountain and East Ridge, Buckingham Co., VA	Q, Ky, Py, Mu, Pa, Rut, Hem, Tz, Ap	intermediate metavolcanic rocks of Chopawamsic fm.	Espenshade and Potter (1960), Bennett (1961),Marr (1980)	World's largest kyanite mine, metamorphosed hydrothermal alteration zone.
2. Woods Mountain, Buckingham Co., Va	Q, Ky, Mu, Pa, Tz, Rut, Py, Hem	intermediate metavolcanic rocks of Chopawamsic fm.	Espenshade and Potter (1960), Marr (1980)	Similar to Willis Mt. deposit, Layers of massive barren quartzite within Ky quartzite.
3. Leigh Mountain, Prince Edward Co., VA	Q, Ky, Mu Py, Sill, Hem	intermediate metavolcanic rocks of Chopawamsic fm.	Espenshade and Potter (1960), Bennett (1961)	Presence of Sill probably reflects eastward increase in metamorphic grade.
4. Baker Mountain, Prince Edward Co., VA	Q, Ky Rut, Py, Tz, Mu, Pa, Hem	intermediate metavolcanic rocks of Chopawamsic fm.	Espenshade and Potter (1960), Bennett (1961)	Abandoned Ky mine.
5. Halifax Co., VA	Q, Ky, Mu	intermediate metavolcanic rocks of Chopawamsic fm.	Espenshade and Potter (1960)	Stratiform nature similar to Willis Mt. and East Ridge.
6. Madiisonville, Charlotte Co., VA	Q, Ky, Mu, Rut, Py, Hem	intermediate metavolcanic rocks of Chopawamsic fm.	Espenshade and Potter (1960)	Also contains fuchsite and barite.
7. Hagers Mountain, Person Co., NC	Q, Ky, Ctd, Mu, Pa, Rut, Chl, Zr	siliceous slates and phyllited, some volcanic breccia, Carolina Slate Belt	Espenshade and Potter (1969), Zen (1961)	Fine-grained Q resembles that of Pyro deposits such as Bowlings Mt., NC
8. Corbett Deposit, Johnston Co., NC	Q, Ky, Py, Tz, Rut, Zr, Pyro	sericitic slate and sericitic quartzite, Eastern Slate Belt	Espenshade and Potter (1960)	Pyro may be secondary.
9. Haile Mine, Lancaster Co., SC	Q, Kao, Pyro, Ser Hem, Py, Tz, Rut, gold	felsic upper Uwharrie fm., Carolina Slate Belt	Spence et al. (1980)	Most productive gold mine in eastern U. S.
10. Clubb Mountain, Gaston and Lincoln Cos., NC	Q, Ky, Mu, Py, Rut, Laz, St, Dia, Pyro, zunyite, goyazite	undifferentiated schists and gneisses of Kings Mt. Belt	Espenshade and Potter (1960)	Ky quartzite occurs as en echelon lenses.
11. Reese Mountain, Lincoln Co., NC	Q, Sill, Rut, Mt	undifferentiated schists and gneisses of Kings Mt. Belt	Espenshade and Potter (1960)	4 km northwest of Clubb Mt.
12. Crowders Mountain, Gaston Co., NC	Q, Ky, And, Mu	undifferentiated schists and gneisses of Kings Mt. Belt	Espenshade and Potter (1960)	Ky quartzite interlayered with St-Ctd quartzite and ferruginous quartzite.
13. The Pinnacle, Gaston Co., NC	Q, Ky, Py, Mu, Rut, Mt, Zr, Ap	undifferentiated schists and gneisses of Kings Mt. Belt	Espenshade and Potter (1960)	Ky quartzite surrounded by Ctd-Mu schist.
14. Will Knox Deposit, Gaston Co., NC	Q, Sill, And, Rut, Mt, Tz, Laz, Ctd, Ky, Dia	undifferentiated schists and gneisses of Kings Mt. Belt	Espenshade and Potter (1960)	Small lenticular outcrops of Sill quartzite.
15. Henry Knob, York Co., SC	Q, Ky, Py, Mu, Pyro, Rut, barite	dacitic to andesitic metavolcanic rocks of Battleground schist, Kings Mt. Belt	Espenshade and Potter (1960), Peiss (1985a,b)	Commercial Ky mine 1948-1969. Ky quartzite lenses within Py-Mu schist.

Mineral abbreviations: And=andalusite, Ap=apatite, Chl=chlorite, Ctd=chloritoid, Dia=diaspore, Dick=dickite, Hem=hematite, Kao=kaolinite, Ky=kyanite, Laz=lazulite, Mt=magnetite, Mu=muscovite, Pa=paragonite, Py=pyrite, Pyro=pyrophyllite, Q=quartz, Rut=rutile, Ser=sericite, Sill=sillimanite, St=staurolite, Tz=topaz, Zr=zircon.

Deposit	Alteration minerals	Host rocks	References	Remarks
16. Little Mountain Newberry Co., SC	Q, Ky, Mu, Py, Rut, Pyro	Q-Ser schist of Carolina Slate Belt	Espenshade and Potter (1960)	Ky quartzite occurs as north-east striking lenses.
17. Graves Mountain, Lincoln Co., GA	Q, Ky, Hem, Py, Rut, Laz	dacitic pyroclastic rocks of Carolina Slate Belt	Espenshade and Potter (1960), Carpenter and Allard (1980, 1982)	Commercially mined for Ky.
18. Bowlings Mountain, Granville Co., NC	Q, Pyro, And, Tz, Py malachite	undifferentiated Carolina Slate Belt	Espenshade and Potter (1960), Zen (1961)	Mined by Carolina Pyro. Co., Ctd occurs in adjacent rocks.
19. Hillsborough, Orange Co., NC	Q, Pyro, And, Ser, Kao, Py, Tz	andesitic to dacitic metavolcanics of Carolina Slate Belt	Espenshade and Potter (1960), Zen (1961), Sykes and Moody (1979), Schmidt (1985)	Operating Pyro mine, Ti vs. Zn ratios correlate with those of surrounding metavolcanics.
20. Snow Camp, Alamance Co., NC	Q, Pyro, Mu, Ctd, Py, Hem, Pa, Rut, Laz, Dia	felsic to intermediate metavolcanic rocks of Carolina Slate Belt	Espenshade and Potter (1960), Zen (1961), Schmidt (1985)	Pyro mined from 1930's to 1960's. Pyro + Q in lenticular body, 120 x 85 m.
21. Staley, Randolph Co., NC	Q, Pyro, Mu, Ctd, And, Chl, Hem, Rut, Py	volcanic ash and tuff of Carolina Slate Belt	Espenshade and Potter (1960), Zen (1961)	Lenticular body, 120 x 60 m.
22. Glendon, Moore Co., NC	Q, Pyro, Kao, Ctd, Mu, Chl, Hem, Py, Rut, Dia, Ap	felsic to intermediate volcanic rocks of Carolina Slate Belt	Espenshade and Potter (1960), Zen (1961), Spence (1975), Schmidt (1985), Klein (1985)	Gold in alteration zone ranges from 0.02-0.04 ppm.
23. Robbins, Moore Co., NC	Q, Pyro, Kao, Ctd, Mu, Py	felsic to intermediate volcanic rocks of Carolina Slate Belt	Espenshade and Potter (1960), Zen (1961), Schmidt (1985), Klein (1985)	Similar to nearby Glendon deposit.
24. Brewer, Chesterfield Co., SC	Q, Pyro, Ser, Py, Tz, Ky, Dick	felsic flows and tuffs of Uwharrie fm., Carolina Slate Belt	Espenshade and Potter (1961), Schmidt (1985), Butler (1985)	Gold mined here from 1928 to present, Schmidt classifies this as a porphyry gold system.
25. Pilot Mountain, Randolph Co., NC	Q, Pyro, And, Ser, Tz, Hem, Py	andesitic and dacitic tuffs and volcaniclastics of Carolina Slate Belt	Schmidt (1985), Klein and Schmidt (1985)	4.5 x 2.0 km, thought to be analogous to porphyry copper system.
26. Nesbit Mine, Union Co., NC	Q, Kao, Mu, Pyro, And, Py, Hem	andesitic tuff of Uwharrie fm, Carolina Slate Belt	McKee (1985)	Mined for gold from 1880's to 1890's, Gold occurs in pyrite, 0.02-0.04 ppm.

Appendix III

Microprobe Analyses

Microprobe analyses were conducted on an ARL-SEMQ electron microprobe at Virginia Polytechnic Institute and State University at an accelerating voltage of 15 kV for silicate analysis and at an accelerating voltage of 20 kV for pyrite analysis using a beam current of 20 nA. Fluorine-rich topaz from Thomas Range, Utah was used as a standard for topaz fluorine analysis because fluorine peaks from topaz differ from fluorine peaks from other minerals (Solberg, 1982). Other standards are specified in Solberg and Speer (1982). Data were converted to oxide weight percent by the data reduction program Bence-Albee from Albee and Ray (1970).

ANALYSIS #	1	2	3	4
PHASE	MUSC	ALS	MUSC	MUSC
SAMPLE #	DW2	DW2	DW2	DW2
CIRCLE #	2	2	2	2
GRAIN #	1	2	3	4
SIO2	46.25	38.21	46.19	47.19
AL2O3	37.95	64.36	37.44	37.65
TIO2	.32	.06	.48	.34
FE2O3	0.00	0.00	0.00	0.00
FEO	.01	0.00	.06	.06
MGO	.17	0.00	.33	.26
MNO	0.00	0.00	0.00	0.00
ZNO	0.00	0.00	0.00	0.00
CAO	.02	0.00	.02	.02
BAO	0.00	.03	0.00	0.00
NA2O	2.55	0.00	2.36	2.27
K2O	6.76	0.00	7.40	6.99
H2O	0.00	0.00	0.00	0.00
F	.28	0.00	.27	.26
CL	0.00	0.00	0.00	0.00
TOTAL	94.31	102.66	94.55	95.04
# ANIONS	12	5	12	12
SI	3.04	1.00	3.04	3.08
AL	2.94	1.99	2.91	2.90
TI	.02	0.00	.02	.02
FE+3	0.00	0.00	0.00	0.00
FE+2	0.00	0.00	0.00	0.00
MG	.02	0.00	.03	.03
MN	0.00	0.00	0.00	0.00
ZN	0.00	0.00	0.00	0.00
CA	0.00	0.00	0.00	0.00
BA	0.00	0.00	0.00	0.00
NA	.33	0.00	.30	.29
K	.57	0.00	.62	.58
OH	1.94	0.00	1.94	1.95
F	.06	0.00	.06	.05
CL	0.00	0.00	0.00	0.00
SI+ALIV	4.00	1.00	4.00	4.00
ALVI+FM+ZN+TI	2.02	1.99	2.01	2.02
CA+BA+NA+K	.89	0.00	.93	.87
OH+F+CL	2.00	0.00	2.00	2.00
FE/FE+MG	.03	*****	.09	.11

ANALYSIS #	1	2	3	4
PHASE	MUSC	MUSC	ALS	MUSC
SAMPLE #	DW4	DW4	DW4	DW4
CIRCLE #	1	1	1	2
GRAIN #	1	2	3	4
SIO2	42.27	46.59	37.49	46.64
AL2O3	36.09	37.69	63.51	37.26
TIO2	.82	.36	0.00	.52
FE2O3	0.00	0.00	0.00	0.00
FEO	.14	.09	.02	.13
MGO	.64	.26	0.00	.38
MNO	0.00	0.00	0.00	0.00
ZNO	0.00	0.00	0.00	0.00
CAO	0.00	0.00	0.00	0.00
BAO	.22	.16	0.00	.23
NA2O	1.94	2.53	.01	2.82
K2O	8.00	6.67	.01	7.00
H2O	0.00	0.00	0.00	0.00
F	.29	.19	.01	.34
CL	0.00	0.00	0.00	0.00
TOTAL	90.41	94.54	101.05	95.32
# ANIONS	12	12	5	12
SI	2.95	3.06	1.00	3.06
AL	2.97	2.92	2.00	2.88
TI	.04	.02	0.00	.03
FE+3	0.00	0.00	0.00	0.00
FE+2	.01	0.00	0.00	.01
MG	.07	.03	0.00	.04
MN	0.00	0.00	0.00	0.00
ZN	0.00	0.00	0.00	0.00
CA	0.00	0.00	0.00	0.00
BA	.01	0.00	0.00	.01
NA	.26	.32	0.00	.36
K	.71	.56	0.00	.59
OH	1.94	1.96	0.00	1.93
F	.06	.04	0.00	.07
CL	0.00	0.00	0.00	0.00
SI+ALIV	4.00	4.00	1.00	4.00
ALVI+FM+ZN+TI	2.03	2.02	2.00	2.00
CA+BA+NA+K	.98	.88	0.00	.95
OH+F+CL	2.00	2.00	0.00	2.00
FE/FE+MG	.11	.16	1.00	.16

ANALYSIS #	1	2	3	4
PHASE				MUSC
SAMPLE #	DW5	DW5	DW5	DW5
CIRCLE #	2	2	0	0
GRAIN #	4	5	6	7
SIO2	32.37	32.34	32.03	44.40
AL203	55.49	55.27	55.35	39.32
TIO2	.01	.02	.02	.20
FE203	0.00	0.00	0.00	0.00
FEO	.01	0.00	.02	.02
MGO	.04	.04	0.00	0.00
MNO	0.00	0.00	0.00	0.00
ZNO	0.00	0.00	0.00	0.00
CAO	0.00	.01	.01	0.00
BAO	0.00	0.00	0.00	0.00
NA20	0.00	0.00	0.00	5.64
K20	0.00	0.00	.01	2.50
H20	0.00	0.00	0.00	0.00
F	14.77	14.46	14.58	.16
CL	0.00	0.00	0.00	0.00
TOTAL	102.69	102.14	102.02	92.24
# ANIONS				12
SI	.99	1.00	.99	2.95
AL	2.01	2.00	2.01	3.08
TI	0.00	0.00	0.00	.01
FE+3	0.00	0.00	0.00	0.00
FE+2	0.00	0.00	0.00	0.00
MG	0.00	0.00	0.00	0.00
MN	0.00	0.00	0.00	0.00
ZN	0.00	0.00	0.00	0.00
CA	0.00	0.00	0.00	0.00
BA	0.00	0.00	0.00	0.00
NA	0.00	0.00	0.00	.73
K	0.00	0.00	0.00	.21
OH	.57	.59	.58	1.97
F	1.43	1.41	1.42	.03
CL	0.00	0.00	0.00	0.00
SI+ALIV				4.00
ALVI+FM+ZN+TI				2.04
CA+BA+NA+K				.94
OH+F+CL				2.00
FE/FE+MG				1.00

ANALYSIS #	5	6	7	8
PHASE	MUSC	MUSC	MUSC	ALS
SAMPLE #	DW5	DW5	DW5	DW5
CIRCLE #	0	0	0	1
GRAIN #	8	9	10	1
SIO2	45.29	45.55	45.57	37.53
AL2O3	39.55	39.15	38.75	63.42
TIO2	.23	.19	.26	0.00
FE2O3	0.00	0.00	0.00	0.00
FEO	0.00	0.00	0.00	.02
MGO	.03	0.00	0.00	0.00
MNO	0.00	0.00	0.00	0.00
ZNO	0.00	0.00	0.00	0.00
CAO	.03	.05	.02	0.00
BAO	0.00	0.00	.09	0.00
NA2O	5.60	5.77	5.29	.01
K2O	2.70	2.44	3.00	0.00
H2O	0.00	0.00	0.00	0.00
F	.17	.14	.25	0.00
CL	0.00	0.00	0.00	0.00
TOTAL	93.60	93.29	93.23	100.98
# ANIONS	12	12	12	5
SI	2.96	2.99	3.00	1.00
AL	3.05	3.02	3.01	2.00
TI	.01	.01	.01	0.00
FE+3	0.00	0.00	0.00	0.00
FE+2	0.00	0.00	0.00	0.00
MG	0.00	0.00	0.00	0.00
MN	0.00	0.00	0.00	0.00
ZN	0.00	0.00	0.00	0.00
CA	0.00	0.00	0.00	0.00
BA	0.00	0.00	0.00	0.00
NA	.71	.73	.68	0.00
K	.23	.20	.25	0.00
OH	1.96	1.97	1.95	0.00
F	.04	.03	.05	0.00
CL	0.00	0.00	0.00	0.00
SI+ALIV	4.00	4.00	4.00	1.00
ALVI+FM+ZN+TI	2.03	2.02	2.02	2.00
CA+BA+NA+K	.94	.94	.93	0.00
OH+F+CL	2.00	2.00	2.00	0.00
FE/FE+MG	0.00	*****	*****	1.00

ANALYSIS #	1	2	3	5
PHASE				
SAMPLE #	DW10	DW10	DW10	DW10
CIRCLE #	1	1	0	
GRAIN #	1	2	3	5
SIO2	32.35	33.15	32.64	32.70
AL2O3	55.10	55.78	55.26	56.25
TIO2	.01	.04	.04	.03
FE2O3	0.00	0.00	0.00	0.00
FEO	.04	.02	0.00	0.00
MGO	0.00	.05	0.00	0.00
MNO	0.00	0.00	0.00	0.00
ZNO	0.00	0.00	0.00	0.00
CAO	0.00	0.00	0.00	0.00
BAO	0.00	0.00	0.00	0.00
NA2O	0.00	0.00	0.00	0.00
K2O	0.00	0.00	0.00	0.00
H2O	0.00	0.00	0.00	0.00
F	13.96	14.22	13.90	13.97
CL	0.00	0.00	0.00	0.00
TOTAL	101.46	103.26	101.84	102.95
# ANIONS				
SI	1.00	1.00	1.00	.99
AL	2.00	1.99	2.00	2.01
TI	0.00	0.00	0.00	0.00
FE+3	0.00	0.00	0.00	0.00
FE+2	0.00	0.00	0.00	0.00
MG	0.00	0.00	0.00	0.00
MN	0.00	0.00	0.00	0.00
ZN	0.00	0.00	0.00	0.00
CA	0.00	0.00	0.00	0.00
BA	0.00	0.00	0.00	0.00
NA	0.00	0.00	0.00	0.00
K	0.00	0.00	0.00	0.00
OH	.64	.64	.65	.66
F	1.36	1.36	1.35	1.34
CL	0.00	0.00	0.00	0.00

SI+ALIV
ALVI+FM+ZN+TI
CA+BA+NA+K
OH+F+CL
FE/FE+MG

ANALYSIS #	1	2	3	4
PHASE	ALS			
SAMPLE #	DW10A	DW10A	DW10A	DW10A
CIRCLE #	1	1	1	1
GRAIN #	1	2	3	4
SIO2	38.49	33.34	33.55	32.68
AL203	65.63	56.56	56.19	56.33
TIO2	.01	.01	.01	0.00
FE203	0.00	0.00	0.00	0.00
FEO	0.00	.03	.04	0.00
MGO	.01	.07	.02	0.00
MNO	0.00	0.00	0.00	0.00
ZNO	0.00	0.00	0.00	0.00
CAO	0.00	0.00	0.00	.01
BAO	0.00	0.00	0.00	0.00
NA20	.02	0.00	0.00	0.00
K20	.01	0.00	0.00	0.00
H20	0.00	0.00	0.00	0.00
F	0.00	13.18	14.02	15.19
CL	0.00	0.00	0.00	0.00
TOTAL	104.17	103.19	103.83	104.21
# ANIONS	5			
SI	1.00	1.00	1.01	.99
AL	2.00	2.00	1.99	2.01
TI	0.00	0.00	0.00	0.00
FE+3	0.00	0.00	0.00	0.00
FE+2	0.00	0.00	0.00	0.00
MG	0.00	0.00	0.00	0.00
MN	0.00	0.00	0.00	0.00
ZN	0.00	0.00	0.00	0.00
CA	0.00	0.00	0.00	0.00
BA	0.00	0.00	0.00	0.00
NA	0.00	0.00	0.00	0.00
K	0.00	0.00	0.00	0.00
OH	0.00	.75	.67	.54
F	0.00	1.25	1.33	1.46
CL	0.00	0.00	0.00	0.00

SI+ALIV	1.00
ALVI+FM+ZN+TI	2.00
CA+BA+NA+K	0.00
OH+F+CL	0.00
FE/FE+MG	0.00

ANALYSIS #	5	6	7
PHASE		MUSC	
SAMPLE #	DW10A	DW10A	DW10A
CIRCLE #	1	0	0
GRAIN #	5	6	7
SIO2	32.97	46.91	32.93
AL2O3	56.20	39.69	55.94
TIO2	0.00	.22	0.00
FE2O3	0.00	0.00	0.00
FEO	.01	0.00	.04
MGO	.05	0.00	0.00
MNO	0.00	0.00	0.00
ZNO	0.00	0.00	0.00
CAO	0.00	.02	.01
BAO	0.00	.08	0.00
NA2O	0.00	5.78	0.00
K2O	.01	2.16	0.00
H2O	0.00	0.00	0.00
F	14.77	.17	15.05
CL	0.00	0.00	0.00
TOTAL	104.01	95.03	103.97
# ANIONS		12	
SI	1.00	3.01	1.00
AL	2.00	3.00	2.00
TI	0.00	.01	0.00
FE+3	0.00	0.00	0.00
FE+2	0.00	0.00	0.00
MG	0.00	0.00	0.00
MN	0.00	0.00	0.00
ZN	0.00	0.00	0.00
CA	0.00	0.00	0.00
BA	0.00	0.00	0.00
NA	0.00	.72	0.00
K	0.00	.18	0.00
OH	.59	1.97	.56
F	1.41	.03	1.44
CL	0.00	0.00	0.00
SI+ALIV		4.00	
ALVI+FM+ZN+TI		2.02	
CA+BA+NA+K		.90	
OH+F+CL		2.00	
FE/FE+MG		*****	

ANALYSIS #	1
PHASE	MUSC
SAMPLE #	DW10C
CIRCLE #	1
GRAIN #	1
SIO2	45.41
AL2O3	38.34
TIO2	.08
FE2O3	0.00
FEO	.01
MGO	.02
MNO	0.00
ZNO	0.00
CAO	.07
BAO	0.00
NA2O	4.84
K2O	3.42
H2O	0.00
F	.13
CL	0.00
TOTAL	92.32
# ANIONS	12
SI	3.01
AL	3.00
TI	0.00
FE+3	0.00
FE+2	0.00
MG	0.00
MN	0.00
ZN	0.00
CA	0.00
BA	0.00
NA	.62
K	.29
OH	1.97
F	.03
CL	0.00
SI+ALIV	4.00
ALVI+FM+ZN+TI	2.02
CA+BA+NA+K	.92
OH+F+CL	2.00
FE/FE+MG	.22

ANALYSIS #	1	2	3	4
PHASE				MUSC
SAMPLE #	DW10D	DW10D	DW10D	DW10D
CIRCLE #	0	0	0	0
GRAIN #	1	2	3	4
SIO2	32.16	32.25	45.93	45.86
AL2O3	56.25	55.80	38.44	39.41
TIO2	.02	.07	.03	.21
FE2O3	0.00	0.00	0.00	0.00
FEO	.02	0.00	0.00	.01
MGO	0.00	0.00	0.00	0.00
MNO	0.00	0.00	0.00	0.00
ZNO	0.00	0.00	0.00	0.00
CAO	0.00	.01	0.00	.01
BAO	0.00	0.00	0.00	0.00
NA2O	0.00	0.00	1.05	6.19
K2O	0.00	0.00	.30	2.06
H2O	0.00	0.00	0.00	0.00
F	14.66	15.10	.02	.16
CL	0.00	0.00	0.00	0.00
TOTAL	103.11	103.23	85.77	93.91
# ANIONS				12
SI	.98	.99	2.00	2.98
AL	2.02	2.01	1.97	3.02
TI	0.00	0.00	0.00	.01
FE+3	0.00	0.00	0.00	0.00
FE+2	0.00	0.00	0.00	0.00
MG	0.00	0.00	0.00	0.00
MN	0.00	0.00	0.00	0.00
ZN	0.00	0.00	0.00	0.00
CA	0.00	0.00	0.00	0.00
BA	0.00	0.00	0.00	0.00
NA	0.00	0.00	.09	.78
K	0.00	0.00	.02	.17
OH	.58	.54	4.00	1.97
F	1.42	1.46	0.00	.03
CL	0.00	0.00	0.00	0.00
SI+ALIV				4.00
ALVI+FM+ZN+TI				2.02
CA+BA+NA+K				.95
OH+F+CL				2.00
FE/FE+MG				1.00

PHASE	MUSC	MUSC	ALS	
SAMPLE #	DW14	DW14	DW14	DW14
CIRCLE #				
GRAIN #	1	2	3	4
SIO2	47.49	47.89	37.86	.28
AL2O3	40.12	39.80	64.42	.50
TIO2	.14	.15	.01	96.13
FE2O3	0.00	0.00	0.00	0.00
FEO	.07	.05	.04	.17
MGO	.15	.12	.03	0.00
MNO	0.00	.02	0.00	.08
ZNO	0.00	0.00	0.00	0.00
CAO	.13	.08	0.00	.04
BAO	0.00	.14	0.00	.59
NA2O	5.23	5.49	0.00	0.00
K2O	1.23	1.59	0.00	.03
H2O	0.00	0.00	0.00	0.00
F	.19	.26	.05	.08
CL	0.00	0.00	0.00	0.00
TOTAL	94.75	95.59	102.41	97.90
# ANIONS	12	12	5	
SI	3.03	3.04	1.00	0.00
AL	3.02	2.98	2.00	.01
TI	.01	.01	0.00	.99
FE+3	0.00	0.00	0.00	0.00
FE+2	0.00	0.00	0.00	0.00
MG	.01	.01	0.00	0.00
MN	0.00	0.00	0.00	0.00
ZN	0.00	0.00	0.00	0.00
CA	.01	.01	0.00	0.00
BA	0.00	0.00	0.00	0.00
NA	.65	.68	0.00	0.00
K	.10	.13	0.00	0.00
OH	1.96	1.95	0.00	0.00
F	.04	.05	0.00	0.00
CL	0.00	0.00	0.00	0.00
SI+ALIV	4.00	4.00	1.00	
ALVI+FM+ZN+TI	2.07	2.05	2.00	
CA+BA+NA+K	.76	.81	0.00	
OH+F+CL	2.00	2.00	0.00	
FE/FE+MG	.21	.19	.43	

PHASE	MUSC	MUSC	MUSC
SAMPLE #	DW14	DW14	DW14
CIRCLE #			
GRAIN #	5	6	7
SIO2	47.02	45.65	45.55
AL2O3	40.10	36.08	36.11
TIO2	.16	.57	.55
FE2O3	0.00	0.00	0.00
FEO	.03	.13	.01
MGO	.12	.78	.56
MNO	0.00	0.00	0.00
ZNO	0.00	0.00	0.00
CAO	.11	.04	.03
BAO	0.00	.09	.06
NA2O	5.46	2.01	2.02
K2O	1.38	6.95	6.97
H2O	0.00	0.00	0.00
F	.29	.35	.33
CL	0.00	0.00	0.00
TOTAL	94.67	92.65	92.19
# ANIONS	12	12	12
SI	3.01	3.07	3.07
AL	3.03	2.86	2.87
TI	.01	.03	.03
FE+3	0.00	0.00	0.00
FE+2	0.00	.01	0.00
MG	.01	.08	.06
MN	0.00	0.00	0.00
ZN	0.00	0.00	0.00
CA	.01	0.00	0.00
BA	0.00	0.00	0.00
NA	.68	.26	.26
K	.11	.60	.60
OH	1.94	1.93	1.93
F	.06	.07	.07
CL	0.00	0.00	0.00
SI+ALIV	4.00	4.00	4.00
ALVI+FM+ZN+TI	2.06	2.04	2.03
CA+BA+NA+K	.80	.86	.87
OH+F+CL	2.00	2.00	2.00
FE/FE+MG	.12	.09	.01

ANALYSIS #	1	2	3	4
PHASE	MUSC	MUSC	MUSC	MUSC
SAMPLE #	DW22	DW22	DW22	DW22
CIRCLE #	A	A	A	A
GRAIN #	1	2	3	4
SIO2	46.46	45.91	45.66	45.89
AL2O3	36.96	37.86	37.38	37.74
TIO2	.27	.27	.27	.27
FE2O3	0.00	0.00	0.00	0.00
FEO	0.00	0.00	0.00	0.00
MGO	.02	.02	.03	.01
MNO	.02	0.00	.02	.01
ZNO	0.00	0.00	0.00	0.00
CAO	0.00	0.00	0.00	0.00
BAO	0.00	0.00	0.00	0.00
NA2O	6.16	5.34	4.98	5.73
K2O	1.90	3.00	3.53	2.68
H2O	0.00	0.00	0.00	0.00
F	.30	.21	.15	.12
CL	0.00	0.00	0.00	0.00
TOTAL	92.09	92.61	92.02	92.45
# ANIONS	12	12	12	12
SI	3.08	3.04	3.04	3.04
AL	2.89	2.95	2.94	2.94
TI	.01	.01	.01	.01
FE+3	0.00	0.00	0.00	0.00
FE+2	0.00	0.00	0.00	0.00
MG	0.00	0.00	0.00	0.00
MN	0.00	0.00	0.00	0.00
ZN	0.00	0.00	0.00	0.00
CA	0.00	0.00	0.00	0.00
BA	0.00	0.00	0.00	0.00
NA	.79	.68	.64	.74
K	.16	.25	.30	.23
OH	1.94	1.96	1.97	1.97
F	.06	.04	.03	.03
CL	0.00	0.00	0.00	0.00
SI+ALIV	4.00	4.00	4.00	4.00
ALVI+FM+ZN+TI	1.99	2.00	2.00	2.00
CA+BA+NA+K	.95	.94	.94	.96
OH+F+CL	2.00	2.00	2.00	2.00
FE/FE+MG	0.00	0.00	0.00	0.00

PHASE	ALS	MUSC	ALS	
SAMPLE #	DW28	DW28	DW28	DW28
CIRCLE #				
GRAIN #	1	3	4	5
SIO2	37.14	46.73	38.16	.13
AL2O3	63.16	35.77	63.28	.10
TIO2	0.00	.57	0.00	95.50
FE2O3	0.00	0.00	0.00	0.00
FEO	.01	.29	.01	.51
MGO	.01	.50	.09	.01
MNO	.02	.02	.03	.08
ZNO	0.00	0.00	0.00	0.00
CAO	.01	.06	.01	.04
BAO	0.00	.57	.09	.41
NA2O	0.00	2.06	.02	.01
K2O	0.00	6.69	0.00	.03
H2O	0.00	0.00	0.00	0.00
F	.01	.30	.14	.01
CL	0.00	0.00	0.00	0.00
TOTAL	100.36	93.56	101.83	96.83
# ANIONS	5	12	5	
SI	1.00	3.11	1.01	0.00
AL	2.00	1.92	1.98	0.00
TI	0.00	.03	0.00	.99
FE+3	0.00	0.00	0.00	0.00
FE+2	0.00	.02	0.00	.01
MG	0.00	.05	0.00	0.00
MN	0.00	0.00	0.00	0.00
ZN	0.00	0.00	0.00	0.00
CA	0.00	0.00	0.00	0.00
BA	0.00	.01	0.00	0.00
NA	0.00	.27	0.00	0.00
K	0.00	.57	0.00	0.00
OH	0.00	1.94	0.00	0.00
F	0.00	.06	.01	0.00
CL	0.00	0.00	0.00	0.00
SI+ALIV	1.00	4.00	1.01	
ALVI+FM+ZN+TI	2.00	1.13	1.98	
CA+BA+NA+K	0.00	.85	0.00	
OH+F+CL	0.00	2.00	.01	
FE/FE+MG	.36	.25	.06	

PHASE	MUSC	MUSC	MUSC	MUSC
SAMPLE #	DW30	DW30	DW30	DW30
CIRCLE #				
GRAIN #	1	2	3	4
SIO2	44.92	45.40	44.60	45.29
AL2O3	35.39	35.58	35.34	34.80
TIO2	.62	.38	.42	.40
FE2O3	0.00	0.00	0.00	0.00
FEO	1.71	1.64	2.31	2.01
MGO	.38	.40	.58	.58
MNO	.02	.02	0.00	.02
ZNO	0.00	0.00	0.00	0.00
CAO	.03	.04	.04	.01
BAO	.10	.29	.27	.41
NA2O	1.46	1.43	1.49	1.36
K2O	7.73	8.02	7.88	7.44
H2O	0.00	0.00	0.00	0.00
F	.16	.35	.28	.33
CL	0.00	0.00	0.00	0.00
TOTAL	92.52	93.55	93.21	92.65
# ANIONS	12	12	12	12
SI	3.05	3.07	3.03	3.08
AL	2.84	2.83	2.83	2.79
TI	.03	.02	.02	.02
FE+3	0.00	0.00	0.00	0.00
FE+2	.10	.09	.13	.11
MG	.04	.04	.06	.06
MN	0.00	0.00	0.00	0.00
ZN	0.00	0.00	0.00	0.00
CA	0.00	0.00	0.00	0.00
BA	0.00	.01	.01	.01
NA	.19	.19	.20	.18
K	.67	.69	.68	.65
OH	1.97	1.93	1.94	1.93
F	.03	.07	.06	.07
CL	0.00	0.00	0.00	0.00
SI+ALIV	4.00	4.00	4.00	4.00
ALVI+FM+ZN+TI	2.06	2.05	2.08	2.07
CA+BA+NA+K	.87	.89	.89	.84
OH+F+CL	2.00	2.00	2.00	2.00
FE/FE+MG	.72	.70	.69	.66

ANALYSIS #	1	2	3	4
PHASE	MUSC	ALS	MUSC	
SAMPLE #	DE31	DE31	DE31	DE31
CIRCLE #				
GRAIN #	1	2	3	4
SIO2	46.90	37.02	48.08	33.17
AL2O3	35.86	64.60	36.02	58.69
TIO2	.65	0.00	.63	0.00
FE2O3	0.00	0.00	0.00	0.00
FEO	.09	0.00	.11	0.00
MGO	.98	.03	.98	0.00
MNO	0.00	0.00	0.00	0.00
ZNO	0.00	0.00	0.00	0.00
CAO	0.00	0.00	.02	0.00
BAO	.34	0.00	.36	0.00
NA2O	1.72	0.00	1.66	0.00
K2O	7.10	0.00	7.37	0.00
H2O	0.00	0.00	0.00	0.00
F	.53	.03	.61	17.65
CL	0.00	0.00	0.00	0.00
TOTAL	94.17	101.68	95.84	109.51
# ANIONS	12	5	12	
SI	3.11	.98	3.13	.98
AL	2.80	2.02	2.77	2.03
TI	.03	0.00	.03	0.00
FE+3	0.00	0.00	0.00	0.00
FE+2	0.00	0.00	.01	0.00
MG	.10	0.00	.10	0.00
MN	0.00	0.00	0.00	0.00
ZN	0.00	0.00	0.00	0.00
CA	0.00	0.00	0.00	0.00
BA	.01	0.00	.01	0.00
NA	.22	0.00	.21	0.00
K	.60	0.00	.61	0.00
OH	1.89	0.00	1.87	.36
F	.11	0.00	.13	1.64
CL	0.00	0.00	0.00	0.00
SI+ALIV	4.00	1.00	4.00	
ALVI+FM+ZN+TI	2.04	2.01	2.03	
CA+BA+NA+K	.83	0.00	.83	
OH+F+CL	2.00	0.00	2.00	
FE/FE+MG	.05	0.00	.06	

ANALYSIS #	5	6	7	8
PHASE				MUSC
SAMPLE #	DE33	DE33	DE33	DE33
CIRCLE #				
GRAIN #	5	6	7	8
SIO2	32.14	32.02	32.27	46.95
AL2O3	56.05	56.16	56.12	38.84
TIO2	0.00	0.00	0.00	.19
FE2O3	0.00	0.00	0.00	0.00
FEO	0.00	0.00	0.00	.14
MGO	0.00	0.00	0.00	.06
MNO	0.00	0.00	0.00	.02
ZNO	0.00	0.00	0.00	0.00
CAO	0.00	0.00	0.00	.03
BAO	0.00	0.00	0.00	0.00
NA2O	0.00	0.00	0.00	4.33
K2O	0.00	0.00	0.00	1.96
H2O	0.00	0.00	0.00	0.00
F	17.07	17.13	17.07	.29
CL	0.00	0.00	0.00	0.00
TOTAL	105.26	105.31	105.46	92.81
# ANIONS				12
SI	.98	.98	.99	3.06
AL	2.02	2.03	2.02	1.12
TI	0.00	0.00	0.00	.01
FE+3	0.00	0.00	0.00	0.00
FE+2	0.00	0.00	0.00	.01
MG	0.00	0.00	0.00	.01
MN	0.00	0.00	0.00	0.00
ZN	0.00	0.00	0.00	0.00
CA	0.00	0.00	0.00	0.00
BA	0.00	0.00	0.00	0.00
NA	0.00	0.00	0.00	.55
K	0.00	0.00	0.00	.16
OH	.35	.34	.35	1.94
F	1.65	1.66	1.65	.06
CL	0.00	0.00	0.00	0.00
SI+ALIV				4.00
ALVI+FM+ZN+TI				.20
CA+BA+NA+K				.71
OH+F+CL				2.00
FE/FE+MG				.57

ANALYSIS #	1	2	3	4
PHASE	MUSC	MUSC	ALS	
SAMPLE #	DE34	DE34	DE34	DE34
CIRCLE #				
GRAIN #	1	2	3	4
SIO2	45.46	46.17	35.83	.01
AL2O3	37.47	37.55	62.75	.30
TIO2	.45	.34	0.00	97.93
FE2O3	0.00	0.00	0.00	0.00
FEO	.03	.01	.01	.08
MGO	.48	.25	.06	.03
MNO	0.00	0.00	0.00	.06
ZNO	0.00	0.00	0.00	0.00
CAO	.01	.02	.01	.02
BAO	.05	0.00	0.00	.61
NA2O	2.28	2.47	0.00	0.00
K2O	6.85	6.51	0.00	.03
H2O	0.00	0.00	0.00	0.00
F	.76	.49	.04	.06
CL	0.00	0.00	0.00	0.00
TOTAL	93.84	93.81	98.70	99.13
# ANIONS	12	12	5	
SI	3.03	3.06	.98	0.00
AL	2.94	2.93	2.02	0.00
TI	.02	.02	0.00	.99
FE+3	0.00	0.00	0.00	0.00
FE+2	0.00	0.00	0.00	0.00
MG	.05	.02	0.00	0.00
MN	0.00	0.00	0.00	0.00
ZN	0.00	0.00	0.00	0.00
CA	0.00	0.00	0.00	0.00
BA	0.00	0.00	0.00	0.00
NA	.29	.32	0.00	0.00
K	.58	.55	0.00	0.00
OH	1.84	1.90	0.00	0.00
F	.16	.10	0.00	0.00
CL	0.00	0.00	0.00	0.00
SI+ALIV	4.00	4.00	1.00	
ALVI+FM+ZN+TI	2.04	2.03	2.01	
CA+BA+NA+K	.88	.87	0.00	
OH+F+CL	2.00	2.00	0.00	
FE/FE+MG	.03	.02	.09	

ANALYSIS #	5	6	8	9
PHASE	MUSC	MUSC	MUSC	MUSC
SAMPLE #	DE34	DE34	DE34	DE34
CIRCLE #				
GRAIN #	5	6	8	9
SIO2	46.11	46.08	46.27	45.53
AL2O3	37.82	39.53	39.47	37.23
TIO2	.48	.11	.07	.47
FE2O3	0.00	0.00	0.00	0.00
FEO	.03	0.00	.01	.05
MGO	.04	.07	.06	.43
MNO	0.00	0.00	0.00	0.00
ZNO	0.00	0.00	0.00	0.00
CAO	.06	.04	.06	.04
BAO	.05	0.00	0.00	.04
NA2O	1.90	4.81	5.44	2.00
K2O	6.33	1.72	1.29	6.52
H2O	0.00	0.00	0.00	0.00
F	.48	.55	.35	.59
CL	0.00	0.00	0.00	0.00
TOTAL	93.30	92.91	93.02	92.90
# ANIONS	12	12	12	12
SI	3.06	3.02	3.02	3.05
AL	2.96	3.05	3.03	2.94
TI	.02	.01	0.00	.02
FE+3	0.00	0.00	0.00	0.00
FE+2	0.00	0.00	0.00	0.00
MG	0.00	.01	.01	.04
MN	0.00	0.00	0.00	0.00
ZN	0.00	0.00	0.00	0.00
CA	0.00	0.00	0.00	0.00
BA	0.00	0.00	0.00	0.00
NA	.24	.61	.69	.26
K	.54	.14	.11	.56
OH	1.90	1.89	1.93	1.88
F	.10	.11	.07	.12
CL	0.00	0.00	0.00	0.00
SI+ALIV	4.00	4.00	4.00	4.00
ALVI+FM+ZN+TI	2.04	2.08	2.06	2.05
CA+BA+NA+K	.79	.76	.80	.82
OH+F+CL	2.00	2.00	2.00	2.00
FE/FE+MG	.28	0.00	.09	.06

ANALYSIS #	10	11	12
PHASE	MUSC		ALS
SAMPLE #	DE34	DE34	DE34
CIRCLE #			
GRAIN #	10	11	12
SIO2	45.76	.10	37.38
AL2O3	38.58	.20	64.21
TIO2	.23	98.05	0.00
FE2O3	0.00	0.00	0.00
FEO	.01	.08	.02
MGO	.12	.03	.01
MNO	0.00	.05	0.00
ZNO	0.00	0.00	0.00
CAO	.05	.04	.01
BAO	0.00	.46	0.00
NA2O	4.22	.01	0.00
K2O	3.80	.04	0.00
H2O	0.00	0.00	0.00
F	.29	.23	.01
CL	0.00	0.00	0.00
TOTAL	93.06	99.29	101.64
# ANIONS	12		5
SI	3.02	0.00	.99
AL	3.00	0.00	2.01
TI	.01	.99	0.00
FE+3	0.00	0.00	0.00
FE+2	0.00	0.00	0.00
MG	.01	0.00	0.00
MN	0.00	0.00	0.00
ZN	0.00	0.00	0.00
CA	0.00	0.00	0.00
BA	0.00	0.00	0.00
NA	.54	0.00	0.00
K	.32	0.00	0.00
OH	1.94	0.00	0.00
F	.06	.01	0.00
CL	0.00	0.00	0.00
SI+ALIV	4.00		1.00
ALVI+FM+ZN+TI	2.04		2.00
CA+BA+NA+K	.86		0.00
OH+F+CL	2.00		0.00
FE/FE+MG	.04		.53

ANALYSIS #	1	2	3	4
PHASE	MUSC	ALS	MUSC	MUSC
SAMPLE #	DE36	DE36	DE36	DE36
CIRCLE #				
GRAIN #	1	2	3	4
SIO2	47.22	36.55	46.54	48.05
AL203	37.38	63.27	36.12	37.25
TIO2	.38	0.00	.53	.53
FE203	0.00	0.00	0.00	0.00
FEO	.03	.01	.07	0.00
MGO	.36	0.00	.48	.46
MNO	0.00	0.00	0.00	0.00
ZNO	0.00	0.00	0.00	0.00
CAO	.04	0.00	.04	.02
BAO	.05	0.00	.04	.06
NA20	2.64	0.00	2.17	2.30
K20	6.73	0.00	6.70	6.73
H20	0.00	0.00	0.00	0.00
F	.55	.02	.69	.53
CL	0.00	0.00	0.00	0.00
TOTAL	95.38	99.85	93.38	95.93
# ANIONS	12	5	12	12
SI	3.08	.99	3.10	3.11
AL	2.87	2.02	2.84	2.84
TI	.02	0.00	.03	.03
FE+3	0.00	0.00	0.00	0.00
FE+2	0.00	0.00	0.00	0.00
MG	.04	0.00	.05	.04
MN	0.00	0.00	0.00	0.00
ZN	0.00	0.00	0.00	0.00
CA	0.00	0.00	0.00	0.00
BA	0.00	0.00	0.00	0.00
NA	.33	0.00	.28	.29
K	.56	0.00	.57	.56
OH	1.89	0.00	1.85	1.89
F	.11	0.00	.15	.11
CL	0.00	0.00	0.00	0.00
SI+ALIV	4.00	1.00	4.00	4.00
ALVI+FM+ZN+TI	2.01	2.00	2.02	2.02
CA+BA+NA+K	.90	0.00	.85	.85
OH+F+CL	2.00	0.00	2.00	2.00
FE/FE+MG	.04	1.00	.08	0.00

ANALYSIS #	1	2	3	4
PHASE	FELD	BIOT	GAR	GAR
SAMPLE #	CC12	CC12	CC12	CC12
CIRCLE #	A	A	A	A
GRAIN #	1	2	3	4
SIO2	64.60	37.51	39.76	30.25
AL2O3	22.79	19.04	21.49	21.38
TIO2	0.00	1.35	.10	.10
FE2O3	0.00	0.00	0.00	0.00
FEO	.04	15.61	29.49	29.70
MGO	.02	11.50	7.05	6.19
MNO	.01	.01	.86	.83
ZNO	0.00	0.00	0.00	0.00
CAO	3.65	.07	1.72	2.37
BAO	0.00	0.00	0.00	0.00
NA2O	9.05	.05	0.00	.03
K2O	.06	8.51	.02	.02
H2O	0.00	0.00	0.00	0.00
F	0.00	0.00	0.00	0.00
CL	0.00	0.00	0.00	0.00
TOTAL	100.22	93.65	100.49	90.87
# ANIONS	8	12	12	12
SI	2.84	2.82	3.07	2.67
AL	1.18	1.69	1.96	2.23
TI	0.00	.08	.01	.01
FE+3	0.00	0.00	0.00	0.00
FE+2	0.00	.98	1.90	2.19
MG	0.00	1.29	.81	.82
MN	0.00	0.00	.06	.06
ZN	0.00	0.00	0.00	0.00
CA	.17	.01	.14	.22
BA	0.00	0.00	0.00	0.00
NA	.77	.01	0.00	.01
K	0.00	.82	0.00	0.00
OH	0.00	2.00	0.00	0.00
F	0.00	0.00	0.00	0.00
CL	0.00	0.00	0.00	0.00
SI+ALIV	4.00	4.00	3.07	3.00
ALVI+FM+ZN+TI	.02	2.85	4.73	4.98
CA+BA+NA+K	.95	.83	.14	.23
OH+F+CL	0.00	2.00	0.00	0.00
FE/FE+MG	.53	.43	.70	.73

ANALYSIS #	1	2	3	4
PHASE	GAR	BIOT	CHL	FELD
SAMPLE #	CC45	CC45	CC45	CC45
CIRCLE #	A	A	A	A
GRAIN #	1	2	3	4
SIO2	38.53	35.98	26.78	62.66
AL2O3	20.97	16.64	21.53	21.67
TIO2	.10	1.83	.11	.03
FE2O3	0.00	0.00	0.00	0.00
FEO	30.54	14.92	17.54	.02
MGO	6.23	13.74	19.45	.03
MNO	1.17	.07	.08	0.00
ZNO	0.00	0.00	0.00	0.00
CAO	.88	.03	0.00	2.29
BAO	0.00	0.00	0.00	0.00
NA2O	.03	.13	0.00	8.49
K2O	.02	8.20	.09	.04
H2O	0.00	0.00	0.00	0.00
F	.06	.39	.11	0.00
CL	0.00	0.00	0.00	0.00
TOTAL	98.53	91.93	85.69	95.23
# ANIONS	12	12	18	8
SI	3.06	2.78	2.77	2.87
AL	1.96	1.51	2.62	1.17
TI	.01	.11	.01	0.00
FE+3	0.00	0.00	0.00	0.00
FE+2	2.03	.96	1.51	0.00
MG	.74	1.58	2.99	0.00
MN	.08	0.00	.01	0.00
ZN	0.00	0.00	0.00	0.00
CA	.07	0.00	0.00	.11
BA	0.00	0.00	0.00	0.00
NA	0.00	.02	0.00	.75
K	0.00	.81	.01	0.00
OH	0.00	1.90	7.96	0.00
F	.02	.10	.04	0.00
CL	0.00	0.00	0.00	0.00
SI+ALIV	3.06	4.00	4.00	4.00
ALVI+FM+ZN+TI	4.81	2.94	5.91	.05
CA+BA+NA+K	.08	.83	.01	.87
OH+F+CL	.02	2.00	8.00	0.00
FE/FE+MG	.73	.38	.34	.27

ANALYSIS #	5	6	7	8
PHASE	FELD	AMPH	AMPH	CHL
SAMPLE #	CC45	CC45	CC45	CC45
CIRCLE #	A	A	A	A
GRAIN #	4	5	6	7
SIO2	62.66	43.07	41.09	43.67
AL2O3	21.67	15.73	14.34	14.25
TIO2	.03	.30	.28	.10
FE2O3	0.00	0.00	0.00	0.00
FEO	.02	20.90	19.78	9.88
MGO	.03	13.77	13.50	7.86
MNO	0.00	.26	.31	.09
ZNO	0.00	0.00	0.00	0.00
CAO	2.29	.23	.21	.75
BAO	0.00	0.00	0.00	0.00
NA2O	8.49	1.63	1.55	3.23
K2O	.04	.02	.15	.19
H2O	0.00	0.00	0.00	0.00
F	0.00	.20	.18	.12
CL	0.00	0.00	0.00	0.00
TOTAL	95.23	96.11	91.39	80.14
# ANIONS	8	24	24	18
SI	2.87	6.41	6.44	4.47
AL	1.17	2.76	2.65	1.72
TI	0.00	.03	.03	.01
FE+3	0.00	0.00	0.00	0.00
FE+2	0.00	2.60	2.59	.85
MG	0.00	3.06	3.15	1.20
MN	0.00	.03	.04	.01
ZN	0.00	0.00	0.00	0.00
CA	.11	.04	.04	.08
BA	0.00	0.00	0.00	0.00
NA	.75	.47	.47	.64
K	0.00	0.00	.03	.02
OH	0.00	1.91	1.91	7.96
F	0.00	.09	.09	.04
CL	0.00	0.00	0.00	0.00
SI+ALIV	4.00	8.00	8.00	4.47
ALVI+FM+ZN+TI	.05	6.90	6.91	3.78
CA+BA+NA+K	.87	.51	.54	.75
OH+F+CL	0.00	2.00	2.00	8.00
FE/FE+MG	.27	.46	.45	.41

ANALYSIS #	1	2	3	4
PHASE	AMPH	AMPH	BIOT	FELD
SAMPLE #	CC53	CC53	CC53	CC53
CIRCLE #	B	B	3	A
GRAIN #	1	2	3	4
SIO2	48.23	47.31	37.19	58.70
AL2O3	9.62	8.74	16.42	23.92
TIO2	.23	.25	1.31	.02
FE2O3	0.00	0.00	0.00	0.00
FEO	19.43	18.50	12.09	.01
MGO	16.72	16.42	15.18	.01
MNO	1.89	.55	.02	0.00
ZNO	0.00	0.00	0.00	0.00
CAO	.84	.53	.16	5.59
BAO	0.00	0.00	0.00	0.00
NA2O	.95	.93	.28	6.96
K2O	.02	.08	7.45	.04
H2O	0.00	0.00	0.00	0.00
F	.10	.07	.19	.05
CL	0.00	0.00	0.00	0.00
TOTAL	98.03	93.38	90.29	95.30
# ANIONS	24	24	12	8
SI	7.00	7.14	2.85	2.72
AL	1.65	1.55	1.49	1.31
TI	.03	.03	.08	0.00
FE+3	0.00	0.00	0.00	0.00
FE+2	2.36	2.34	.78	0.00
MG	3.62	3.69	1.74	0.00
MN	.23	.07	0.00	0.00
ZN	0.00	0.00	0.00	0.00
CA	.13	.09	.01	.28
BA	0.00	0.00	0.00	0.00
NA	.27	.27	.04	.63
K	0.00	.02	.73	0.00
OH	1.95	1.97	1.95	0.00
F	.05	.03	.05	.01
CL	0.00	0.00	0.00	0.00
SI+ALIV	8.00	8.00	4.00	4.00
ALVI+FM+ZN+TI	6.88	6.82	2.93	.03
CA+BA+NA+K	.40	.37	.78	.91
OH+F+CL	2.00	2.00	2.00	.01
FE/FE+MG	.39	.39	.31	.36

ANALYSIS #	1	2	3	4
PHASE	GAR	GAR	BIOT	BIOT
SAMPLE #	CC75	CC75	CC75	CC75
CIRCLE #	1	A	A	A
GRAIN #	1	2	3	4
SIO2	38.64	38.43	36.73	36.67
AL2O3	21.06	20.92	18.26	17.67
TIO2	.09	.09	1.39	1.54
FE2O3	0.00	0.00	0.00	0.00
FEO	29.80	30.52	13.05	13.66
MGO	6.31	5.60	14.60	14.17
MNO	3.15	3.25	.04	.03
ZNO	0.00	0.00	0.00	0.00
CAO	.20	.47	.10	.10
BAO	0.00	0.00	0.00	0.00
NA2O	.03	.03	.53	.58
K2O	.03	.03	7.36	7.79
H2O	0.00	0.00	0.00	0.00
F	.07	.09	.17	.20
CL	0.00	0.00	0.00	0.00
TOTAL	99.38	99.43	92.23	92.41
# ANIONS	12	12	12	12
SI	3.05	3.05	2.77	2.78
AL	1.96	1.96	1.62	1.58
TI	.01	.01	.08	.09
FE+3	0.00	0.00	0.00	0.00
FE+2	1.97	2.02	.82	.87
MG	.74	.66	1.64	1.60
MN	.21	.22	0.00	0.00
ZN	0.00	0.00	0.00	0.00
CA	.02	.04	.01	.01
BA	0.00	0.00	0.00	0.00
NA	0.00	0.00	.08	.09
K	0.00	0.00	.71	.75
OH	0.00	0.00	1.96	1.95
F	.02	.02	.04	.05
CL	0.00	0.00	0.00	0.00
SI+ALIV	3.05	3.05	4.00	4.00
ALVI+FM+ZN+TI	4.89	4.87	2.94	2.92
CA+BA+NA+K	.02	.05	.79	.85
OH+F+CL	.02	.02	2.00	2.00
FE/FE+MG	.73	.75	.33	.35

ANALYSIS #	6	7	8	9
PHASE	FELD	ALS		
SAMPLE #	CC75	CC75	CC75	CC75
CIRCLE #	A	A	A	A
GRAIN #	6	7	8	9
SIO2	66.84	37.28	.65	.68
AL203	20.11	59.78	.19	.18
TIO2	.02	.01	47.25	96.24
FE203	0.00	0.00	0.00	0.00
FEO	.12	.56	46.20	1.86
MGO	.01	.05	.44	0.00
MNO	0.00	0.00	.60	.02
ZNO	0.00	0.00	0.00	0.00
CAO	.82	0.00	.04	.05
BAO	0.00	0.00	0.00	0.00
NA20	9.97	.01	0.00	0.00
K20	.02	0.00	.05	.04
H20	0.00	0.00	0.00	0.00
F	.02	0.00	.09	.09
CL	0.00	0.00	0.00	0.00
TOTAL	97.93	97.69	95.51	99.16
# ANIONS	8	5		
SI	2.97	1.03	.02	.01
AL	1.05	1.95	.01	0.00
TI	0.00	0.00	.95	.98
FE+3	0.00	0.00	0.00	0.00
FE+2	0.00	.01	1.03	.02
MG	0.00	0.00	.02	0.00
MN	0.00	0.00	.01	0.00
ZN	0.00	0.00	0.00	0.00
CA	.04	0.00	0.00	0.00
BA	0.00	0.00	0.00	0.00
NA	.86	0.00	0.00	0.00
K	0.00	0.00	0.00	0.00
OH	0.00	0.00	0.00	0.00
F	0.00	0.00	.01	0.00
CL	0.00	0.00	0.00	0.00
SI+ALIV	4.00	1.03		
ALVI+FM+ZN+TI	.03	1.96		
CA+BA+NA+K	.90	0.00		
OH+F+CL	0.00	0.00		
FE/FE+MG	.87	.86		

ANALYSIS #	1	2
PHASE	STAUR	STAUR
SAMPLE #	CC75ST	CC75ST
CIRCLE #	1	1
GRAIN #	1	1
SIO2	28.57	28.43
AL2O3	48.14	48.80
TIO2	.72	.71
FE2O3	0.00	0.00
FEO	13.31	13.10
MGO	3.05	3.02
MNO	.23	.22
ZNO	.60	.62
CAO	.02	.02
BAO	0.00	0.00
NA2O	.01	0.00
K2O	.01	.01
H2O	0.00	0.00
F	.03	.02
CL	0.00	0.00
TOTAL	94.69	94.95
# ANIONS	48	48
SI	8.23	8.16
AL	16.34	16.50
TI	.16	.15
FE+3	0.00	0.00
FE+2	3.21	3.14
MG	1.31	1.29
MN	.06	.05
ZN	.13	.13
CA	.01	.01
BA	0.00	0.00
NA	.01	0.00
K	0.00	0.00
OH	3.97	3.98
F	.03	.02
CL	0.00	0.00
SI+ALIV		
ALVI+FM+ZN+TI		
CA+BA+NA+K		
OH+F+CL		
FE/FE+MG	.71	.71

ANALYSIS #	1	2	3	4
PHASE	STAUR	AMPH	ALS	FELD
SAMPLE #	CC95	CC95	CC95	CC95
CIRCLE #	A	A	A	A
GRAIN #	1	2	3	4
SIO2	27.92	41.00	36.95	64.31
AL2O3	49.64	18.04	58.76	19.77
TIO2	.49	.28	0.00	.01
FE2O3	0.00	0.00	0.00	0.00
FEO	12.59	19.08	.89	.02
MGO	2.79	13.17	.06	0.00
MNO	.09	.41	0.00	0.00
ZNO	0.00	0.00	0.00	0.00
CAO	0.00	.11	0.00	1.08
BAO	0.00	0.00	0.00	0.00
NA2O	.02	2.03	0.00	9.88
K2O	.01	.02	0.00	.04
H2O	0.00	0.00	0.00	0.00
F	0.00	0.00	0.00	0.00
CL	0.00	0.00	0.00	0.00
TOTAL	93.55	94.14	96.66	95.11
# ANIONS	48	24	5	8
SI	8.07	6.19	1.03	2.95
AL	16.91	3.21	1.94	1.07
TI	.11	.03	0.00	0.00
FE+3	0.00	0.00	0.00	0.00
FE+2	3.04	2.41	.02	0.00
MG	1.20	2.96	0.00	0.00
MN	.02	.05	0.00	0.00
ZN	0.00	0.00	0.00	0.00
CA	0.00	.02	0.00	.05
BA	0.00	0.00	0.00	0.00
NA	.01	.59	0.00	.88
K	0.00	0.00	0.00	0.00
OH	4.00	2.00	0.00	0.00
F	0.00	0.00	0.00	0.00
CL	0.00	0.00	0.00	0.00
SI+ALIV		8.00	1.03	4.00
ALVI+FM+ZN+TI		6.86	1.96	.02
CA+BA+NA+K		.62	0.00	.93
OH+F+CL		2.00	0.00	0.00
FE/FE+MG	.72	.45	.89	1.00

ANALYSIS #	1	2
PHASE	BIOT	FELD
SAMPLE #	CC111	CC111
CIRCLE #	A	A
GRAIN #	1	2
SIO2	37.69	61.11
AL2O3	17.51	23.58
TIO2	1.44	.01
FE2O3	0.00	0.00
FEO	13.43	.04
MGO	14.50	.03
MNO	.09	0.00
ZNO	0.00	0.00
CAO	.02	4.97
BAO	0.00	0.00
NA2O	.22	8.31
K2O	8.50	.05
H2O	0.00	0.00
F	0.00	0.00
CL	0.00	0.00
TOTAL	93.40	98.10
# ANIONS	12	8
SI	2.82	2.76
AL	1.54	1.25
TI	.08	0.00
FE+3	0.00	0.00
FE+2	.84	0.00
MG	1.62	0.00
MN	.01	0.00
ZN	0.00	0.00
CA	0.00	.24
BA	0.00	0.00
NA	.03	.73
K	.81	0.00
OH	2.00	0.00
F	0.00	0.00
CL	0.00	0.00
SI+ALIV	4.00	4.00
ALVI+FM+ZN+TI	2.91	.01
CA+BA+NA+K	.84	.97
OH+F+CL	2.00	0.00
FE/FE+MG	.34	.43

ANALYSIS #	1	2	3	4
PHASE	GAR	GAR	FELD	MUSC
SAMPLE #	CC115	CC115	CC115	CC115
CIRCLE #	A	A	A	A
GRAIN #	1	1B	2	3
SIO2	37.99	38.14	64.87	45.89
AL2O3	20.63	20.55	21.00	33.10
TIO2	.11	.11	0.00	.07
FE2O3	0.00	0.00	0.00	0.00
FEO	23.73	23.73	0.00	2.27
MGO	5.10	4.42	.02	.99
MNO	9.93	10.79	0.00	0.00
ZNO	0.00	0.00	0.00	0.00
CAO	1.31	.94	1.84	.01
BAO	0.00	0.00	0.00	0.00
NA2O	.03	.04	10.16	1.05
K2O	.02	.03	.07	8.97
H2O	0.00	0.00	0.00	0.00
F	0.00	0.00	0.00	0.00
CL	0.00	0.00	0.00	0.00
TOTAL	98.85	98.75	97.96	92.35
# ANIONS	12	12	8	12
SI	3.04	3.06	2.90	3.14
AL	1.95	1.95	1.11	2.67
TI	.01	.01	0.00	0.00
FE+3	0.00	0.00	0.00	0.00
FE+2	1.59	1.59	0.00	.13
MG	.61	.53	0.00	.10
MN	.67	.73	0.00	0.00
ZN	0.00	0.00	0.00	0.00
CA	.11	.08	.09	0.00
BA	0.00	0.00	0.00	0.00
NA	0.00	.01	.88	.14
K	0.00	0.00	0.00	.78
OH	0.00	0.00	0.00	2.00
F	0.00	0.00	0.00	0.00
CL	0.00	0.00	0.00	0.00
SI+ALIV	3.04	3.06	4.00	4.00
ALVI+FM+ZN+TI	4.82	4.81	.01	2.05
CA+BA+NA+K	.12	.09	.97	.92
OH+F+CL	0.00	0.00	0.00	2.00
FE/FE+MG	.72	.75	0.00	.56

ANALYSIS #	5	6	7	8
PHASE	GAR	GAR	GAR	FELD
SAMPLE #	CC115	CC115	CC115	CC115
CIRCLE #	B	B	B	X
GRAIN #	5	4B	5	6
SIO2	37.52	38.19	38.16	64.20
AL2O3	19.88	20.74	20.38	21.12
TIO2	.15	.09	.09	.01
FE2O3	0.00	0.00	0.00	0.00
FEO	22.94	23.34	23.75	.01
MGO	5.16	5.25	5.58	0.00
MNO	8.75	10.19	9.28	.01
ZNO	0.00	0.00	0.00	0.00
CAO	2.33	.69	.72	2.18
BAO	0.00	0.00	0.00	0.00
NA2O	.06	.03	.07	9.71
K2O	.02	.02	.03	.05
H2O	0.00	0.00	0.00	0.00
F	0.00	0.00	0.00	0.00
CL	0.00	0.00	0.00	0.00
TOTAL	96.81	98.54	98.06	97.29
# ANIONS	12	12	12	8
SI	3.06	3.06	3.07	2.89
AL	1.91	1.96	1.93	1.12
TI	.01	.01	.01	0.00
FE+3	0.00	0.00	0.00	0.00
FE+2	1.56	1.56	1.60	0.00
MG	.63	.63	.67	0.00
MN	.60	.69	.63	0.00
ZN	0.00	0.00	0.00	0.00
CA	.20	.06	.06	.11
BA	0.00	0.00	0.00	0.00
NA	.01	0.00	.01	.85
K	0.00	0.00	0.00	0.00
OH	0.00	0.00	0.00	0.00
F	0.00	0.00	0.00	0.00
CL	0.00	0.00	0.00	0.00
SI+ALIV	3.06	3.06	3.07	4.00
ALVI+FM+ZN+TI	4.71	4.84	4.83	.02
CA+BA+NA+K	.21	.07	.08	.96
OH+F+CL	0.00	0.00	0.00	0.00
FE/FE+MG	.71	.71	.70	1.00

ANALYSIS #	1	2	3	4
PHASE	AMPH	ALS	BIOT	CHL
SAMPLE #	CC139A	CC139A	CC139A	CC139A
CIRCLE #	1	1	1	2
GRAIN #	1	2	3	1
SIO2	46.20	36.99	38.80	44.62
AL203	14.00	58.89	16.61	14.47
TIO2	.18	.03	.81	.26
FE203	0.00	0.00	0.00	0.00
FEO	15.15	.54	9.19	14.38
MGO	17.95	.07	17.70	17.38
MNO	.49	0.00	.05	.63
ZNO	0.00	0.00	0.00	0.00
CAO	.40	0.00	.18	.35
BAO	0.00	0.00	0.00	0.00
NA2O	1.51	0.00	.37	1.61
K2O	.01	.01	7.67	.01
H2O	0.00	0.00	0.00	0.00
F	0.00	0.00	0.00	0.00
CL	0.00	0.00	0.00	0.00
TOTAL	95.89	96.53	91.38	93.71
# ANIONS	24	5	12	18
SI	6.68	1.03	2.89	4.01
AL	2.38	1.94	1.46	1.53
TI	.02	0.00	.05	.02
FE+3	0.00	0.00	0.00	0.00
FE+2	1.83	.01	.57	1.08
MG	3.87	0.00	1.96	2.33
MN	.06	0.00	0.00	.05
ZN	0.00	0.00	0.00	0.00
CA	.06	0.00	.01	.03
BA	0.00	0.00	0.00	0.00
NA	.42	0.00	.05	.28
K	0.00	0.00	.73	0.00
OH	2.00	0.00	2.00	8.00
F	0.00	0.00	0.00	0.00
CL	0.00	0.00	0.00	0.00
SI+ALIV	8.00	1.03	4.00	4.01
ALVI+FM+ZN+TI	6.84	1.96	2.93	5.01
CA+BA+NA+K	.49	0.00	.80	.32
OH+F+CL	2.00	0.00	2.00	8.00
FE/FE+MG	.32	.81	.23	.32

ANALYSIS #	1	2	3	4
PHASE	AMPH	FELD	GAR	AMPH
SAMPLE #	CC157	CC157	CC157	CC157
CIRCLE #	B	B	A	A
GRAIN #	1	2	3	4
SIO2	42.90	61.28	39.68	43.61
AL2O3	15.41	24.51	21.06	14.70
TIO2	.29	.05	.12	.41
FE2O3	0.00	0.00	0.00	0.00
FEO	15.17	0.00	33.24	15.55
MGO	10.34	0.00	6.54	11.64
MNO	.19	0.00	1.72	.21
ZNO	0.00	0.00	0.00	0.00
CAO	10.83	6.16	3.34	10.97
BAO	.11	0.00	0.00	.10
NA2O	2.30	7.66	.03	2.21
K2O	.19	.02	.01	.16
H2O	0.00	0.00	0.00	0.00
F	.11	0.00	.06	.12
CL	0.00	0.00	0.00	0.00
TOTAL	97.84	99.68	105.80	99.68
# ANIONS	24	8	12	24
SI	6.34	2.72	2.99	6.33
AL	2.68	1.28	1.87	2.52
TI	.03	0.00	.01	.04
FE+3	0.00	0.00	0.00	0.00
FE+2	1.87	0.00	2.09	1.89
MG	2.28	0.00	.73	2.52
MN	.02	0.00	.11	.03
ZN	0.00	0.00	0.00	0.00
CA	1.71	.29	.27	1.71
BA	.01	0.00	0.00	.01
NA	.66	.66	0.00	.62
K	.04	0.00	0.00	.03
OH	1.95	0.00	0.00	1.94
F	.05	0.00	.01	.06
CL	0.00	0.00	0.00	0.00
SI+ALIV	8.00	4.00	3.00	8.00
ALVI+FM+ZN+TI	5.22	.01	4.79	5.33
CA+BA+NA+K	2.41	.95	.27	2.36
OH+F+CL	2.00	0.00	.01	2.00
FE/FE+MG	.45	*****	.74	.43

ANALYSIS #	5	6	7	8
PHASE		FELD	AMPH	GAR
SAMPLE #	CC157	CC157	CC157	CC157
CIRCLE #	A	A	X	X
GRAIN #	5	6	7	8
SIO2	.23	61.21	43.17	39.27
AL2O3	.48	23.50	14.19	21.13
TIO2	18.51	.04	.49	.12
FE2O3	0.00	0.00	0.00	0.00
FEO	76.40	0.00	14.93	31.99
MGO	.10	0.00	11.54	6.82
MNO	.16	.05	.25	1.45
ZNO	0.00	0.00	0.00	0.00
CAO	.02	5.23	9.78	3.56
BAO	.31	.01	.05	0.00
NA2O	0.00	7.98	2.49	.03
K2O	.04	.02	.13	.08
H2O	0.00	0.00	0.00	0.00
F	.05	.02	.14	0.00
CL	0.00	0.00	0.00	0.00
TOTAL	96.30	98.06	97.16	104.45
# ANIONS		8	24	12
SI	.01	2.76	6.40	2.98
AL	.02	1.25	2.48	1.89
TI	.60	0.00	.05	.01
FE+3	0.00	0.00	0.00	0.00
FE+2	2.73	0.00	1.85	2.03
MG	.01	0.00	2.55	.77
MN	.01	0.00	.03	.09
ZN	0.00	0.00	0.00	0.00
CA	0.00	.25	1.55	.29
BA	.01	0.00	0.00	0.00
NA	0.00	.70	.72	0.00
K	0.00	0.00	.02	.01
OH	0.00	0.00	1.93	0.00
F	.01	0.00	.07	0.00
CL	0.00	0.00	0.00	0.00
SI+ALIV		4.00	8.00	3.00
ALVI+FM+ZN+TI		.01	5.37	4.77
CA+BA+NA+K		.95	2.30	.30
OH+F+CL		0.00	2.00	0.00
FE/FE+MG		*****	.42	.72

ANALYSIS #	1	2	3	4
PHASE	AMPH	AMPH	AMPH	ALS
SAMPLE #	CC194	CC194	CC194	
CIRCLE #	A	A	A	
GRAIN #	1	2	4	
SIO2	53.54	55.05	53.90	0.00
AL2O3	6.03	4.09	4.38	0.00
TIO2	.17	.12	.18	0.00
FE2O3	0.00	0.00	0.00	0.00
FEO	17.82	16.99	16.64	0.00
MGO	22.41	22.18	21.31	0.00
MNO	.56	.57	.51	0.00
ZNO	0.00	0.00	0.00	0.00
CAO	.48	.44	.49	0.00
BAO	.13	.07	.05	0.00
NA2O	.64	.37	.41	0.00
K2O	0.00	0.00	0.00	0.00
H2O	0.00	0.00	0.00	0.00
F	.09	.13	0.00	0.00
CL	0.00	0.00	0.00	0.00
TOTAL	101.87	100.01	97.87	0.00
# ANIONS	24	24	24	0
SI	7.33	7.62	7.61	0.00
AL	.97	.67	.73	0.00
TI	.02	.01	.02	0.00
FE+3	0.00	0.00	0.00	0.00
FE+2	2.04	1.97	1.97	0.00
MG	4.57	4.58	4.49	0.00
MN	.06	.07	.06	0.00
ZN	0.00	0.00	0.00	0.00
CA	.07	.07	.07	0.00
BA	.01	0.00	0.00	0.00
NA	.17	.10	.11	0.00
K	0.00	0.00	0.00	0.00
OH	1.96	1.94	2.00	0.00
F	.04	.06	0.00	0.00
CL	0.00	0.00	0.00	0.00
SI+ALIV	8.00	8.00	8.00	0.00
ALVI+FM+ZN+TI	7.00	6.91	6.87	0.00
CA+BA+NA+K	.25	.17	.19	0.00
OH+F+CL	2.00	2.00	2.00	0.00
FE/FE+MG	.31	.30	.30	*****

ANALYSIS #	1	2	3	4
PHASE	AMPH	AMPH	CHL	BIOT
SAMPLE #	CC210	CC210	CC210	CC210
CIRCLE #	A	A	A	A
GRAIN #	1	2	3	4
SIO2	44.77	54.90	27.80	40.09
AL2O3	13.76	1.58	22.19	16.72
TIO2	.47	.07	.10	1.31
FE2O3	0.00	0.00	0.00	0.00
FEO	11.35	17.82	12.52	10.41
MGO	12.81	21.99	24.70	18.41
MNO	.16	.44	.04	.03
ZNO	0.00	0.00	0.00	0.00
CAO	9.99	.41	.01	.02
BAO	0.00	.08	.04	.03
NA2O	2.20	.14	0.00	.41
K2O	.14	.02	.01	8.44
H2O	0.00	0.00	0.00	0.00
F	.21	.04	.07	.42
CL	0.00	0.00	0.00	0.00
TOTAL	95.86	97.49	87.48	96.29
# ANIONS	24	24	18	12
SI	6.59	7.82	2.73	2.87
AL	2.39	.27	2.57	1.41
TI	.05	.01	.01	.07
FE+3	0.00	0.00	0.00	0.00
FE+2	1.40	2.12	1.03	.62
MG	2.81	4.67	3.62	1.96
MN	.02	.05	0.00	0.00
ZN	0.00	0.00	0.00	0.00
CA	1.58	.06	0.00	0.00
BA	0.00	0.00	0.00	0.00
NA	.63	.04	0.00	.06
K	.03	0.00	0.00	.77
OH	1.90	1.98	7.98	1.90
F	.10	.02	.02	.10
CL	0.00	0.00	0.00	0.00
SI+ALIV	8.00	8.00	4.00	4.00
ALVI+FM+ZN+TI	5.26	6.95	5.97	2.94
CA+BA+NA+K	2.23	.11	0.00	.83
OH+F+CL	2.00	2.00	8.00	2.00
FE/FE+MG	.33	.31	.22	.24

ANALYSIS #	5	6	7	8
PHASE		AMPH	FELD	AMPH
SAMPLE #	CC210	CC210	CC210	CC210
CIRCLE #	A	D	D	C
GRAIN #	5	6	7	8
SIO2	0.00	48.15	62.17	51.48
AL2O3	.12	11.54	23.53	7.78
TIO2	98.23	.28	.02	.17
FE2O3	0.00	0.00	0.00	0.00
FEO	.56	12.99	0.00	16.04
MGO	.03	20.67	0.00	19.99
MNO	.07	.36	0.00	.44
ZNO	0.00	0.00	0.00	0.00
CAO	.04	.61	5.22	.50
BAO	.57	.02	0.00	0.00
NA2O	0.00	1.53	8.28	1.12
K2O	.02	0.00	.04	.01
H2O	0.00	0.00	0.00	0.00
F	.01	.17	0.00	.09
CL	0.00	0.00	0.00	0.00
TOTAL	99.65	96.32	99.26	97.62
# ANIONS		24	8	24
SI	0.00	6.87	2.77	7.30
AL	0.00	1.94	1.24	1.30
TI	.99	.03	0.00	.02
FE+3	0.00	0.00	0.00	0.00
FE+2	.01	1.55	0.00	1.90
MG	0.00	4.39	0.00	4.23
MN	0.00	.04	0.00	.05
ZN	0.00	0.00	0.00	0.00
CA	0.00	.09	.25	.08
BA	0.00	0.00	0.00	0.00
NA	0.00	.42	.72	.31
K	0.00	0.00	0.00	0.00
OH	0.00	1.92	0.00	1.96
F	0.00	.08	0.00	.04
CL	0.00	0.00	0.00	0.00
SI+ALIV		8.00	4.00	8.00
ALVI+FM+ZN+TI		6.83	0.00	6.80
CA+BA+NA+K		.52	.97	.39
OH+F+CL		2.00	0.00	2.00
FE/FE+MG		.26	*****	.31

ANALYSIS #	9	10	11	12
PHASE	AMPH	BIOT	FELD	BIOT
SAMPLE #	CC210	CC210	CC210	CC210
CIRCLE #	C	C	B	A
GRAIN #	9	10	11	12
SIO2	45.56	39.89	62.83	39.83
AL2O3	14.63	16.89	23.83	16.74
TIO2	.49	1.30	0.00	1.22
FE2O3	0.00	0.00	0.00	0.00
FEO	11.11	11.07	.01	10.78
MGO	14.48	18.83	0.00	18.73
MNO	.15	.04	.01	.04
ZNO	0.00	0.00	0.00	0.00
CAO	10.69	.03	4.76	.02
BAO	0.00	.16	0.00	.15
NA2O	2.06	.39	8.62	.25
K2O	.14	8.64	.05	8.72
H2O	0.00	0.00	0.00	0.00
F	.25	.46	.01	.26
CL	0.00	0.00	0.00	0.00
TOTAL	99.56	97.70	100.12	96.74
# ANIONS	24	12	8	12
SI	6.46	2.83	2.77	2.85
AL	2.44	1.41	1.24	1.41
TI	.05	.07	0.00	.07
FE+3	0.00	0.00	0.00	0.00
FE+2	1.32	.66	0.00	.64
MG	3.06	1.99	0.00	1.99
MN	.02	0.00	0.00	0.00
ZN	0.00	0.00	0.00	0.00
CA	1.62	0.00	.23	0.00
BA	0.00	0.00	0.00	0.00
NA	.57	.05	.74	.03
K	.03	.78	0.00	.79
OH	1.89	1.90	0.00	1.94
F	.11	.10	0.00	.06
CL	0.00	0.00	0.00	0.00
SI+ALIV	8.00	4.00	4.00	4.00
ALVI+FM+ZN+TI	5.35	2.97	.01	2.96
CA+BA+NA+K	2.21	.84	.97	.84
OH+F+CL	2.00	2.00	0.00	2.00
FE/FE+MG	.30	.25	1.00	.24

ANALYSIS #	1	2	3	4
PHASE	AMPH	BIOT	CHL	FELD
SAMPLE #	CC239	CC239	CC239	CC239
CIRCLE #	E	E	E	E
GRAIN #	1	2	3	4
SIO2	43.49	39.97	28.82	60.81
AL2O3	14.90	17.12	21.47	25.01
TIO2	.74	1.31	.10	.02
FE2O3	0.00	0.00	0.00	0.00
FEO	13.32	10.73	13.79	.06
MGO	12.40	16.94	24.97	0.00
MNO	.26	.04	.09	0.00
ZNO	0.00	0.00	0.00	0.00
CAO	9.89	.06	.05	6.38
BAO	.03	.03	0.00	0.00
NA2O	2.23	.52	.02	7.87
K2O	.21	7.70	.02	.03
H2O	0.00	0.00	0.00	0.00
F	.14	.33	.11	0.00
CL	0.00	0.00	0.00	0.00
TOTAL	97.61	94.75	89.44	100.18
# ANIONS	24	12	18	8
SI	6.36	2.89	2.79	2.70
AL	2.57	1.46	2.45	1.31
TI	.08	.07	.01	0.00
FE+3	0.00	0.00	0.00	0.00
FE+2	1.63	.65	1.12	0.00
MG	2.70	1.83	3.60	0.00
MN	.03	0.00	.01	0.00
ZN	0.00	0.00	0.00	0.00
CA	1.55	0.00	.01	.30
BA	0.00	0.00	0.00	0.00
NA	.63	.07	0.00	.68
K	.04	.71	0.00	0.00
OH	1.94	1.92	7.97	0.00
F	.06	.08	.03	0.00
CL	0.00	0.00	0.00	0.00
SI+ALIV	8.00	4.00	4.00	4.00
ALVI+FM+ZN+TI	5.38	2.91	5.97	.01
CA+BA+NA+K	2.22	.79	.01	.98
OH+F+CL	2.00	2.00	8.00	0.00
FE/FE+MG	.38	.26	.24	1.00

ANALYSIS #	5	6	7	8
PHASE		AMPH	AMPH	FELD
SAMPLE #	CC239	CC239	CC239	CC239
CIRCLE #	E	D	D	D
GRAIN #	5	6	7	8
SIO2	.06	51.19	44.64	61.52
AL2O3	.07	6.95	13.33	24.65
TIO2	96.23	.19	.70	0.00
FE2O3	0.00	0.00	0.00	0.00
FEO	.25	19.49	14.20	.08
MGO	0.00	19.54	13.68	0.00
MNO	.05	.54	.25	0.00
ZNO	0.00	0.00	0.00	0.00
CAO	.05	.64	9.39	5.70
BAO	.50	.01	0.00	0.00
NA2O	0.00	.94	2.06	8.25
K2O	.03	.01	.19	.03
H2O	0.00	0.00	0.00	0.00
F	0.00	.01	.12	0.00
CL	0.00	0.00	0.00	0.00
TOTAL	97.24	99.51	98.56	100.23
# ANIONS		24	24	8
SI	0.00	7.25	6.48	2.72
AL	0.00	1.16	2.28	1.29
TI	.99	.02	.08	0.00
FE+3	0.00	0.00	0.00	0.00
FE+2	0.00	2.31	1.72	0.00
MG	0.00	4.12	2.96	0.00
MN	0.00	.06	.03	0.00
ZN	0.00	0.00	0.00	0.00
CA	0.00	.10	1.46	.27
BA	0.00	0.00	0.00	0.00
NA	0.00	.26	.58	.71
K	0.00	0.00	.04	0.00
OH	0.00	2.00	1.94	0.00
F	0.00	0.00	.06	0.00
CL	0.00	0.00	0.00	0.00
SI+ALIV		8.00	8.00	4.00
ALVI+FM+ZN+TI		6.92	5.54	.01
CA+BA+NA+K		.36	2.07	.98
OH+F+CL		2.00	2.00	0.00
FE/FE+MG		.36	.37	1.00

ANALYSIS #	1	2	3	4
PHASE	CHL	BIOT	CHL	
SAMPLE #	CC264	CC264	CC264	CC264
CIRCLE #	C	D	D	B
GRAIN #	1	2	3	4
SIO2	27.64	40.10	27.36	.15
AL2O3	21.64	15.31	22.01	.11
TIO2	.08	1.43	.11	96.78
FE2O3	0.00	0.00	0.00	0.00
FEO	12.10	10.58	11.50	.54
MGO	23.13	18.27	23.23	.01
MNO	.19	.15	.13	.05
ZNO	0.00	0.00	0.00	0.00
CAO	.03	.12	.02	.09
BAO	0.00	.20	0.00	.40
NA2O	0.00	.13	0.00	.01
K2O	.02	9.19	.01	.03
H2O	0.00	0.00	0.00	0.00
F	.07	.53	.10	.01
CL	0.00	0.00	0.00	0.00
TOTAL	84.90	96.01	84.47	98.18
# ANIONS	18	12	18	
SI	2.79	2.91	2.77	0.00
AL	2.58	1.31	2.63	0.00
TI	.01	.08	.01	.99
FE+3	0.00	0.00	0.00	0.00
FE+2	1.02	.64	.97	.01
MG	3.49	1.97	3.51	0.00
MN	.02	.01	.01	0.00
ZN	0.00	0.00	0.00	0.00
CA	0.00	.01	0.00	0.00
BA	0.00	.01	0.00	0.00
NA	0.00	.02	0.00	0.00
K	0.00	.85	0.00	0.00
OH	7.98	1.88	7.97	0.00
F	.02	.12	.03	0.00
CL	0.00	0.00	0.00	0.00
SI+ALIV	4.00	4.00	4.00	
ALVI+FM+ZN+TI	5.91	2.91	5.90	
CA+BA+NA+K	.01	.88	0.00	
OH+F+CL	8.00	2.00	8.00	
FE/FE+MG	.23	.25	.22	

ANALYSIS #	5	6	7	8
PHASE	FELD	BIOT	AMPH	BIOT
SAMPLE #	CC264	CC264	CC264	CC264
CIRCLE #	B	B	A	A
GRAIN #	5	6	7	8
SIO2	64.64	39.99	59.10	39.26
AL2O3	22.14	16.27	2.02	15.51
TIO2	0.00	1.04	.11	1.34
FE2O3	0.00	0.00	0.00	0.00
FEO	0.00	11.78	7.18	10.53
MGO	0.00	19.07	27.21	18.32
MNO	0.00	.16	.11	.14
ZNO	0.00	0.00	0.00	0.00
CAO	2.97	.03	.02	.03
BAO	0.00	.11	.06	.12
NA2O	9.82	.18	.16	.12
K2O	.04	9.59	.76	9.64
H2O	0.00	0.00	0.00	0.00
F	0.00	.50	.28	.49
CL	0.00	0.00	0.00	0.00
TOTAL	99.61	98.72	97.01	95.50
# ANIONS	8	12	24	12
SI	2.85	2.84	8.03	2.87
AL	1.15	1.36	.32	1.34
TI	0.00	.06	.01	.07
FE+3	0.00	0.00	0.00	0.00
FE+2	0.00	.70	.82	.64
MG	0.00	2.02	5.51	2.00
MN	0.00	.01	.01	.01
ZN	0.00	0.00	0.00	0.00
CA	.14	0.00	0.00	0.00
BA	0.00	0.00	0.00	0.00
NA	.84	.02	.04	.02
K	0.00	.87	.13	.90
OH	0.00	1.89	1.88	1.89
F	0.00	.11	.12	.11
CL	0.00	0.00	0.00	0.00
SI+ALIV	4.00	4.00	8.03	4.00
ALVI+FM+ZN+TI	.01	2.98	6.67	2.93
CA+BA+NA+K	.98	.90	.18	.92
OH+F+CL	0.00	2.00	2.00	2.00
FE/FE+MG	*****	.26	.13	.24

ANALYSIS #	9	10
PHASE	CHL	FELD
SAMPLE #	CC264	CC264
CIRCLE #	A	A
GRAIN #	9	10
SIO2	28.00	65.69
AL2O3	21.73	22.30
TIO2	.12	0.00
FE2O3	0.00	0.00
FEO	13.04	0.00
MGO	24.37	0.00
MNO	.18	0.00
ZNO	0.00	0.00
CAO	.03	2.87
BAO	0.00	.01
NA2O	0.00	9.43
K2O	.14	.05
H2O	0.00	0.00
F	.03	.02
CL	0.00	0.00
TOTAL	87.64	100.37
# ANIONS	18	8
SI	2.76	2.87
AL	2.52	1.15
TI	.01	0.00
FE+3	0.00	0.00
FE+2	1.07	0.00
MG	3.58	0.00
MN	.02	0.00
ZN	0.00	0.00
CA	0.00	.13
BA	0.00	0.00
NA	0.00	.80
K.	.02	0.00
OH	7.99	0.00
F	.01	0.00
CL	0.00	0.00
SI+ALIV	4.00	4.00
ALVI+FM+ZN+TI	5.96	.02
CA+BA+NA+K	.02	.94
OH+F+CL	8.00	0.00
FE/FE+MG	.23	*****

ANALYSIS #	1	2	3	4
PHASE	GAR	BIOT	FELD	AMPH
SAMPLE #	CC296	CC296	CC296	CC296
CIRCLE #	C	C	C	C
GRAIN #	1	2	3	4
SIO2	38.75	38.15	65.31	45.22
AL2O3	20.74	17.46	23.31	15.26
TIO2	.02	1.21	0.00	.20
FE2O3	0.00	0.00	0.00	0.00
FEO	29.77	13.88	0.00	20.35
MGO	6.06	15.04	0.00	14.90
MNO	2.55	.06	0.00	.54
ZNO	0.00	0.00	0.00	0.00
CAO	1.71	.01	3.75	.36
BAO	.09	.31	0.00	0.00
NA2O	0.00	.31	9.45	2.08
K2O	.02	8.16	.03	.01
H2O	0.00	0.00	0.00	0.00
F	.05	.14	0.00	.13
CL	0.00	0.00	0.00	0.00
TOTAL	99.76	94.73	101.85	99.05
# ANIONS	12	12	8	24
SI	3.05	2.82	2.82	6.51
AL	1.93	1.52	1.19	2.59
TI	0.00	.07	0.00	.02
FE+3	0.00	0.00	0.00	0.00
FE+2	1.96	.86	0.00	2.45
MG	.71	1.66	0.00	3.20
MN	.17	0.00	0.00	.07
ZN	0.00	0.00	0.00	0.00
CA	.14	0.00	.17	.06
BA	0.00	.01	0.00	0.00
NA	0.00	.04	.79	.58
K	0.00	.77	0.00	0.00
OH	0.00	1.97	0.00	1.94
F	.01	.03	0.00	.06
CL	0.00	0.00	0.00	0.00
SI+ALIV	3.05	4.00	4.00	8.00
ALVI+FM+ZN+TI	4.77	2.93	.01	6.83
CA+BA+NA+K	.15	.82	.97	.64
OH+F+CL	.01	2.00	0.00	2.00
FE/FE+MG	.73	.34	*****	.43

ANALYSIS #	1	2	3	4
PHASE	AMPH	FELD	GAR	AMPH
SAMPLE #	CC344	CC344	CC344	CC344
CIRCLE #	C	C	A	B
GRAIN #	1	2	3	4
SIO2	42.24	62.55	38.99	43.26
AL2O3	16.27	23.04	21.49	15.55
TIO2	.21	0.00	.07	.22
FE2O3	0.00	0.00	0.00	0.00
FEO	20.66	.09	28.99	20.33
MGO	14.19	0.00	7.67	14.04
MNO	.26	0.00	.86	.30
ZNO	0.00	0.00	0.00	0.00
CAO	.35	3.84	2.00	.35
BAO	0.00	0.00	0.00	.02
NA2O	2.07	8.67	0.00	1.98
K2O	.01	.04	.02	.01
H2O	0.00	0.00	0.00	0.00
F	.06	0.00	.06	.11
CL	0.00	0.00	0.00	0.00
TOTAL	96.32	98.23	100.15	96.17
# ANIONS	24	8	12	24
SI	6.28	2.80	3.02	6.43
AL	2.85	1.22	1.96	2.72
TI	.02	0.00	0.00	.02
FE+3	0.00	0.00	0.00	0.00
FE+2	2.57	0.00	1.88	2.53
MG	3.15	0.00	.89	3.11
MN	.03	0.00	.06	.04
ZN	0.00	0.00	0.00	0.00
CA	.06	.18	.17	.06
BA	0.00	0.00	0.00	0.00
NA	.60	.75	0.00	.57
K	0.00	0.00	0.00	0.00
OH	1.97	0.00	0.00	1.95
F	.03	0.00	.01	.05
CL	0.00	0.00	0.00	0.00
SI+ALIV	8.00	4.00	3.02	8.00
ALVI+FM+ZN+TI	6.91	.02	4.79	6.85
CA+BA+NA+K	.65	.94	.17	.63
OH+F+CL	2.00	0.00	.01	2.00
FE/FE+MG	.45	1.00	.68	.45

ANALYSIS #	1	2	3	4
PHASE	BIOT	BIOT	GAR	GAR
SAMPLE #	CC357	CC357	CC357	CC357
CIRCLE #	A	A	A	A
GRAIN #	1	2	3	4
SIO2	38.60	38.13	39.12	39.83
AL2O3	17.27	17.61	21.37	20.99
TIO2	1.37	1.35	.07	.08
FE2O3	0.00	0.00	0.00	0.00
FEO	12.09	12.07	26.89	26.57
MGO	16.04	15.75	6.53	6.51
MNO	.04	.07	2.00	2.06
ZNO	0.00	0.00	0.00	0.00
CAO	.02	.04	3.32	3.66
BAO	.14	.14	.11	.11
NA2O	.39	.44	0.00	.02
K2O	8.04	7.80	.01	.02
H2O	0.00	0.00	0.00	0.00
F	.25	.12	.06	.03
CL	0.00	0.00	0.00	0.00
TOTAL	94.25	93.52	99.48	99.88
# ANIONS	12	12	12	12
SI	2.84	2.82	3.05	3.09
AL	1.50	1.54	1.97	1.92
TI	.08	.08	0.00	0.00
FE+3	0.00	0.00	0.00	0.00
FE+2	.74	.75	1.76	1.72
MG	1.76	1.74	.76	.75
MN	0.00	0.00	.13	.14
ZN	0.00	0.00	0.00	0.00
CA	0.00	0.00	.28	.30
BA	0.00	0.00	0.00	0.00
NA	.06	.06	0.00	0.00
K	.76	.74	0.00	0.00
OH	1.94	1.97	0.00	0.00
F	.06	.03	.01	.01
CL	0.00	0.00	0.00	0.00
SI+ALIV	4.00	4.00	3.05	3.09
ALVI+FM+ZN+TI	2.92	2.93	4.62	4.54
CA+BA+NA+K	.82	.81	.28	.31
OH+F+CL	2.00	2.00	.01	.01
FE/FE+MG	.30	.30	.70	.70

ANALYSIS #	5	6	7	8
PHASE	AMPH	BIOT	GAR	BIOT
SAMPLE #	CC357	CC357	CC357	CC357
CIRCLE #	A	B	B	B
GRAIN #	5	6	7	8
SIO2	43.12	38.31	39.09	38.34
AL2O3	15.79	17.45	21.10	17.12
TIO2	.51	1.24	.13	1.24
FE2O3	0.00	0.00	0.00	0.00
FEO	14.30	13.11	27.64	12.57
MGO	11.47	16.17	6.49	15.85
MNO	.29	0.00	1.83	.09
ZNO	0.00	0.00	0.00	0.00
CAO	9.70	.02	3.80	.02
BAO	0.00	.09	.04	.13
NA2O	1.96	.39	.01	.38
K2O	.21	8.25	.02	8.04
H2O	0.00	0.00	0.00	0.00
F	.08	.15	0.00	.24
CL	0.00	0.00	0.00	0.00
TOTAL	97.43	95.18	100.15	94.02
# ANIONS	24	12	12	12
SI	6.33	2.81	3.04	2.84
AL	2.73	1.51	1.94	1.49
TI	.06	.07	.01	.07
FE+3	0.00	0.00	0.00	0.00
FE+2	1.76	.80	1.80	.78
MG	2.51	1.77	.75	1.75
MN	.04	0.00	.12	.01
ZN	0.00	0.00	0.00	0.00
CA	1.53	0.00	.32	0.00
BA	0.00	0.00	0.00	0.00
NA	.56	.06	0.00	.05
K	.04	.77	0.00	.76
OH	1.96	1.97	0.00	1.94
F	.04	.03	0.00	.06
CL	0.00	0.00	0.00	0.00
SI+ALIV	8.00	4.00	3.04	4.00
ALVI+FM+ZN+TI	5.42	2.95	4.62	2.93
CA+BA+NA+K	2.12	.83	.32	.82
OH+F+CL	2.00	2.00	0.00	2.00
FE/FE+MG	.41	.31	.70	.31

ANALYSIS #	18	19	20	21
PHASE	FELD	AMPH	AMPH	FELD
SAMPLE #	CC357	CC357	CC357	CC357
CIRCLE #	E	E	E	E
GRAIN #	17	18	19	20
SIO2	61.22	52.97	43.95	61.04
AL2O3	24.88	3.47	13.77	25.51
TIO2	.01	.09	.70	.01
FE2O3	0.00	0.00	0.00	0.00
FEO	.02	19.66	14.79	0.00
MGO	0.00	19.75	11.80	0.00
MNO	0.00	.58	.27	0.00
ZNO	0.00	0.00	0.00	0.00
CAO	5.51	.42	9.42	5.95
BAO	0.00	.06	0.00	.01
NA2O	8.02	.31	1.85	7.87
K2O	.04	.01	.23	.05
H2O	0.00	0.00	0.00	0.00
F	0.00	.05	.07	.08
CL	0.00	0.00	0.00	0.00
TOTAL	99.70	97.37	96.85	100.52
# ANIONS	8	24	24	8
SI	2.72	7.64	6.50	2.69
AL	1.30	.59	2.40	1.33
TI	0.00	.01	.08	0.00
FE+3	0.00	0.00	0.00	0.00
FE+2	0.00	2.37	1.83	0.00
MG	0.00	4.25	2.60	0.00
MN	0.00	.07	.03	0.00
ZN	0.00	0.00	0.00	0.00
CA	.26	.06	1.49	.28
BA	0.00	0.00	0.00	0.00
NA	.69	.09	.53	.67
K	0.00	0.00	.04	0.00
OH	0.00	1.98	1.97	0.00
F	0.00	.02	.03	.01
CL	0.00	0.00	0.00	0.00
SI+ALIV	4.00	8.00	8.00	4.00
ALVI+FM+ZN+TI	.02	6.94	5.44	.02
CA+BA+NA+K	.95	.16	2.07	.96
OH+F+CL	0.00	2.00	2.00	.01
FE/FE+MG	1.00	.36	.41	*****

ANALYSIS #	1	2	3	4
PHASE	FELD	BIOT	AMPH	AMPH
SAMPLE #	CC375	CC375	CC375	CC375
CIRCLE #	B	B	B	B
GRAIN #	1	2	3	4
SIO2	63.98	36.68	41.49	41.48
AL2O3	22.19	18.80	18.12	18.47
TIO2	0.00	1.49	.23	.21
FE2O3	0.00	0.00	0.00	0.00
FEO	.03	10.39	13.73	14.33
MGO	.03	15.76	15.13	14.68
MNO	.01	.09	.79	.83
ZNO	0.00	0.00	0.00	0.00
CAO	2.41	.10	.16	.18
BAO	.07	.17	.01	0.00
NA2O	10.56	.42	2.11	2.10
K2O	.04	7.50	0.00	.01
H2O	0.00	0.00	0.00	0.00
F	0.00	.20	.10	.09
CL	0.00	0.00	0.00	0.00
TOTAL	99.32	91.60	91.87	92.38
# ANIONS	8	12	24	24
SI	2.84	2.75	6.27	6.25
AL	1.16	1.66	3.23	3.28
TI	0.00	.08	.03	.02
FE+3	0.00	0.00	0.00	0.00
FE+2	0.00	.65	1.73	1.80
MG	0.00	1.76	3.41	3.30
MN	0.00	.01	.10	.11
ZN	0.00	0.00	0.00	0.00
CA	.11	.01	.03	.03
BA	0.00	.01	0.00	0.00
NA	.91	.06	.62	.61
K	0.00	.72	0.00	0.00
OH	0.00	1.95	1.95	1.96
F	0.00	.05	.05	.04
CL	0.00	0.00	0.00	0.00
SI+ALIV	4.00	4.00	8.00	8.00
ALVI+FM+ZN+TI	.01	2.93	6.76	6.75
CA+BA+NA+K	1.03	.79	.64	.64
OH+F+CL	0.00	2.00	2.00	2.00
FE/FE+MG	.36	.27	.34	.35

ANALYSIS #	1	2	3	4
PHASE	FELD	AMPH	AMPH	AMPH
SAMPLE #	CC410	CC410	CC410	CC410
CIRCLE #	A	A	A	A
GRAIN #	1	2	3	4
SIO2	63.14	43.82	54.31	44.02
AL2O3	22.92	11.30	.76	11.79
TIO2	0.00	.43	.06	.45
FE2O3	0.00	0.00	0.00	0.00
FEO	.11	14.95	20.08	15.30
MGO	0.00	10.97	18.20	11.25
MNO	.02	.66	2.26	.67
ZNO	0.00	0.00	0.00	0.00
CAO	3.80	10.21	.98	10.09
BAO	.03	.04	0.00	.04
NA2O	9.07	2.02	.07	1.95
K2O	.05	.24	.02	.24
H2O	0.00	0.00	0.00	0.00
F	.03	.02	.01	.14
CL	0.00	0.00	0.00	0.00
TOTAL	99.17	94.66	96.75	95.94
# ANIONS	8	24	24	24
SI	2.81	6.69	7.96	6.64
AL	1.20	2.03	.13	2.09
TI	0.00	.05	.01	.05
FE+3	0.00	0.00	0.00	0.00
FE+2	0.00	1.91	2.46	1.93
MG	0.00	2.49	3.97	2.53
MN	0.00	.09	.28	.09
ZN	0.00	0.00	0.00	0.00
CA	.18	1.67	.15	1.63
BA	0.00	0.00	0.00	0.00
NA	.78	.60	.02	.57
K	0.00	.05	0.00	.05
OH	0.00	1.99	2.00	1.93
F	0.00	.01	0.00	.07
CL	0.00	0.00	0.00	0.00
SI+ALIV	4.00	8.00	8.00	8.00
ALVI+FM+ZN+TI	.01	5.26	6.81	5.32
CA+BA+NA+K	.97	2.32	.18	2.25
OH+F+CL	0.00	2.00	2.00	2.00
FE/FE+MG	1.00	.43	.38	.43

ANALYSIS #	6	7	8	9
PHASE	AMPH	AMPH	AMPH	AMPH
SAMPLE #	CC410	CC410	CC410	CC410
CIRCLE #	A	B	B	B
GRAIN #	6	7	8	9
SIO2	43.54	52.88	47.60	43.71
AL2O3	11.47	2.18	8.53	12.20
TIO2	.38	.13	.18	.35
FE2O3	0.00	0.00	0.00	0.00
FEO	15.73	19.80	17.25	15.38
MGO	9.89	17.75	13.29	10.55
MNO	.55	1.39	.91	.52
ZNO	0.00	0.00	0.00	0.00
CAO	9.90	1.31	6.69	10.19
BAO	.06	.03	.09	0.00
NA2O	1.87	.31	1.34	2.01
K2O	.26	.03	.22	.27
H2O	0.00	0.00	0.00	0.00
F	.12	.07	.13	0.00
CL	0.00	0.00	0.00	0.00
TOTAL	93.77	95.88	96.23	95.18
# ANIONS	24	24	24	24
SI	6.73	7.81	7.10	6.63
AL	2.09	.38	1.50	2.18
TI	.04	.01	.02	.04
FE+3	0.00	0.00	0.00	0.00
FE+2	2.03	2.45	2.15	1.95
MG	2.28	3.91	2.95	2.39
MN	.07	.17	.11	.07
ZN	0.00	0.00	0.00	0.00
CA	1.64	.21	1.07	1.66
BA	0.00	0.00	.01	0.00
NA	.56	.09	.39	.59
K	.05	.01	.04	.05
OH	1.94	1.97	1.94	2.00
F	.06	.03	.06	0.00
CL	0.00	0.00	0.00	0.00
SI+ALIV	8.00	8.00	8.00	8.00
ALVI+FM+ZN+TI	5.24	6.73	5.84	5.26
CA+BA+NA+K	2.25	.30	1.50	2.30
OH+F+CL	2.00	2.00	2.00	2.00
FE/FE+MG	.47	.38	.42	.45

ANALYSIS #	10	11	12	13
PHASE	AMPH	FELD	FELD	BIOT
SAMPLE #	CC410	CC410	CC410	CC410
CIRCLE #	B	B	B	B
GRAIN #	10	11	12	13
SIO2	53.58	63.68	63.53	37.62
AL2O3	1.74	23.18	23.13	16.65
TIO2	.12	0.00	0.00	1.41
FE2O3	0.00	0.00	0.00	0.00
FEO	19.62	.02	.03	15.32
MGO	17.75	0.00	0.00	13.55
MNO	1.71	0.00	0.00	.13
ZNO	0.00	0.00	0.00	0.00
CAO	1.14	3.94	3.99	.04
BAO	0.00	.03	.07	0.00
NA2O	.26	9.14	9.08	.19
K2O	.02	.04	.05	8.12
H2O	0.00	0.00	0.00	0.00
F	.03	0.00	0.00	.15
CL	0.00	0.00	0.00	0.00
TOTAL	95.97	100.03	99.88	93.18
# ANIONS	24	8	8	12
SI	7.89	2.81	2.81	2.85
AL	.30	1.20	1.20	1.49
TI	.01	0.00	0.00	.08
FE+3	0.00	0.00	0.00	0.00
FE+2	2.42	0.00	0.00	.97
MG	3.90	0.00	0.00	1.53
MN	.21	0.00	0.00	.01
ZN	0.00	0.00	0.00	0.00
CA	.18	.19	.19	0.00
BA	0.00	0.00	0.00	0.00
NA	.07	.78	.78	.03
K	0.00	0.00	0.00	.78
OH	1.99	0.00	0.00	1.96
F	.01	0.00	0.00	.04
CL	0.00	0.00	0.00	0.00
SI+ALIV	8.00	4.00	4.00	4.00
ALVI+FM+ZN+TI	6.73	.01	.01	2.92
CA+BA+NA+K	.26	.97	.97	.82
OH+F+CL	2.00	0.00	0.00	2.00
FE/FE+MG	.38	1.00	1.00	.39

ANALYSIS #	14	15	16	17
PHASE	AMPH		AMPH	AMPH
SAMPLE #	CC410	CC410	CC410	CC410
CIRCLE #	B	B	C	C
GRAIN #	14	15	16	17
SIO2	44.63	.20	53.62	44.84
AL2O3	11.70	.17	1.42	11.44
TIO2	.35	17.20	.08	.36
FE2O3	0.00	0.00	0.00	0.00
FEO	14.71	71.99	19.81	15.38
MGO	11.35	.07	18.01	11.35
MNO	.58	.49	2.31	.62
ZNO	0.00	0.00	0.00	0.00
CAO	10.41	.07	.72	10.32
BAO	.04	.29	.03	.06
NA2O	1.96	0.00	.24	1.94
K2O	.27	.05	.01	.26
H2O	0.00	0.00	0.00	0.00
F	.10	0.00	.07	.12
CL	0.00	0.00	0.00	0.00
TOTAL	96.10	90.53	96.32	96.69
# ANIONS	24		24	24
SI	6.69	.01	7.89	6.70
AL	2.07	.01	.25	2.02
TI	.04	.44	.01	.04
FE+3	0.00	0.00	0.00	0.00
FE+2	1.84	2.06	2.44	1.92
MG	2.54	0.00	3.95	2.53
MN	.07	.01	.29	.08
ZN	0.00	0.00	0.00	0.00
CA	1.67	0.00	.11	1.65
BA	0.00	0.00	0.00	0.00
NA	.57	0.00	.07	.56
K	.05	0.00	0.00	.05
OH	1.95	0.00	1.97	1.94
F	.05	0.00	.03	.06
CL	0.00	0.00	0.00	0.00
SI+ALIV	8.00		8.00	8.00
ALVI+FM+ZN+TI	5.25		6.83	5.29
CA+BA+NA+K	2.30		.19	2.27
OH+F+CL	2.00		2.00	2.00
FE/FE+MG	.42		.38	.43

The vita has been removed from the scanned document